Improving Energy Resource Availability and Resilience with the Strategic Placement of Microgrids

By

Melvin Lugo Alvarez

A thesis submitted in partial fulfillment of the requirements for the degree of

MASTER OF SCIENCE

In

ELECTRICAL ENGINEERING

UNIVERSITY OF PUERTO RICO

MAYAGUEZ CAMPUS

2019

Approved by:

_____	_____
Eduardo I. Ortiz Rivera, PhD.	Date
President, Graduate Committee	
_____	_____
José R. Cedeño Maldonado, PhD	Date
Member, Graduate Committee	
_____	_____
Lionel R. Orama Exclusa, DEng	Date
Member, Graduate Committee	
_____	_____
Silvestre Colón Ramírez, M.S.	Date
Graduate Studies Office Representative	
_____	_____
Dept. Director or Representative	Date
Dr. Omell Pagán Parés	

Improving Energy Resource Availability and Resilience with the Strategic Placement of Microgrids

By

Melvin Lugo Alvarez

October 2019

Chair: Dr. Eduardo I. Ortiz-Rivera

Department: Electrical and Computer Engineering Department

Natural disasters are increasingly impacting the power availability to communities around the world causing long term blackouts. Rural and remote communities are at a greater risk of suffering longer blackouts due to being lower priority or more difficult to power during the energy restoration efforts. Utilities may not have a complete picture of the restoration of power across time, this is where previous work done by NASA comes in by providing a time series of the recovery process using nighttime satellite imagery.

This work proposes a methodology regarding microgrid planning and critical asset clustering using GIS, census, and the nighttime imagery provided by NASA. The work presents a workflow as well as the decision criteria involved. The aftermath of Hurricane María in Puerto Rico is presented as the test case, with a more detailed example based in the town of Jayuya.

Mejoramiento de la disponibilidad de recursos energéticos y la resiliencia con la colocación estratégica de microrredes

Por

Melvin Lugo Álvarez

Octubre 2019

Consejero: Dr. Eduardo I. Ortiz-Rivera
Departamento: Ingeniería Eléctrica y Computadoras

Los desastres naturales afectan cada vez más la disponibilidad de energía para las comunidades de todo el mundo, causando apagones. Las comunidades rurales corren un mayor riesgo de sufrir apagones más largos por ser de menor prioridad o ser más difícil su reconexión al sistema. Los proveedores de servicio eléctrico no necesariamente tienen una imagen completa de la restauración a través del tiempo. Aquí entra el trabajo realizado por la NASA, quienes validaron un método de rastrear la recuperación usando imágenes satelitales nocturnas.

Este trabajo propone una metodología para la planificación de microrredes y la agrupación de cargas criticas mediante la utilización de SIG y las imágenes nocturnas creadas por la NASA. Se presenta un flujo de trabajo, así como los criterios de decisión involucrados. El paso del huracán María en Puerto Rico se presentan como el caso de prueba, con un ejemplo más detallado basado en pueblo de Jayuya.

Acknowledgements

I would like to begin by thanking Indra M. Gonzalez Ojeda who inspired me to not settle and set me on the path to begin my graduate studies.

I would like to thank my advisor Dr. Eduardo I. Ortiz Rivera for showing me how to navigate graduate school and graduate research. As well as thank the graduate committee Dr. José R. Cedeño Maldonado and Dr. Lionel R. Orama Exclusa for their feedback and support during the master's degree.

I would like to thank Dr. Matthew Lave and Mr. Robert Broderick for providing commentary and guidance during the research and development part of this work as well as guidance during the internships at SNL.

Contents

List of Tables:

List of Figures:

Chapter 1:   INTRODUCTION

1.1   Motivation:

The use of electricity is so commonplace for people in modern countries that it has become an essential part of daily life. Everything from, health, security, communications and economic transactions depends on electricity in some way. This is the case in Puerto Rico. Puerto Rico's electricity consumption per capita is around 5GWh with a total population of 3.5 million [1]. PR has the biggest electricity consumption comparing to other major islands in the Caribbean (e.g. Cuba: 1,434kWh, Jamaica: 1,055kWh, Dominican Republic: 1,578 kWh).

The power generation, transmission and distribution system in Puerto Rico is controlled by a single public entity known as the Puerto Rico Electric Power Authority (PREPA) [2]. PREPA is the biggest public power utility in the United States. There are seven different types of power sources; they can be seen in Figure 1. The majority consumption of energy is at the north of Puerto Rico and the production at the south; because of this the transmission lines must cross the island's mountainous terrain. This creates difficult access for maintenance and recovery of the transmission lines. In Figure 2 shows where the biggest power consumption is concentrated [3]. Also, when these lines or the generation is affected the north and northeast is greatly affected creating long periods of blackouts. The transmission lines that cross the island can be seen in Figure 3.

As was mentioned before the majority consumption is in the north and northeast. This unbalanced power generation and consumption has affected the electrical services of the citizens of Puerto Rico in these past days. Puerto Rico was hit by hurricane María on September 20, 2017, creating the biggest blackout in history, not only for Puerto Rico, but also for the USA [3]. The atmospheric event has exposed how the island was not prepared for the devastation caused by the total power and communication loss; not unlike what could happen after a coordinated terrorist attack [4].

María is not alone as the only hurricane that has caused costly damages to the economy and the infrastructure in Puerto Rico. Hurricane George on September 21, 1998, also wreaked havoc and caused around $6 billion in combined infrastructure and cost to the economy [5].

Figure 1 Percentage of Generation by Energy Type. [6]
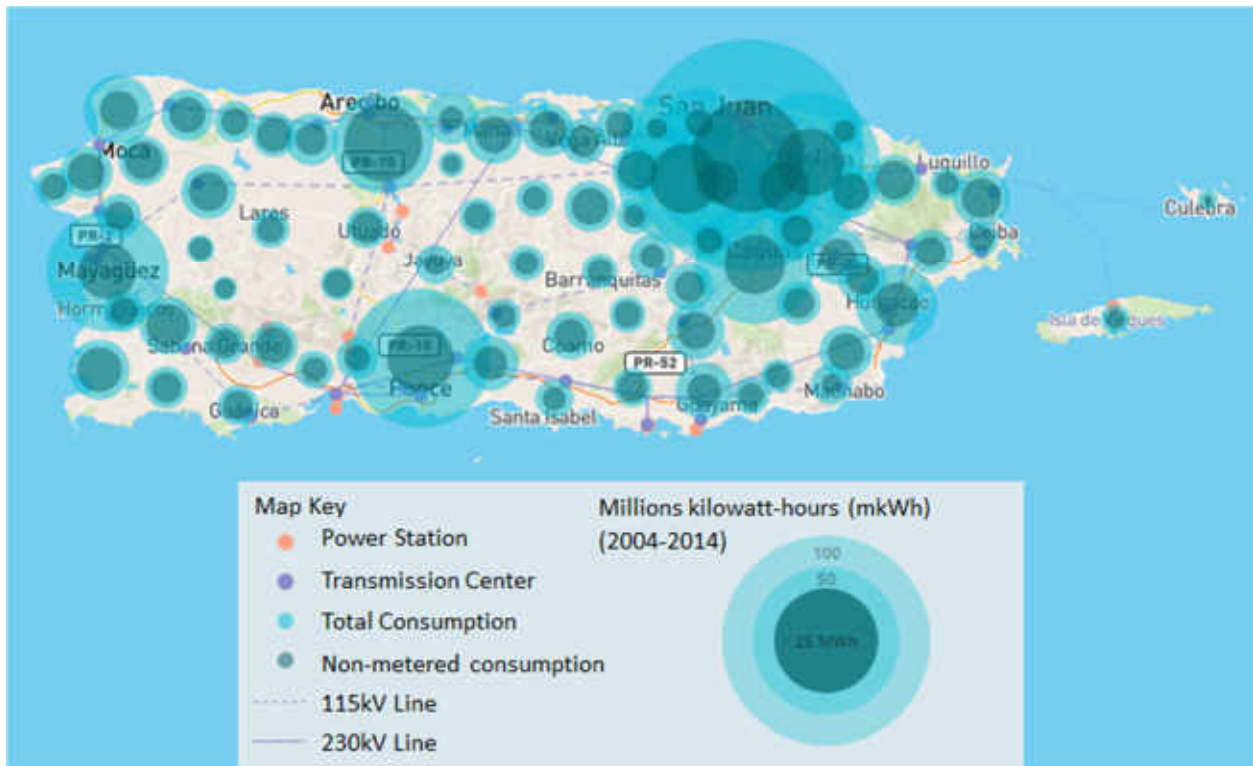
Figure 2 Municipal Energy Consumption of Puerto Rico. [7]

Figure 3 All transmission lines for electrical system in Puerto Rico. [8]
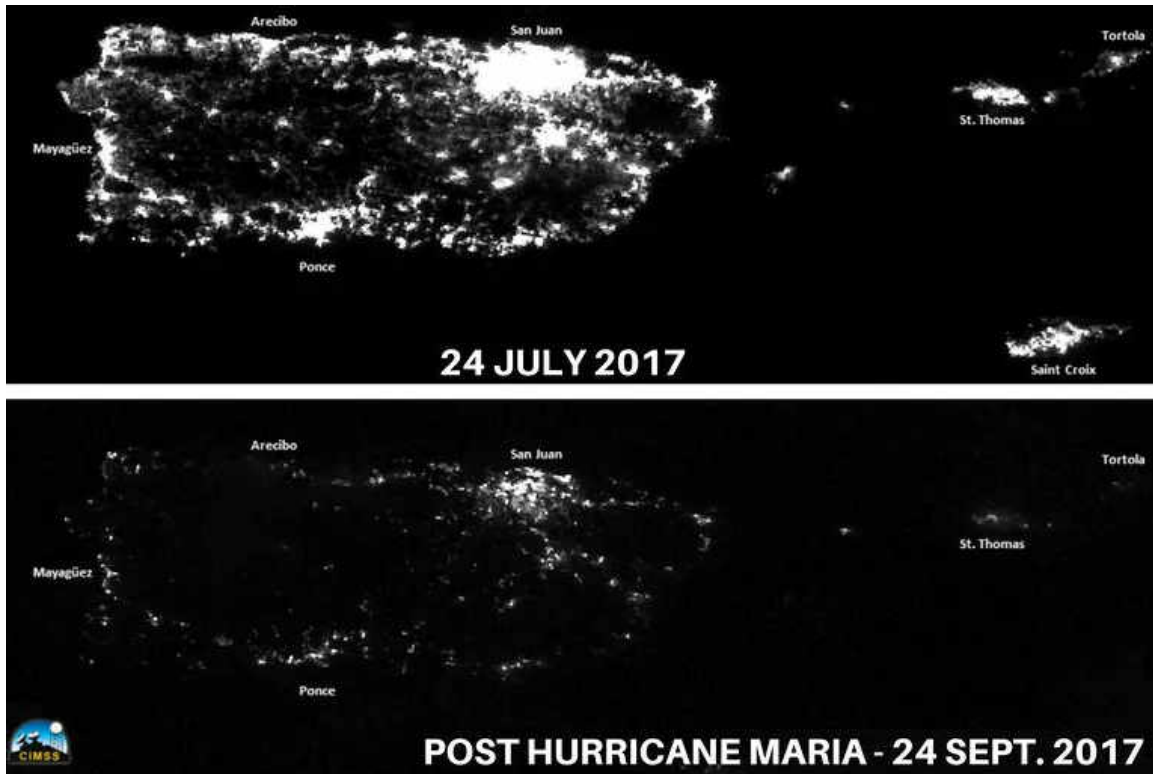
Figure 4 Pre hurricane and post hurricane raw nighttime satellite images of Puerto Rico and some US Virgin Islands.

In most countries, the different systems or products depend of electricity to function or to be produced. Human error, natural phenomena and terrorist attack could cause electric system failure. Electric system failure poses a threat on the daily functioning of the different customers. Prolonged blackouts cause a domino effect that affects society daily life and essential services. Figure 4 shows just how massive the impact of Hurricane María was on the electrical system.

The failure of the electrical system has, without a doubt, a direct impact in daily life and the life supporting systems that make up modern society. The systems impacted by the lack of power in Puerto Rico can be categorized as follows: *water and sanitary system, the health system and public health, communications, the economy, and security*.

The blackout rendered the water authority out of commission during the aftermath of the hurricane. The pumping stations lost power and only those who had cisterns had running water [9]. Nine months after the hurricane, there were still 4% of customers without running water, and those that did have water could have had intermittent service due to failure of the backup generators that were powering the pumping stations [10].

Another direct victim of the power outage were the hospitals. The timeline for hospital availability is as follows:

- 3 days after impact – 12/69 hospitals are in service [11]

- 6 days after impact – hospitals that were in service due to generators required police escort for refueling [12]

- 30 days after impact – 63/69 hospitals. 45 powered by the grid, 18 powered by auxiliary generators, 6 out of service. [13]

A more fundamental aspect of health that was affected, was that of hygiene. The lack of hygiene is directly related to the loss of water.

The transfer of information is crucial to the coordination of recovery efforts and in locating people in need of help. Therefore, chaos ensues when communication services are lost like in the aftermath of the hurricane. Nine days after impact there were only 96 functioning telecom towers of a total 1600 in Puerto Rico. This is equivalent of only a 30% accessibility to communication services [14]. These telecom towers could have been out of service due to damage from the storm, loss of grid power or loss of emergency generator power.

To say the restoration of power in Puerto Rico was slow, would be the biggest understatement in this entire work. "When compared to the restoration of power after Sandy and Irene in Connecticut, New Jersey, New York and Pennsylvania, the restoration in Puerto Rico was painfully slow. Up to November 9, 2017 only 41% had been restored, 45 days after the hurricane. This same amount of generation was reached in 3 days by the slowest utility in NY after Sandy. It has taken 15 times longer in Puerto Rico than it did in New York after Sandy." [15] The restoration effort is slowed down by many factors, one is the fact that it is an island; help cannot get to Puerto Rico as fast as other jurisdictions. Even within the island, the mountainous terrain makes it difficult to get to all clients. The most likely culprit in Puerto Rico's case thought, was a bankrupt utility and an already weakened electric grid. The hurricane only exposed the years of neglected equipment, unmaintained right of way easements and old power generation plants [16].

1.2   Justification

Natural disasters, operator negligence, operator error, location, installation cost and other factors make delivering power to remote communities challenging. All these factors were observed in the electric power recovery efforts after hurricane María hit Puerto Rico in September 20, 2017. [15] Six months after the hurricane made landfall, 8.79% of all electric power customers in Puerto Rico had not been reconnected. [17] This created isolated distribution level customers in remote locations, where the town center may have had power but customers in the mountainous regions did not have power. The first challenge faced by a utility is the identification of these isolated customers. The next step would be to determine what challenges are present in the reconnection of these customers. This analysis might determine that reconnection is simply not viable, because of the cost and labor required, required time, unavailable supplies, etc. While all this is being considered, the customer is still without electric power. Due to the remoteness of

these locations, it is likely that power would once again be lost in the wake of a similar event and emergency precautions should be taken to reduce the impact.

It is important to note that a loss of electric power implies a loss of other critical infrastructure services, such as water, radio, telecommunications, food supply, shelters, emergency personnel, life support systems, etc. The water treatment facilities and pumping stations should not suffer much damage in an incident, man-made or natural, that was centered on the electrical system.

The focus of this work is not to reestablish electric power to an isolated community or customer, but to develop a methodology to strategically increase the energy availability for selected critical infrastructure to increase the resilience of a community using. The system is shown in Figure 5 Grid-tied microgrid configuration, a grid tied PV array with storage and an AC backup generator. The generator could be used to increase the amount of up time for the system and should the fuel supply be compromised; the PV array would take the full load and power the system for a smaller interval.
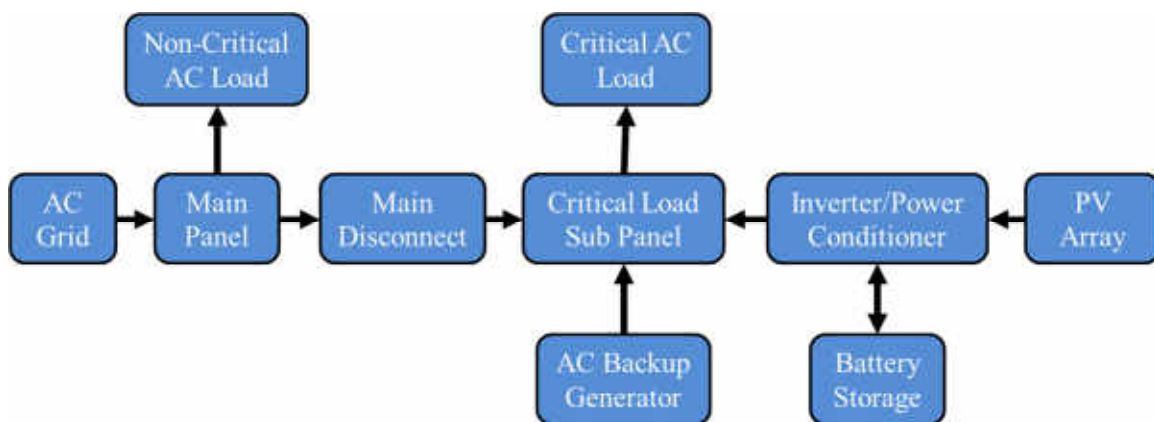
Figure 5 Grid-tied microgrid configuration.

1.3   Objective:

Develop a methodology to aid in the identification of electrically isolated communities and improve energy resource resilience using microgrids to power critical infrastructure.

1.3.1   Sub tasks:

+ Identify communities in Puerto Rico that did not have electricity for more than six months after the island-wide blackout caused by hurricane María. These communities could fall into the "last 10%" of the utility customers to be reconnected.

+ Identify water management resources, telecommunications, radio, hospitals, supermarkets, pharmacies or other loads deemed important during an emergency.

+ Select a test case and perform the complete methodology to serve as a guide for future researchers.

Chapter 2:   PREVIOIUS WORK

2.1   Nighttime satellite imagery

The use of nighttime satellite imagery to monitor power outages has been explored by NASA. They have performed extensive image processing to remove stray and reflected light sources and have managed to isolate the residential, industrial and streetlight sources. Their analysis demonstrated that: "41 percent of Puerto Rico's rural municipalities experienced prolonged periods of outage, compared to 29 percent of urban areas. When combined, power failures across Puerto Rico's rural communities accounted for 61 percent of the estimated cost of 3.9 billion customer-interruption hours, six months after Hurricane María. These regions are primarily rural in the mountainous interior of the island where residents were without power for over 120 days." [18] These results are not surprising and are great news in terms of the geographic areas this work will focus on, which will mostly be "end of the line" rural communities.

One of the most important aspects of this work is that the information obtained through the use of satellite imagery and compiled using the methods found in [19] and [20] is completely independent of the energy supplier. Blackout data for a region is dependent on the metering instrumentation put in place by a utility or microgrid operator. This data may not be present at the distribution level or may not be readily available to a researcher. Moreover, this data would not be able to accurately describe sub-circuit outages unless metering instruments were part of it, thus localized outages would not be recorded. "Satellite data of nighttime lights (NTL), can help meet this need. Unlike utility records, satellite-based measurements are collected onboard space-based platforms that can provide global and consistent coverage. Daily satellite overpasses enable repetitive measurements over time and space, and can survey, not only outages, but the speed of restoration, both within cities and in remote and isolated areas that may be difficult to reach." [20]

There is one disadvantage that arises in using this to gauge the recovery of power in an area; the light gathered is mostly street lighting or other night time outside illumination. As such rural and residential areas with low or no street lighting might not get accurately represented. An example the restoration estimates generated by NASA compared to the utility reports in Puerto Rico is shown in Figure 6.

An explanation offered by NASA for the discrepancy is daytime power availability that would fail during nighttime (brownouts). Another explanation is that because the method relies on street lighting, other loads would be powered first due to higher priority such as hospitals, fire stations, shelters etc. This second reason may explain why the discrepancy is higher towards the end of the study in stages 2 and 3. A possible explanation for the discrepancy in stage 1, where the Black Marble product is indicating there is more power than is being presented in the official reports is that the light being sensed during that time was a combination of available power, which was low, and consumer generators. The light pollution generated by individuals and industry powering their homes and businesses would have been picked up before any grid restoration, this coupled with the fact that the number of available generators did not increase due to a shortage of generator across the island.
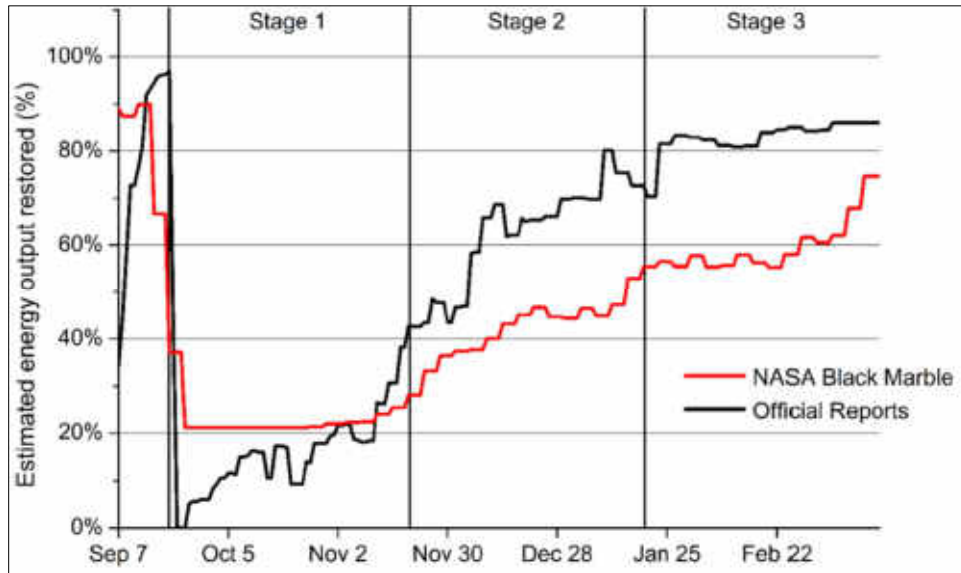
Figure 6 Comparison of estimated restored power per official reports and NASA Black Marble nighttime light based approach. [20]

As luck would have it the NASA Black Marble product was being validated in Puerto Rico 8 months prior to the hit of Hurricane María. This validation even included the deployment of known stable single point light sources. [20] This work helped determine that the nighttime imagery approach was sufficient to track power outages and recovery times. The data used in this work are three composite snapshots created from 195 days' worth of nighttime satellite images taken from September 20, 2017 to March 20, 2018.

2.2 Microgrids

Using distributed generation and microgrids to improve system resilience is not a new idea. The electric grid can benefit greatly from the use of microgrids, but their function should not only be limited to electric power. Microgrids should be thought of as potential energy hubs [21], where other critical infrastructure such as water, gas, and telecommunications are tied in with the grid. Their role in improving system resilience in radial distribution systems has also been studied [22]. This characteristic of microgrids in radial distribution systems is convenient, as many of the affected communities are most likely at the ends of feeders or are all clustered around a single feeder and will operate as islands during emergency situations. Inter-microgrid support has also been shown to be beneficial [23], therefore creating microgrids based on assets that may then in turn support each other is a valid way to cluster high priority loads.

2.3 Synthetic distribution system circuits

While it would be ideal to use real world feeder models of the selected areas, this may not be possible to do in many cases as this information is considered a matter of national security. There are additional difficulties when dealing with the electric grid in a post hurricane María Puerto Rico; many of the distribution level systems were destroyed and haphazardly reconnected; this is where the use of sample circuits is convenient. The National Renewable Energy Lab (NREL) has developed a way to create synthetic distribution system models that are more realistic than traditional IEEE test circuits. "The Synthetic Models for Advanced, Realistic Testing: Distribution Systems and Scenarios, or SMART-DS, offers high-quality, "realistic but not real" distribution network models and advanced tools to generate automated scenarios on those models… The networks are generated by the Reference Network Model developed by Universidad Pontificia Comillas and include high-, medium-, and low-voltage networks and geographical

12

constraints such as topography and street maps" [24] This tool allows the researcher to perform

most types of integration, control, automation and other emerging types of analysis and simulation.

Chapter 3:   METHODOLOGY

The proposed methodology workflow is summarized in Fig. 2. and can be divided into four major steps:

1. Loss of Service Area Identification
2. Number of Affected Customer Estimation
3. Infrastructure Identification
4. Microgrid Design

They can be divided into two categories: broad view event evaluation and local impact evaluation. Steps 1 and 2 are of the broad view type and Steps 3 and 4 are more localized. Steps 1 and 2 only require that a researcher selects a broad area, in this case Puerto Rico excluding the uninhabited island of Mona. Step 3 is a hybrid, where it can be computationally demanding if all the infrastructure for the broader area is desired. A much more convenient approach is to select a smaller region or regions of interest and continue with step 4.
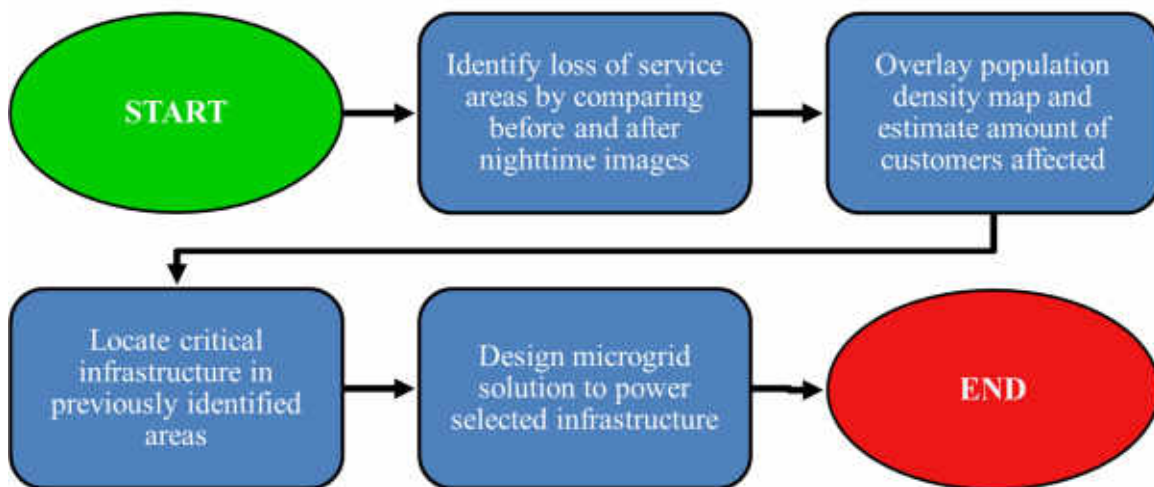
Figure 7 Methodology workflow of proposal.

3.1 Loss of Service Area Identification

The first and arguably most important group of data required for the execution of this methodology are the nighttime satellite imagery sets. These provide the basis for the time series that allows the researcher to evaluate the gradual recovery of power in the areas under evaluation. While there may be private sources for such data, in the interest of keeping with the free and open sources for data, a researcher may be able to get raw nightly data from the NASA/NOAA Suomi National Polar-orbiting Partnership (Suomi-NPP). This and other satellite imagery data can be obtained through the NASA World View App [25]. Another source for this type of nighttime imagery is the Visible Infrared Imager Radiometer Suite Day/Night Band (VIIRS DNB) Nighttime Lights Monthly Composites provided by Esri ArcGIS through their website [26]. It is important to note that the origin of this data is still the Suomi-NPP. The main difference is that data obtained from [26] is a composite created from a range of dates and has been processed to remove the effects of clouds, lighting, fires and other sources of visible light that are not desired.

Satellite images are not taken by a very large camera, nor are they a single image; this is a common misconception. Data is taken by the NPP satellite through an array of onboard sensors, the data used for this work is generated from the data provided by the onboard VIIRS. The satellite orbits the earth at 512 miles (824 kilometers) above the surface. It orbits the earth 14 times a day from pole to pole [27]. These 14 orbits are 1,900 mile wide swaths that are then stitched together into images [28] as can be seen in Figure 8 and Figure 9. Each North-South band corresponds to one orbit. There is some variation that is introduced when using composite images, as the satellite does not take a snapshot of the same area each time it performs a complete scan of the earth. This can be seen in the location of Puerto Rico (circled in red) on Figure 8 it lies on the eastern part of

15

the 4th band and lies roughly in the center of the 5th band on Figure 9. Gaps can also appear, such

as the gap between the 8th and 9th bands around the equator in Figure 9.
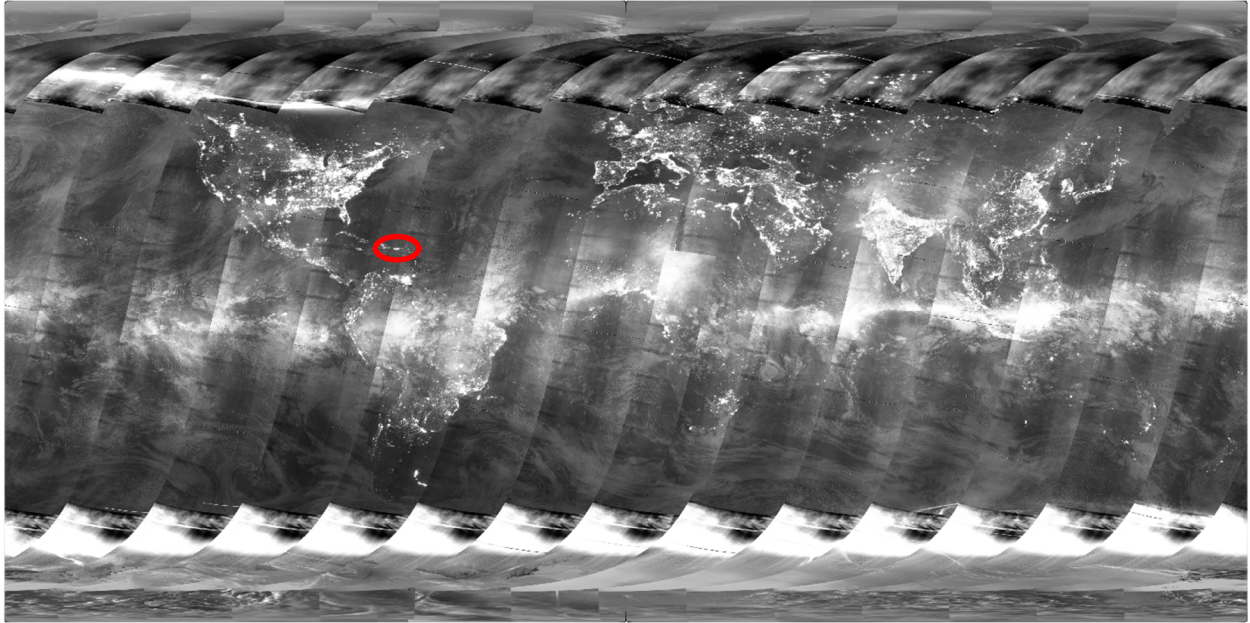
Figure 8 Nighttime VIIR Composite image. Puerto Rico circled in red. [25]
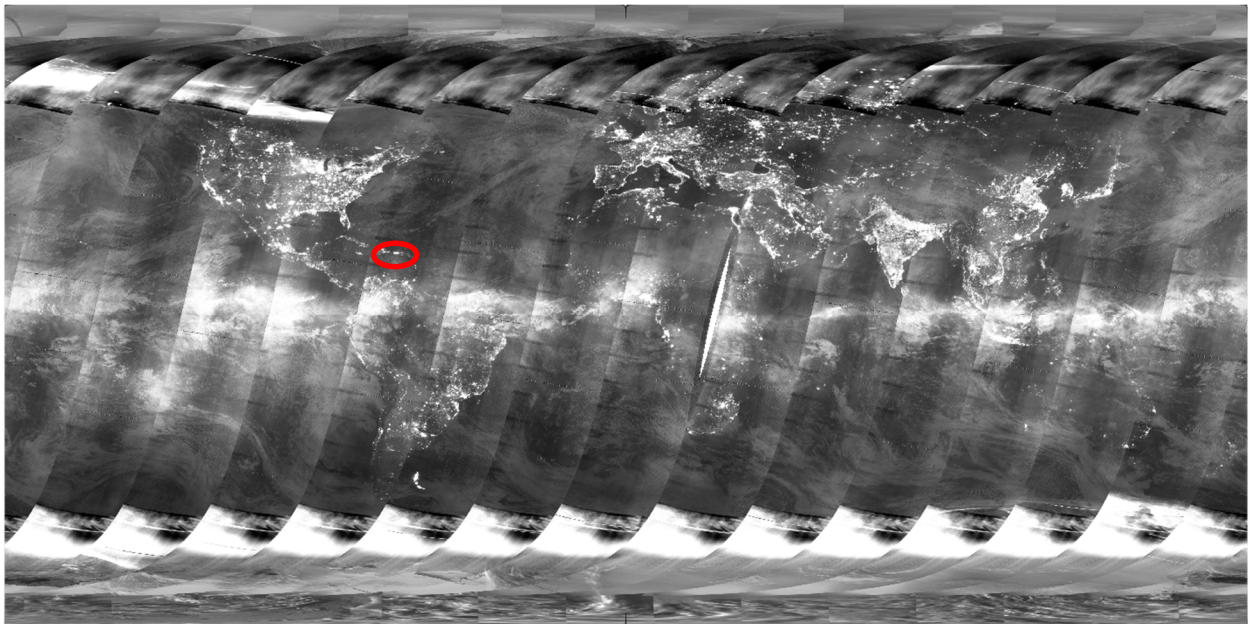
Figure 9 Nighttime VIIR composite image. Puerto Rico circled in red. [25]

16

As previously discussed, the use of satellite imagery can be used to track the power system and estimate the number of affected customers. For this work a four image sample from NASA's work was used to compare a pre hurricane baseline (Figure 10) and three stages: 1-2 months, 3-4 months, and 5-6 months after the hurricane. These images are composites taken over a time period and have been processed to remove bad data such as: cloudy nights, light sources from fire, lightning, and albedo; the methods and procedure behind the pre-processing of this data can be found in [20] [19]. The resolution of the images is 5760x3240 pixels and encompasses the whole island Puerto Rico, but excludes Mona, Desecheo, Vieques and Culebra.

Those that know the island and its people, specifically the population distribution may expect more light than the one presented in Figure 10. This is amplified if the reader compares Figure 35 to the light distribution in Figure 10. The lack of light in some of these expected areas may be explained by the resolution of the image, a close-up may provide more information than is currently presented as there may be sub-pixel features that were averaged out during the creation of the image. Another explanation is that most of the light that is being perceived by the satellite comes from street lighting. This type of lighting would be scarce or non-existent in the more rural areas of the area. This would be worsened by thick vegetation of the rural regions, characteristic of the Caribbean island. This, however, does not hinder the methodology as areas that do not show up in the baseline, would not show up in the recovery either and the work would focus on areas of known power availability before the hurricane.

17
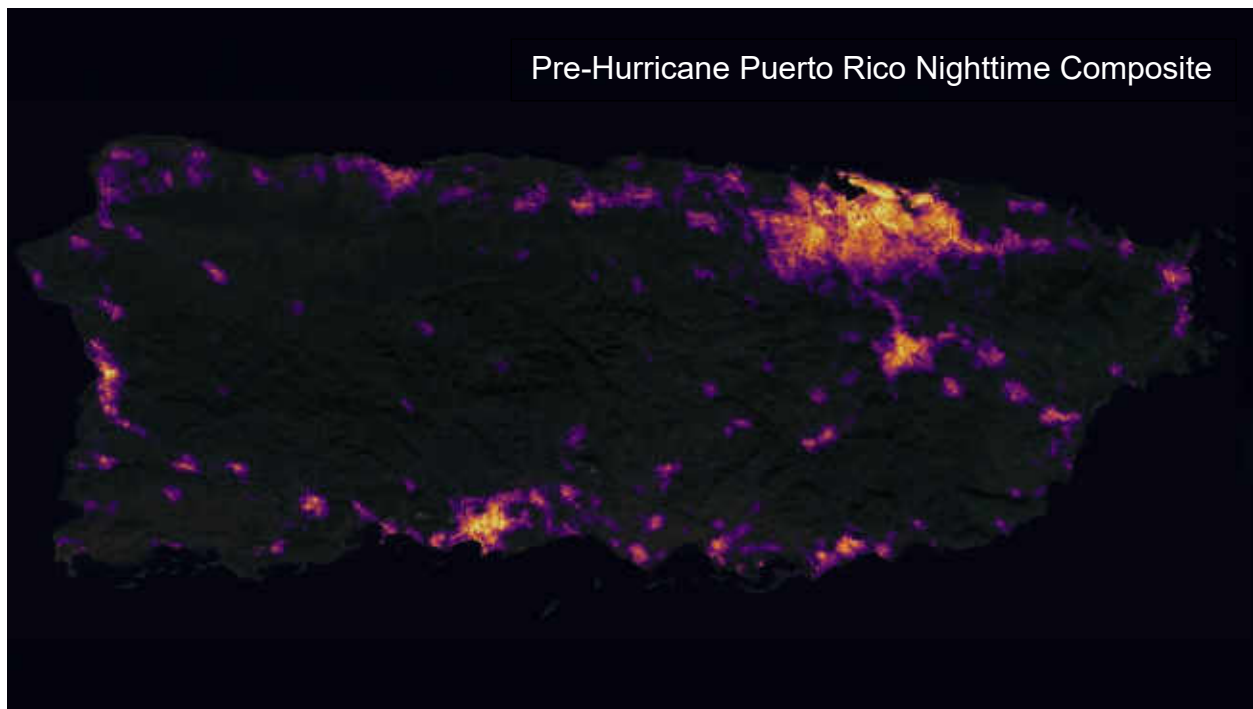
Figure 10 Baseline Image, Pre-Hurricane nighttime satellite imagery, colored areas indicate nighttime lights. [29]
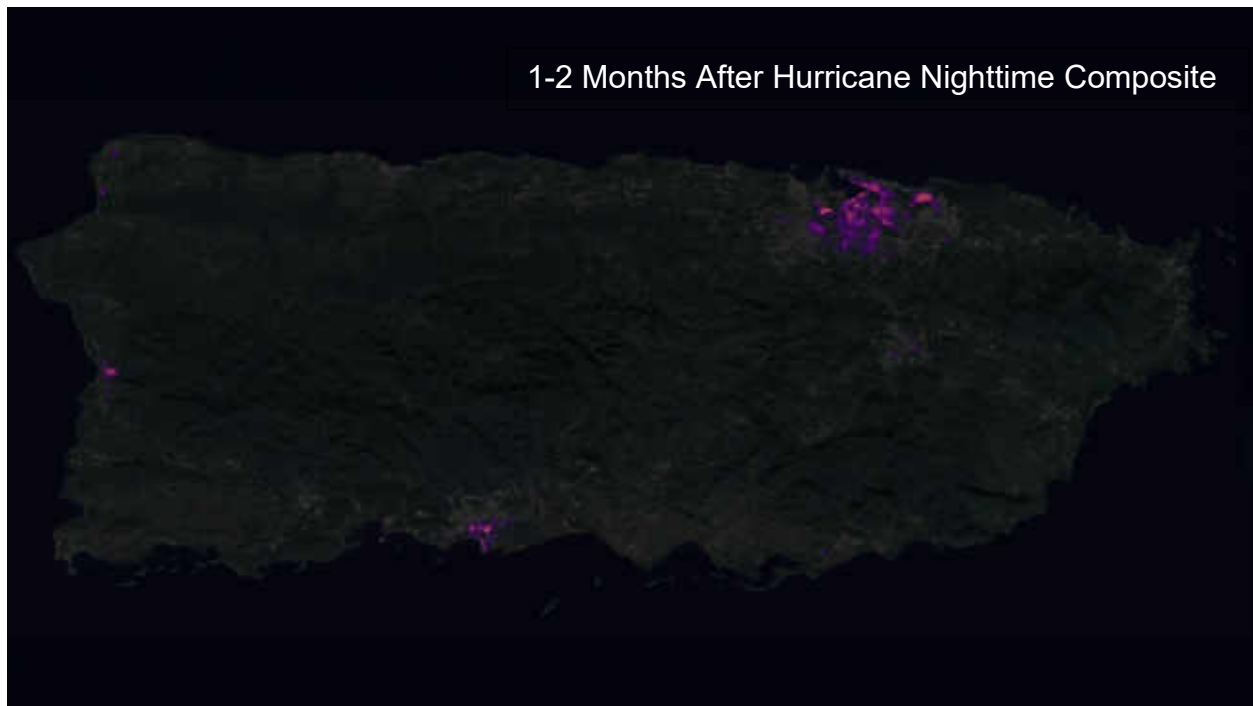
Figure 11 Stage 1 nighttime imagery 1-2 months after hurricane colored areas indicate nighttime lights. [29]

18
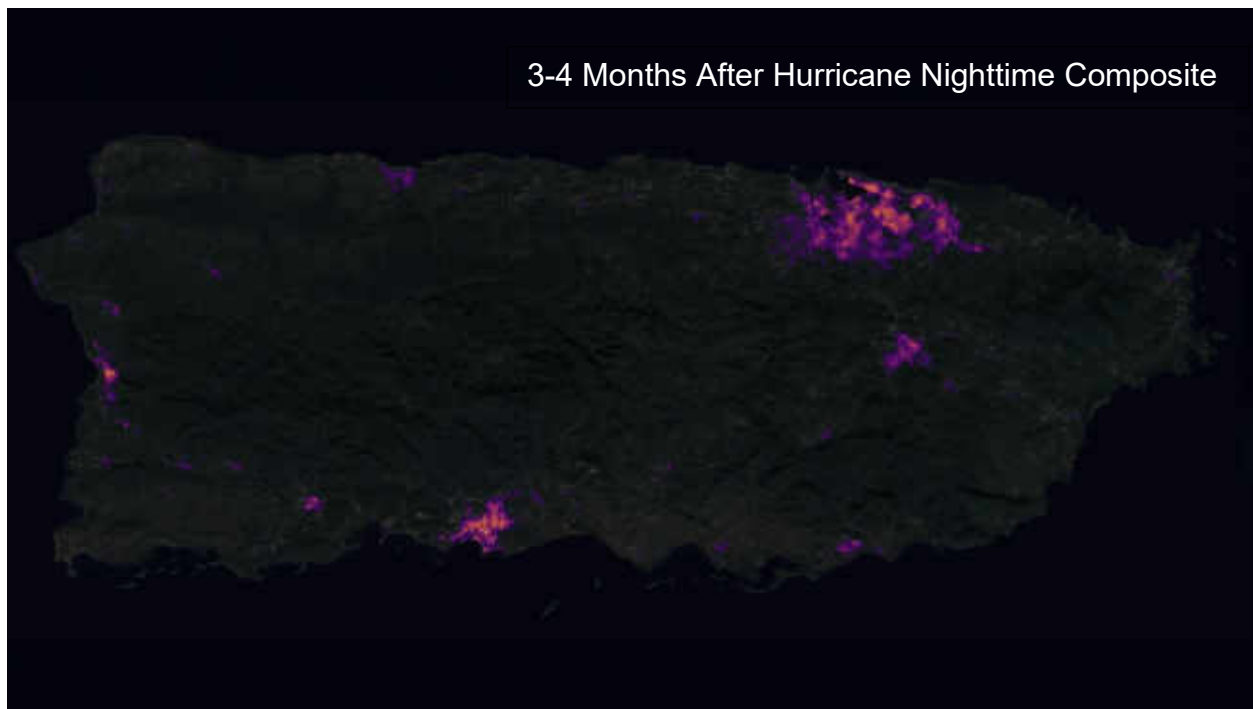
Figure 12 Stage 2 nighttime imagery 3-4 months after hurricane colored areas indicate nighttime lights. [29]
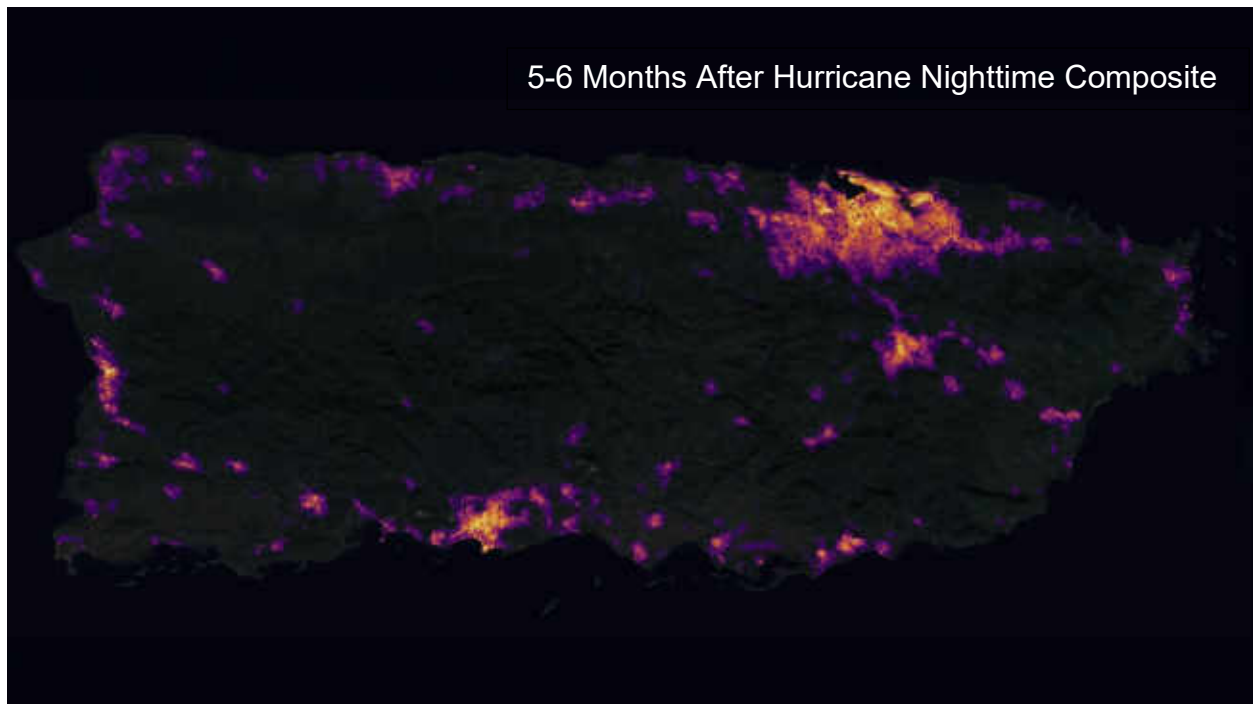
Figure 13 Stage 3 nighttime imagery 5-6 months after hurricane colored areas indicate nighttime lights. [29]

The python package scikit-image [30] was used throughout the image processing portion of this work. It was selected for the broad range of peer reviewed algorithms, it is also currently active with a history of regular updates, has very good documentation and many examples. Most scikit-image functions are based on NumPy [31] arrays, which means that standard array manipulation can be done to the function inputs and outputs. The processing done for this portion of the work was based off the RGB to HSV example found in [32].

This processing is based on the manipulation of the Red-Green-Blue (RGB) color space and the Hue-Saturation-Value (HSV) color space. The original image is imported as an M x N x 3 matrix where each of the color channels R-G-B has an M x N matrix assigned to it. Each pixel has a value assigned from 0 – 255 corresponding to the R-G-B value from the original image. The image is then converted to the HSV color space where it is again represented as an M x N x 3 matrix. As before, each channel has an assigned matrix, but each pixel now has a decimal float that ranges from 0 – 1 that corresponds to the H-S-V value. From this, the Values and Hue channel can be plotted individually as shown on the left side of Figure 14 and Figure 15 respectively.
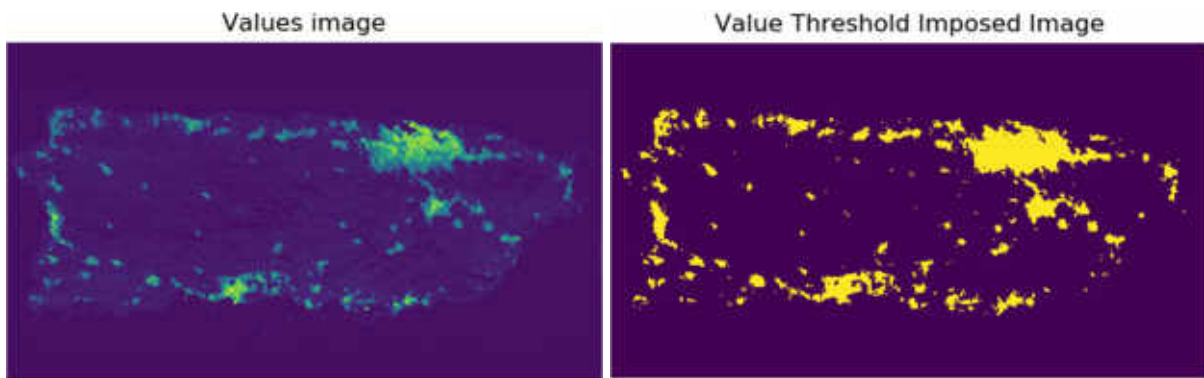
Figure 14 Values channel from HSV converted image (left) and result for imposed threshold (right).
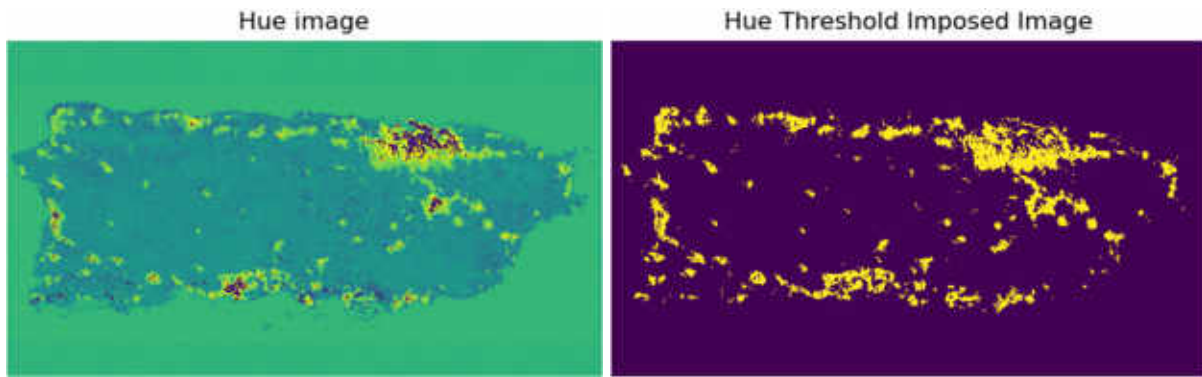
Figure 15 Hue channel from HSV converted image (left) and result for imposed threshold (right).

A binary image, one where all the selected pixels are either 0 or 1 on the selected H-S-V color channel, can be created by imposing a threshold value to separate the desired pixels from the background. A histogram, like that presented in Figure 16, becomes very useful when evaluating an appropriate threshold value. A good example of this is the Hue values histogram in Figure 16, there are two distinct regions: pixels with a hue of under 0.63 and pixels with a hue value of above 0.687. These two upper and lower values are used to create a band-pass filter, where all pixels that do not have a hue value within these two outer bounds are assigned a pixel value of 0 and all within the bounds are assigned a value of 1; the resulting image can be seen in the right part of Figure 15. A similar analysis is done using the values channel; a value threshold of 0.198 is selected. In this case a high pass filter is created; all pixels with values over 0.198 are assigned a 1 and all others a 0, the result of this can be seen in Figure 14. The hue and value binary matrices are re-combined into the HSV for the now processed image. The color space is then converted into a black and white image and exported as a mask for the next processing steps.

The masks can be seen in Figure 19 through Figure 22. If it was not clear from the original images, Figure 19 shows which areas showed up as lit under the night sky. This is not to say that there are no other electrified areas pre-hurricane. Rural areas with very little to no street lighting or artificial sources as well as single homes in remote areas with poor outside lighting would not show up in the nighttime imagery. For the purpose of this work, only the areas that appear lit were considered as these are the only areas that had confirmed power. The recovery of these lit areas can be observed by comparing each stage with the previous one.
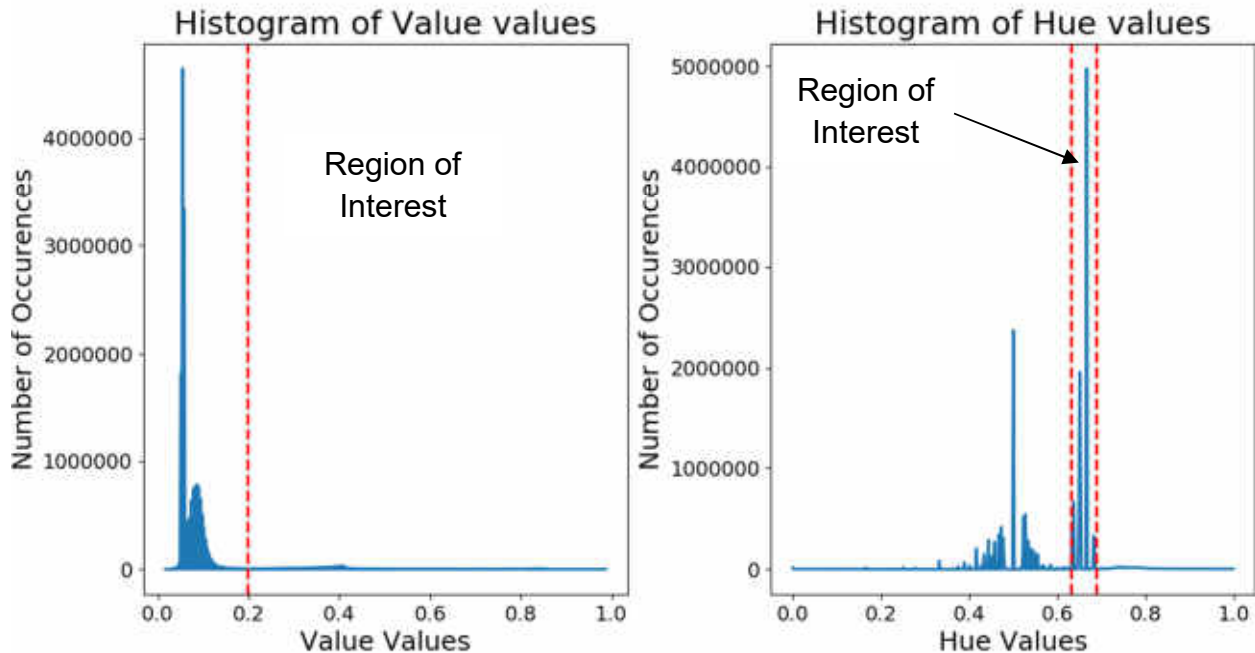
Figure 16 Histograms of the Hue (right) and Value (left) color spaces for pixels in the HSV converted Stage 3 image. Vertical axis is number of pixels, horizontal axis is the Hue or Value from 0 to 1 of each pixel.

The filter boundaries described above, can have some leeway into the undesired areas. For the case of the band-pass filter a value of 7% over the upper bound (which equates to 0.735) and 7% under the lower bound (0.586) can be applied. The high-pass filter had a much higher leeway due to how the pixel values were distributed. This one allowed a 34% lower value (0.13) than the one selected as the threshold for the filter. The desired areas are shown in green; the leeway areas are shown in yellow and the avoid at all cost areas are shown in red in
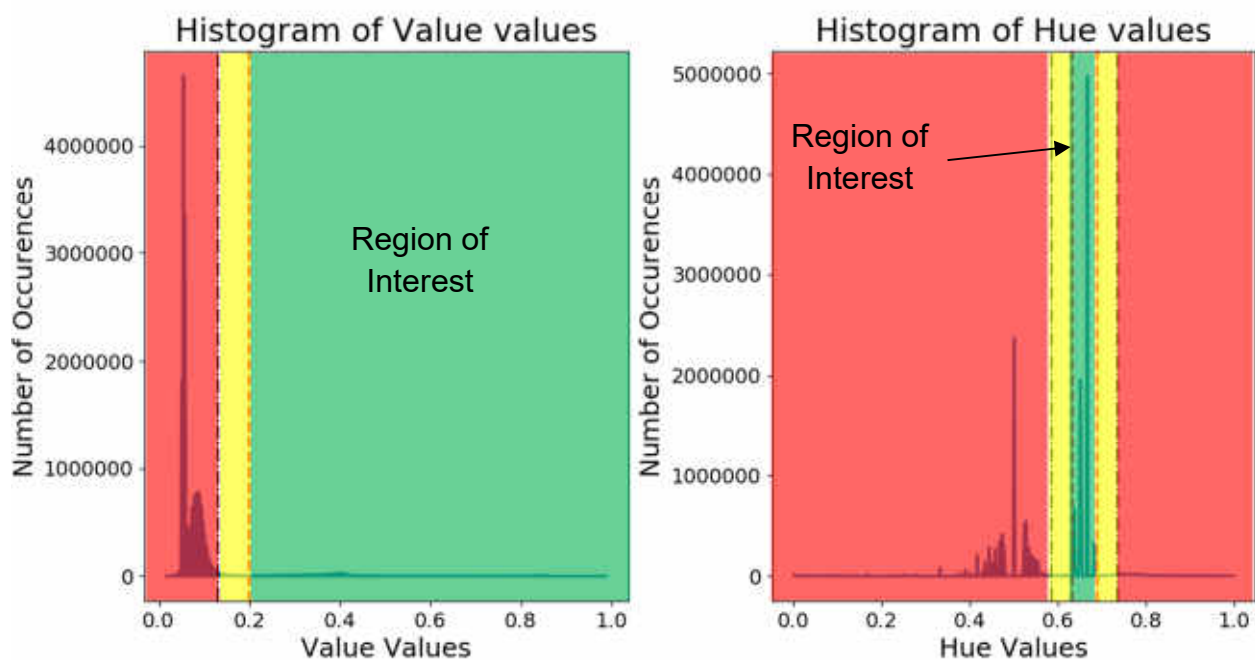
Figure 17 Color coded leeway areas for image processing steps. Green is desired, yellow is leeway area, and red is avoid at all costs
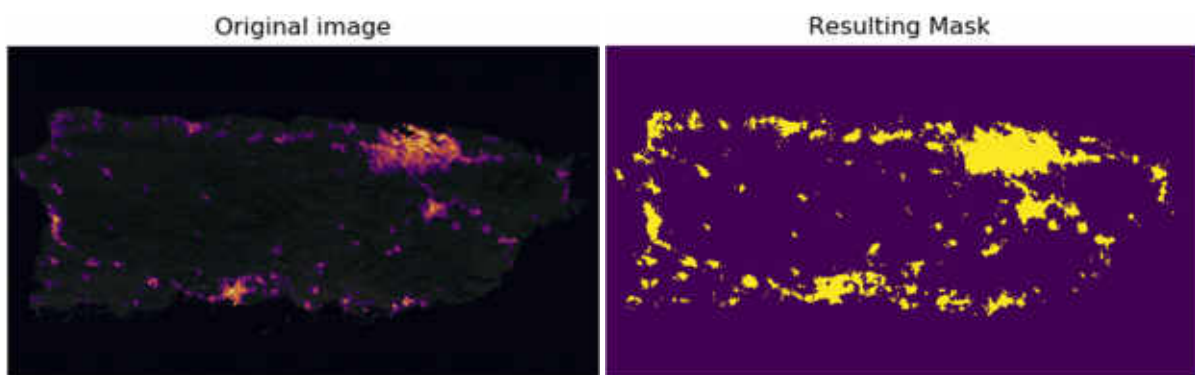
Figure 18 Original RGB image (left) and resulting HSV threshold-imposed mask (right).

Baseline Nighttime Lights Mask
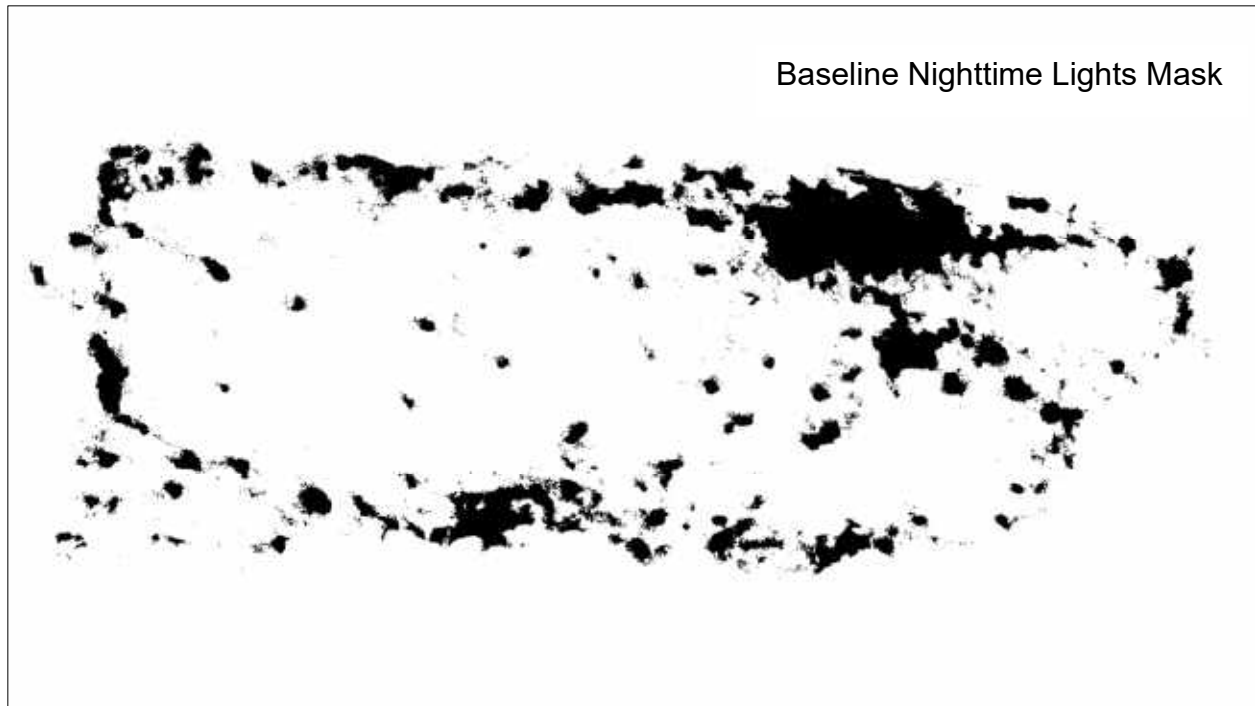
Figure 19 Binary mask of Baseline image, dark areas indicate location of nighttime lights.

1-2 Months after Hurricane Nighttime Lights Mask
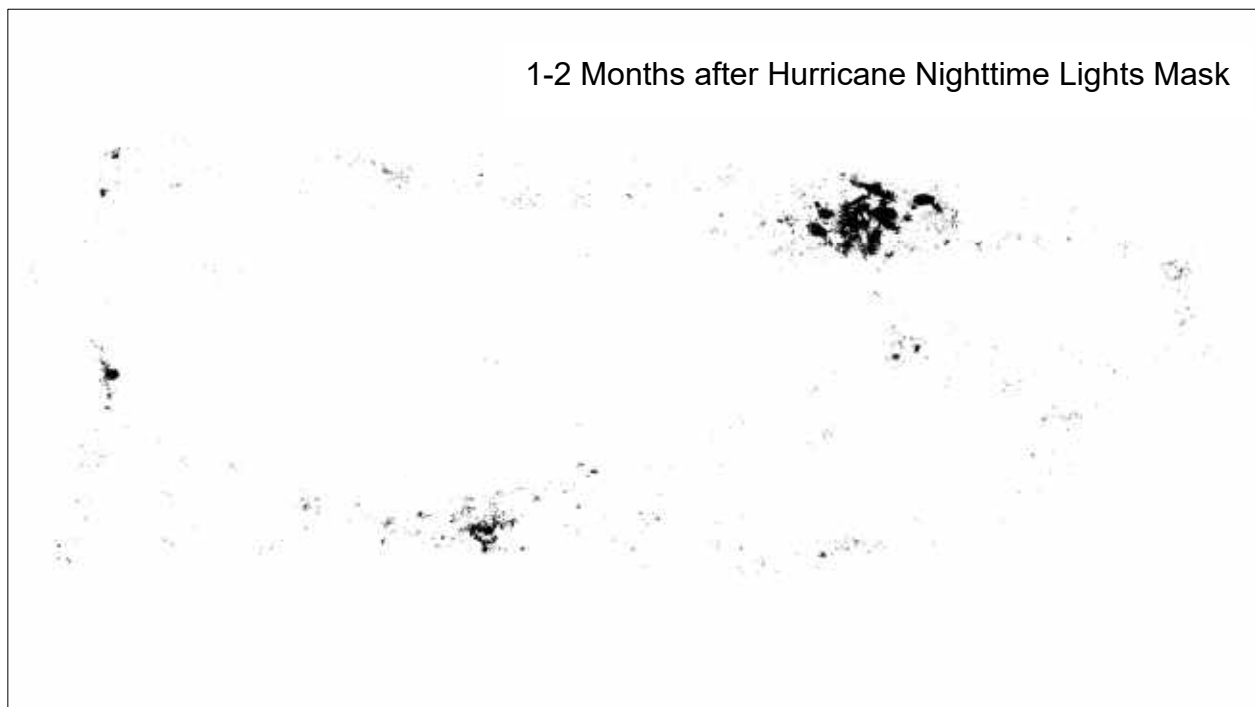
Figure 20 Binary mask of Stage 1 image, dark areas indicate location of nighttime lights.

3-4 Months after Hurricane Nighttime Lights Mask
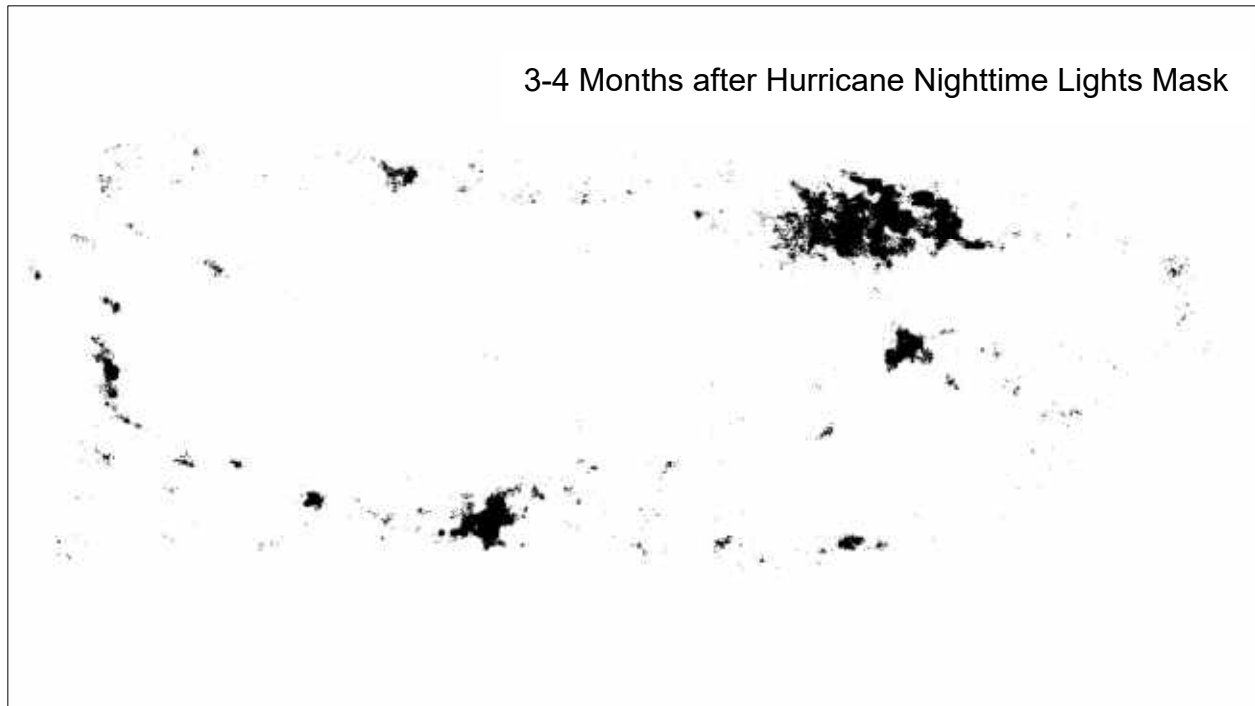
Figure 21 Binary mask of Stage 2 image, dark areas indicate location of nighttime lights.

5-6 Months after Hurricane Nighttime Lights Mask
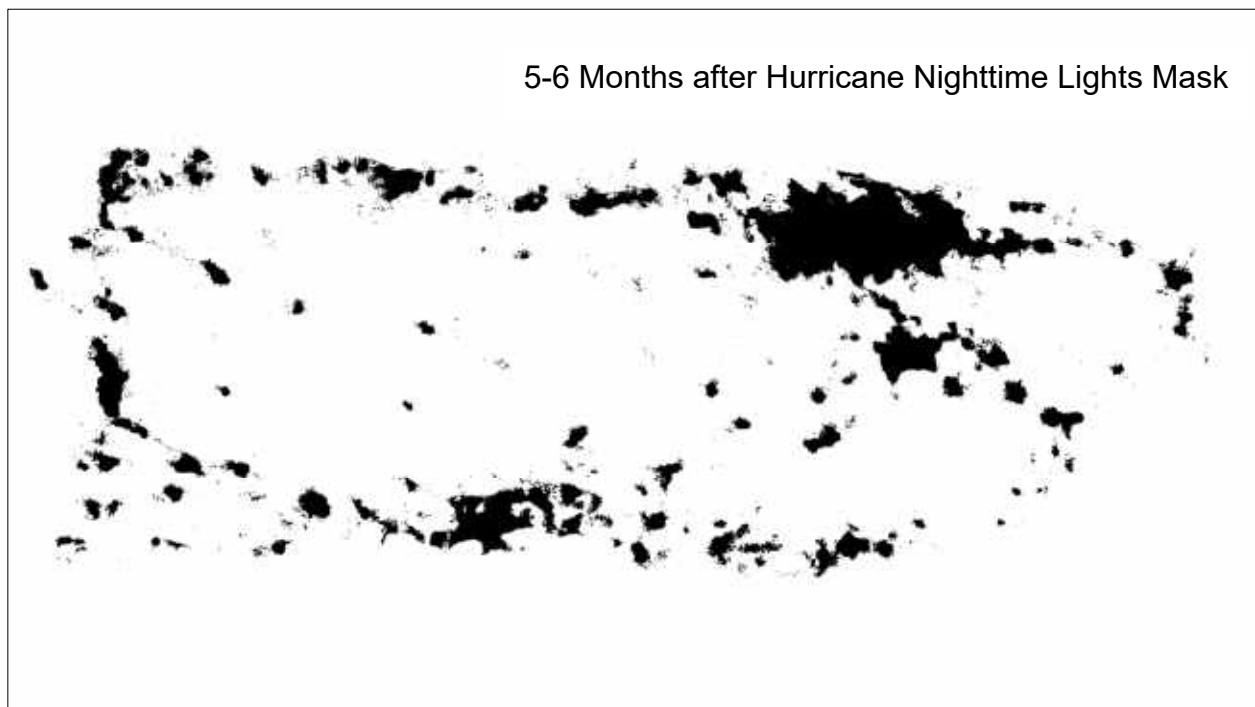
Figure 22 Binary mask of Stage 3 image, dark areas indicate location of nighttime lights.

The masks created in the previous step only show the amount of light for the current time step. A comparison between the baseline, Figure 10, and all the other stages is necessary to calculate which areas did not have power.. The general process for this is to compare pixel by pixel and assign a value of zero for any pixels that have a non-zero value for the baseline and the stage being processed. A simplification of this is to say that the stage area being processed is subtracted from the area in the baseline mask, the resulting image is the representation of the areas that did not have power from the hurricane up to the time being evaluated as shown below:

$$Blackout\ Area = Baseline\ Area - Stage\ N\ Area \qquad (1)$$

Figure 23,Figure 24, and Figure 25 show the final desired result of the image processing. It is important to note the change in meaning from the highlighted areas in each of these images. All highlighted areas now show areas that were **<u>WITHOUT</u>** power. Now the stage 1, 1-2 months after the hurricane, a large highlighted area meaning that most places were under blackout conditions for this time period. There is a reduction in this highlighted area as one moves on through the stages. The most telling picture is Figure 25, the highlighted areas seem to form borders around areas. Some of these areas are rings of blackout areas surrounding places that had been powered previously. One could deduce that power was reestablished to the centers of populated areas and the bordering population had not been given the same priority.
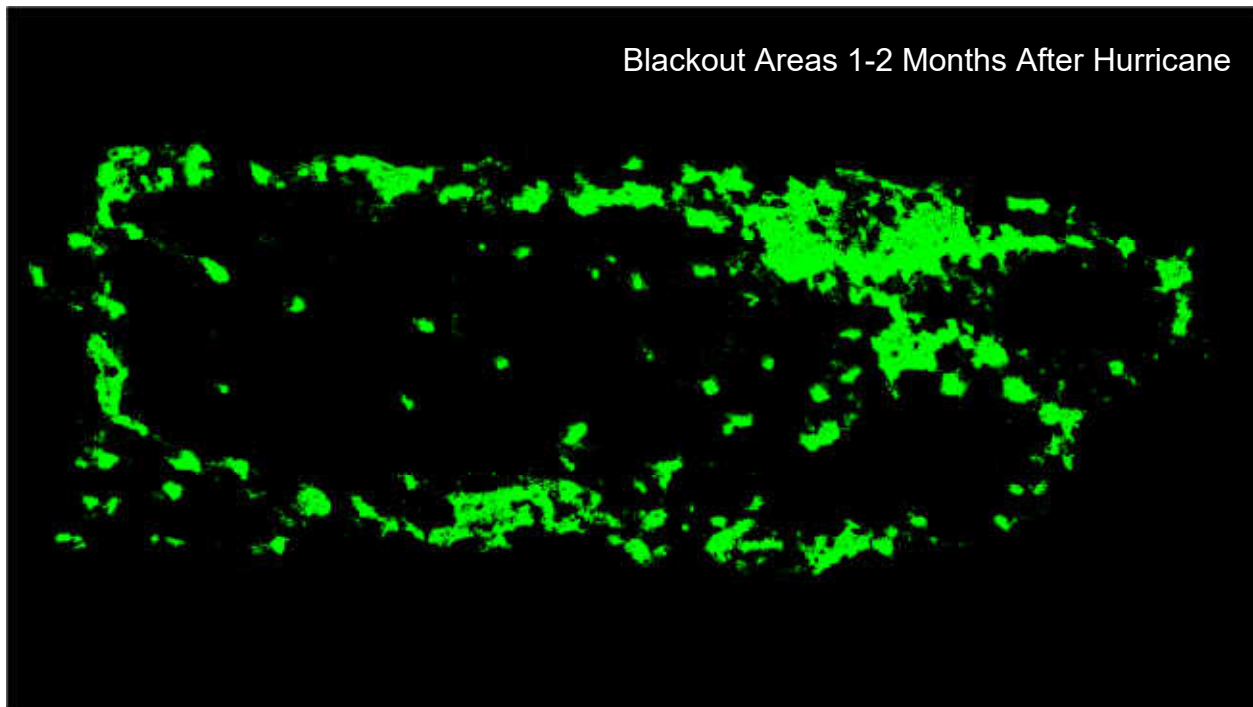
Figure 23 Result of Baseline minus Stage 1, green areas indicate areas without power 1-2 months after hurricane hit.
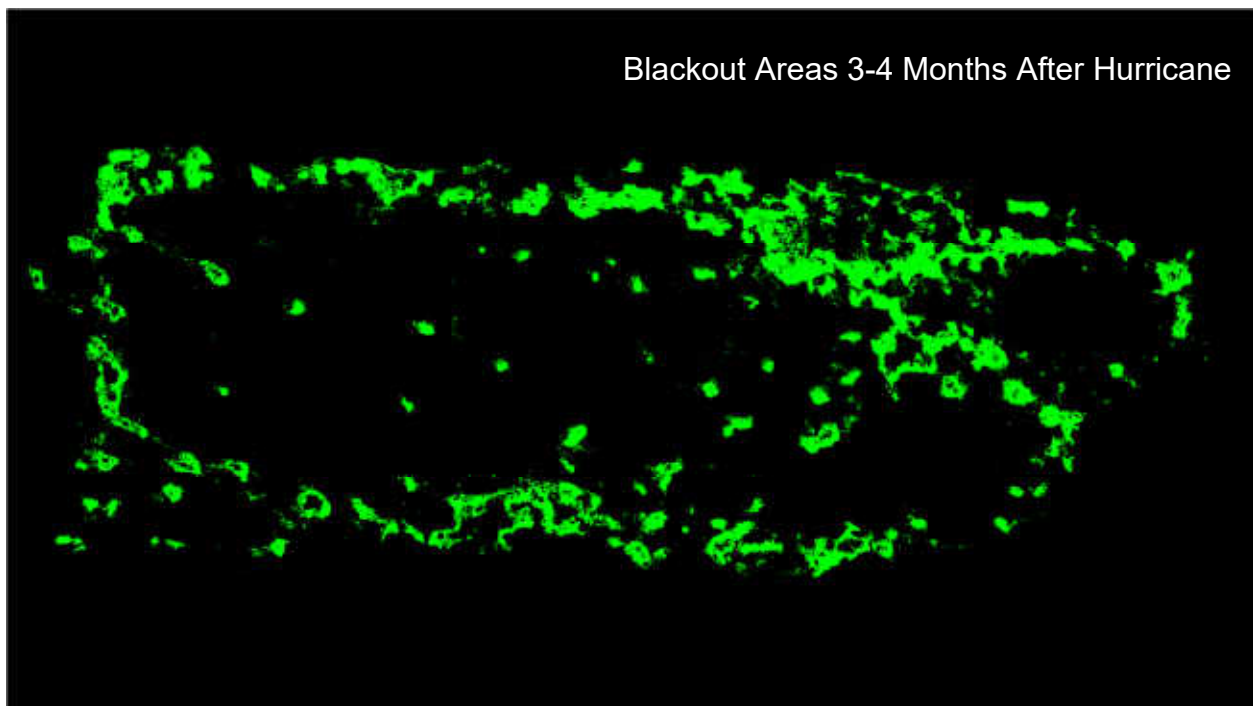
Figure 24 Result of Baseline minus Stage 2, green areas indicate areas without power 3-4 months after hurricane hit.

Blackout Areas 5-6 Months After Hurricane
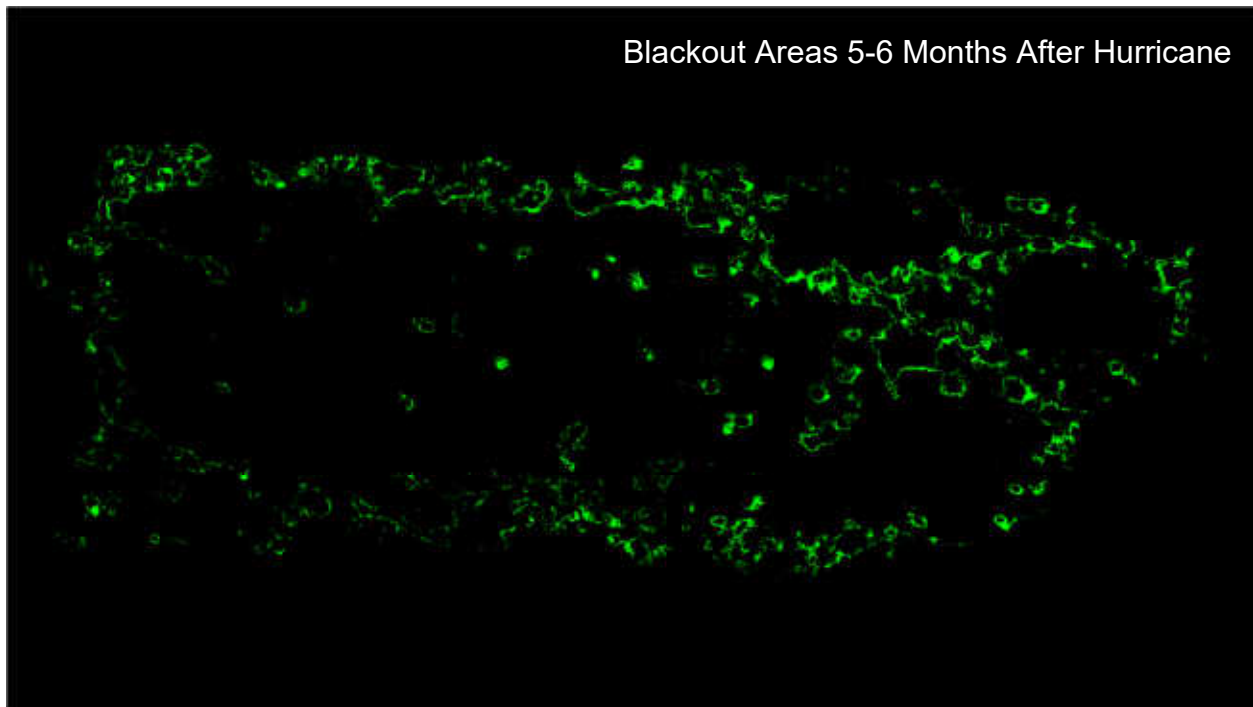
Figure 25 Result of Baseline minus Stage 3, green areas indicate areas without power 5-6 months after hurricane hit.

The images can now be described as highlighted areas on a blank canvas. The human eye can intuitively differentiate and trace the borders of these areas, this is not necessarily the case for computers. This is where the *"find_contours"* function in scikit-image becomes very helpful. This function will find the borders of all the features in an image, this includes outside and inside features. The images at this point of the workflow are binary and the algorithm has no problem finding the contours of the features, as the intensity change from background to highlighted feature is quite sharp. These contours are then saved for the next step in the processing, projecting them onto a map.

The images exist as 5760 pixels wide and 3240 pixels high with no geotagging. They offer one advantage, all the masks and the original images are all the same size and are all centered in the same way, such that if the geotagging was obtained for one, it would apply to all remaining images. Images obtained from [25] can be geotagged by the researcher at the moment of extraction and do not require this step. The use of GeoTiff images is particularly useful at this point and would allow skipping the next step, pixel to lat-lon conversion. The conversion from pixels to latitude longitude requires that the researcher pick a pixel with known coordinates or with the best approximation possible. The images can be mapped using a modified Mercator projection, where equations (2) to (4) are directly the appropriate equations for Mercator conversion from longitude to an X-Y grid, but equations (6) to (8) are used for latitude conversion based off the longitude conversion. Equations (5) and (9) are valid for images of locations in the western hemisphere and north of the equator and exist to accurately reflect the origin for conversion. The normal conversion for pixel (0,0) in an image is the upper left corner, while the origin for this conversion needs to be the lower right corner.

The use of the longitude equations requires a λ_0 that is greater than all the possible longitudes to be mapped; all other longitudes will be mapped off this coordinate. For an image with a single known, or approximately known, coordinate, the radius R_l would most likely be unknown. This value can be calculated by picking a pixel and a λ_0, the value obtained using equation (2) can then be used in equation (4) to calculate the longitude for all remaining pixels in the contours. This can be done by picking a feature in the image and a pixel in the feature to go along with it and then finding the coordinates for that spot in the feature using a known reference map such as Google Earth. The pixel x position in the image is transformed to an equivalent cartesian X using equation (5) before substituting into equation (2) to get the initial R_l required for the rest of the pixel remapping. In this work a λ_0 of -65.538913° was selected, with pixel (319,2618) mapped to coordinate (-67.183825° ,17.931478°) and from this an R_l of 189521.5891979 pixels was calculated using an image width of 5760 pixels the summary is located in Table 1. The equations are nothing more than arc length derivations of a circle from a reference angle λ_0, to a desired angle λ. This then means that the value X is the distance, in this case pixels, from that reference angle. The reference angle could be selected as 0, which would be equivalent to mapping all distances to the prime meridian. The factor of $\frac{\pi}{180}$ is just the degrees to radians conversion factor as the arc length equation is only valid for angles in radians. The radius R_l is the equivalent radius of the earth at that longitude. This, of course is an approximation, as the earth is not a sphere and does not have the same radius at the poles and the equator. Therefore, this equivalent radius is equal for all longitudes at the latitude from which the original feature was selected for conversion. Small deviations, less than 1 degree north or south from this point are acceptable, greater deviations require that a new R_l is computed. Equations can be found in [33]

30

For longitude transformation:

$$R_l = \frac{180 * X}{\pi * (\lambda - \lambda_0)} \tag{2}$$

$$X = \frac{R_l * \pi * (\lambda - \lambda_0)}{180} \tag{3}$$

$$\lambda = \lambda_0 + \frac{X * 180}{\pi * R_l} \tag{4}$$

$$X = pixel\ position - image\ width \tag{5}$$

In a similar fashion as the longitude transformation, a known pixel is selected, the same pixel used for the longitude transformation. A φ_0 is selected to be closer to the equator than any point to be mapped, an R_p is calculated using equation (6) and the remaining pixel latitude assignments are done using equation (8). For this work a φ_0 of 17.7565° , with image height of 3240 pixels and reference pixel (319,2618) mapped to (-67.183825° ,17.931478°),which gives an R_p of 203671.174988 pixels. The equations used are based on the longitude transformation equations and are also just arc length derivations, but unlike the previous transformations special care must be taken to ensure that an adequate φ_0 is selected. The φ_0 must be closer to the equator but only far enough to just be outside of the image being converted, it cannot be 0 as in the longitude conversion case. As stated in the previous section, only small deviations are allowed when converting the latitude due to the oblate spheroid shape of the earth and how the latitude and longitude system is placed over it. By moving north or south of the selected latitude, the radius of the earth changes. The radius is largest at the equator and progressively smaller as one moves closer to the poles. The clear example of this is the difference in percent difference for the longitudes vs the latitudes. The latitudes' percent differences are, in general, an order of magnitude larger than the longitudes' percent difference shown in Table 2

31

For latitude transformation:

$$R_p = \frac{180 * Y}{\pi * (\varphi - \varphi_0)} \tag{6}$$

$$Y = \frac{R_p * \pi * (\varphi - \varphi_0)}{180} \tag{7}$$

$$\varphi = \varphi_0 + \frac{Y * 180}{\pi * R_p} \tag{8}$$

$$Y = image\ height - pixel\ position \tag{9}$$

The percent difference calculations for latitude and longitude found in Table 2 were done using equation (10) shown below:

$$Percent\ Difference = 100 * \frac{|Approximation - Calculated|}{\left|\frac{Approximation + Calculated}{2}\right|} \tag{10}$$

Table 1 Summary of the geotagging parameters used

Geotagging Parameters	
Image height	3240 pixels
Image width	5760 pixels
Reference pixel	(-319,2618)
Mapping of reference pixel	(-67.183825° ,17.931478°)
λ_0	-65.538913°
φ_0	17.7565°
R_l	189521.589198 pixels
R_p	203671.174988 pixels

32

Table 2 Reference Pixels for Geotagging and Error Calculations

	Exact coordinate on Image		Approximation Selected on Map		As Calculated Based off Pixel 1		Percent Difference Between Map Approximation and Calculation	
	Pixel X Coord	**Pixel Y Coord**	**Lat. (deg.)**	**Lon. (deg.)**	**Lat. (deg.)**	**Lon. (deg.)**	**Percent Diff. Lat.**	**Percent Diff Lon.**
Pixel 1	319	2618	17.931478	-67.183825	17.931478	-67.183825	0.0000%	0.0000%
Pixel 2	2959	2606	17.937946	-66.385597	17.934854	-66.385706	0.0172%	0.0002%
Pixel 3	5493	1031	18.387951	-65.618640	18.377925	-65.619632	0.0545%	0.0015%
Pixel 4	5558	1642	18.212323	-65.599709	18.206042	-65.599981	0.0345%	0.0004%
Pixel 5	3333	708	18.479016	-66.269744	18.468790	-66.272639	0.0554%	0.0044%
Pixel 6	47	1108	18.365191	-67.268694	18.356264	-67.266055	0.0486%	0.0039%

A visual aid to the explanation of the geotagging process is located in Figure 26 and Figure 27. A very distinct feature on the south-western shore of the island in the municipality of Cabo Rojo is selected. A pushpin is placed using Google Earth, the coordinates can be seen in the white square in Figure 26, then the closest corresponding pixel is selected from the image that is to be geotagged; Figure 27. This process is then repeated five more times, with features going around the perimeter of the island, the summary of the pixel and lat-lon coordinates can be found in Table 2 above and a Google Earth overlay in Figure 28. The inland features where avoided as it was harder to determine unique features.

Pixel 1 was selected as the reference pixel for convenience, as it was the easiest feature to differentiate in the dark background of the baseline nighttime images. The comparison of the selected locations and how they were re-mapped using the pixel to lat-lon equations (equations (2) through (9)) can be seen in Figure 29. The yellow pushpins are the original locations, white pushpins are the calculated ones. It can be observed that the distortion and percent difference increase as the latitudes increase towards the poles.

Figure 26 Zoomed in Google Earth screen capture of approximate location of Pixel 1.
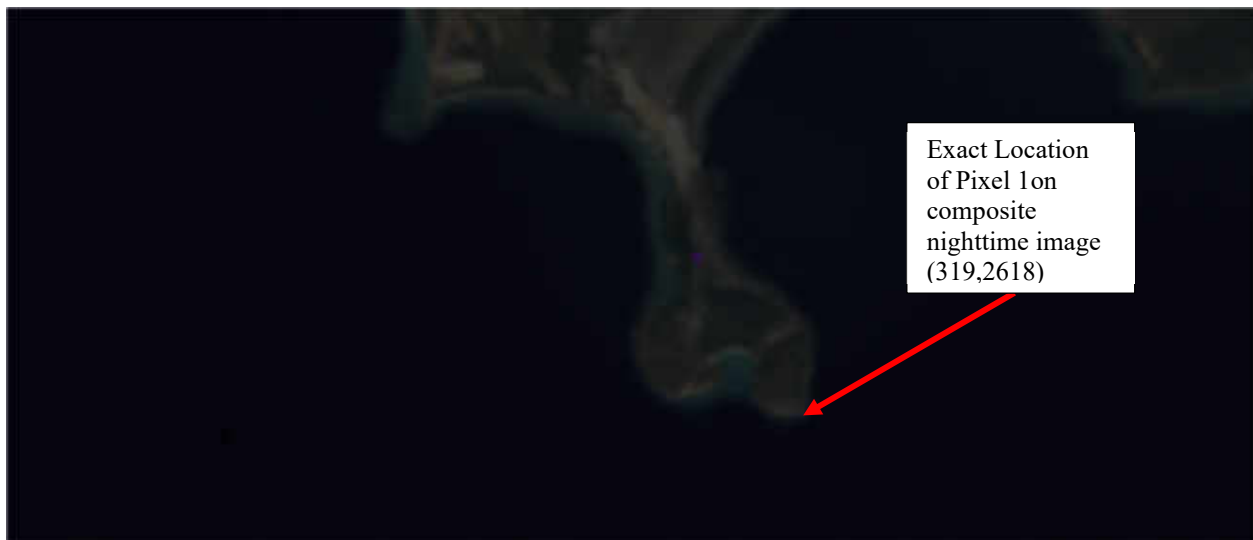
Figure 27 Zoomed in screen capture of exact location of Pixel 1 on baseline nighttime image.

Figure 28 Approximated locations of the six reference pixels.

Figure 29 Approximated pixel locations (yellow pushpins), calculated locations of pixels based off pixel 1 (white pushpins).

The equations used in the latitude section are loosely based on the Mercator projection idea of a cylindrical projection and should not be used in maps encompassing large areas. Proper conversion efforts or sectionalizing of the image should be made for areas larger than the one portrayed in this work. Although it should be reiterated, properly geotagged images would completely forgo the pixel to latitude longitude conversion shown here.

The generated contours have now been saved and converted to latitude longitude coordinates from the X-Y pixel grid and are ready to be mapped onto Google Earth. Google Earth (GE) maps features using the keyhole markup language (KML) [34], these features can be as simple as single placemarks, line paths, polygons, image overlays and even create 3D features. This file format is not unlike html in structure and files are easily created as text using the language structures. The rest of the work from this point forward is done with the creation, edition, and manipulation of KML files. The purpose behind the contour find and latitude longitude conversion for the images is to import the processing results into GE. The KML format specifies that only contours are necessary for the plotting of polygons; the inner areas are filled automatically with any desired color and opacity expressed in an opacity-RGB format (#ffffffff). A python script was created to insert the latitude longitude contour coordinates into a KML script. The result can be seen in Figure 30 through Figure 32, the green polygons represent the blackout areas for the specific time range. Figure 32 shows the mapping was successful and helps validate the theory put forward, that power was restored in the urban centers and the surrounding areas were left in the dark for longer.
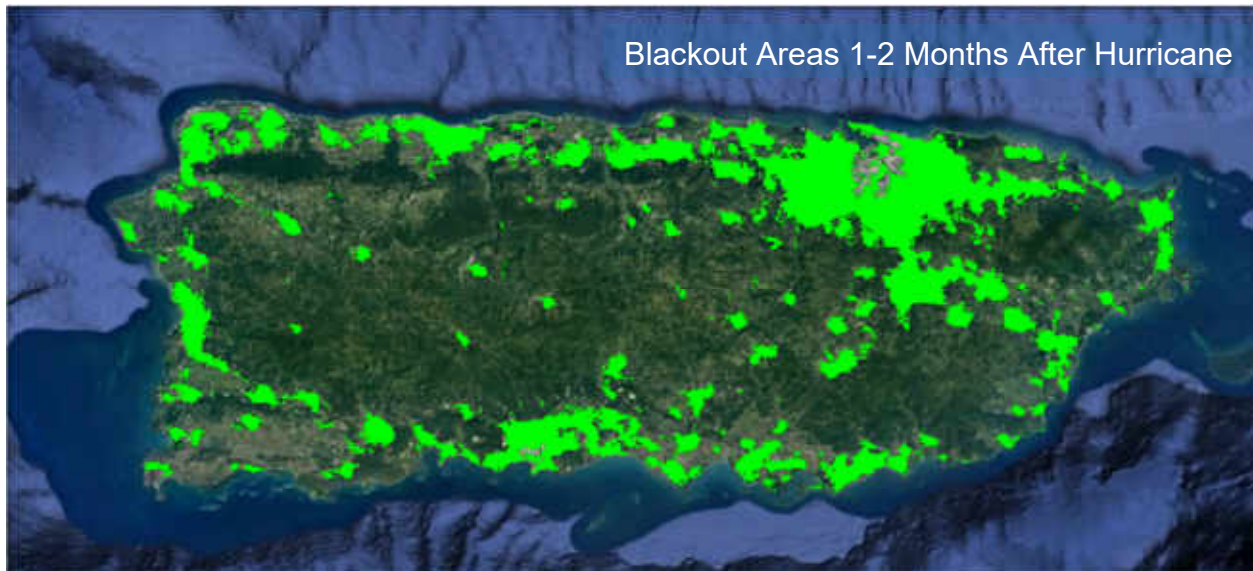
Figure 30 Blackout areas in Stage 1, Google Earth overlay. Bright green polygons indicate areas that do not have power in stage 1 but had power when compared to the baseline image.
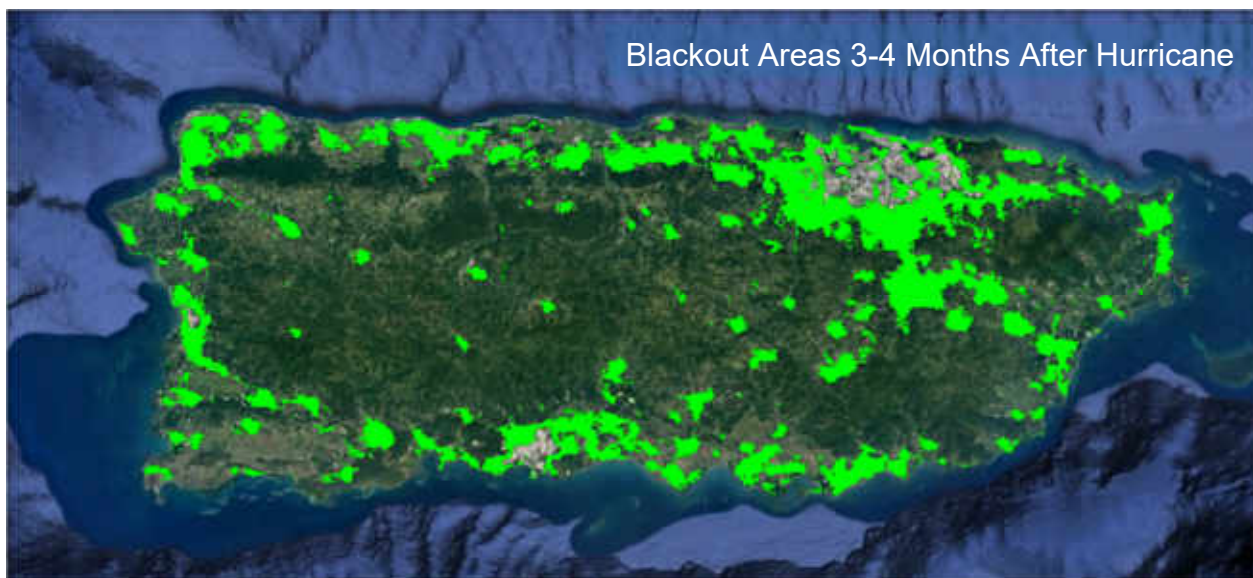
Figure 31 Blackout areas in Stage 2, Google Earth Overlay. Bright green polygons indicate areas that do not have power in stage 2 but had power when compared to the baseline image.
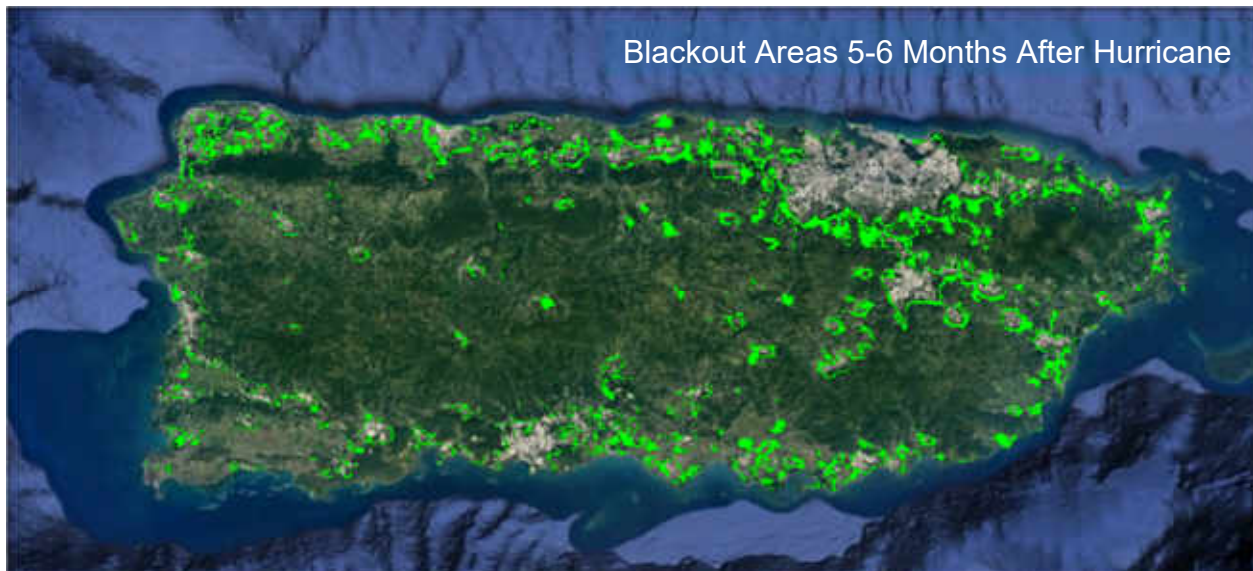
Figure 32 Blackout areas in Stage 3, Google Earth Overlay. Bright green polygons indicate areas that do not have power in stage 3 but had power when compared to the baseline image.

3.2   Number of Affected Customer Estimation

The blackout areas have been ascertained and plotted into GE; this opens up the possibility to have this information now interact with other types of data that can be plotted in GE. One such type of data is population data obtained from the United States Census Bureau [1]. The information can be downloaded as several data types, the one used here is the shapefile, which is an "Esri vector data storage format for storing the location, shape, and attributes of geographic features." [35]. While this file format is an Esri proprietary format, it is convenient to use because GE will import and convert to KML without and data loss or corruption. This information comes in three group levels: State, County, County Sub-Division. An example of the County and County Sub-Division can be seen in Figure 33 and Figure 34 respectively. The County Sub-Division data sets were selected for use, this is due to the relative size of the blackout polygons and the sub-divisions. The county divisions are too large and information resolution would be lost as information is lumped together. For example, the total population of a county may just be

concentrated in one urban center, but only the county subdivision would provide enough information to locate where in the county the population is grouped. This is also critical when calculating average population density. A large county with evenly distributed population would have the same average density as a large county where the population is concentrated in one place. Using the sub-divisions does not completely solve this problem, but it allows average population density calculations that resemble reality more closely.
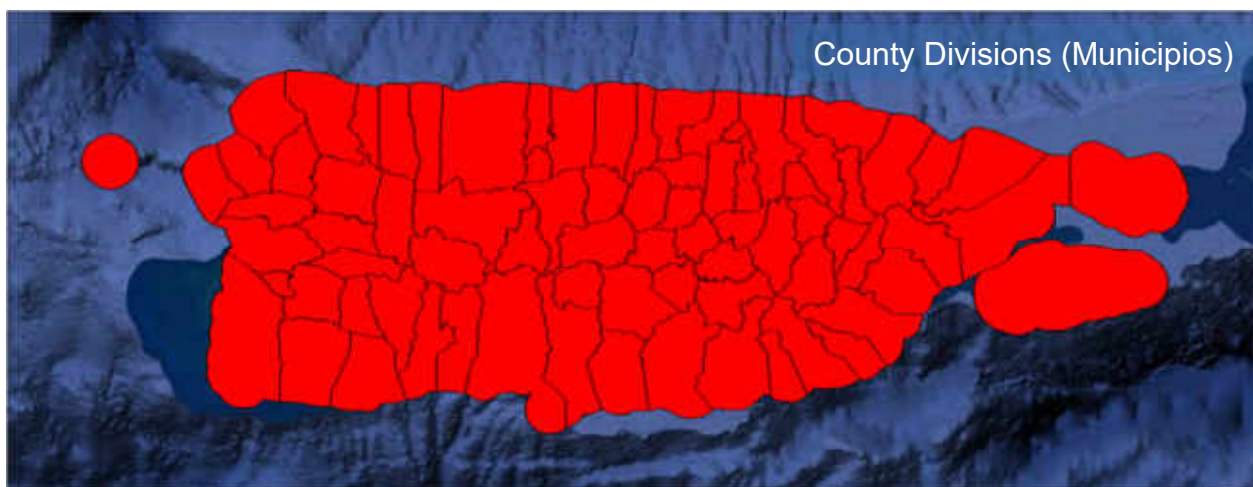
Figure 33 County division shapefile. Includes all 78 "*municipios*" in Puerto Rico. [1]
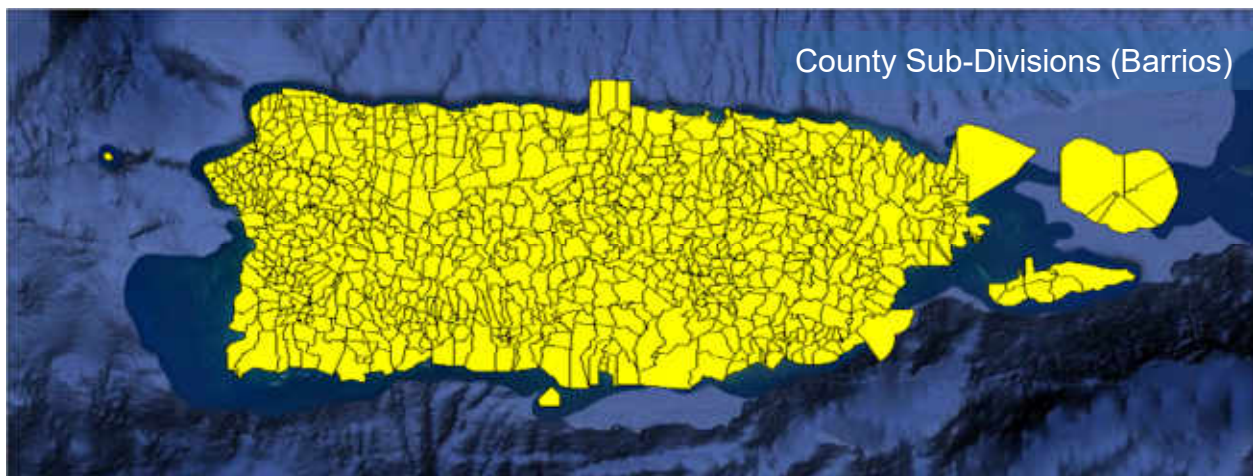
Figure 34 County Sub-Division shapefile. Includes all 902 "*barrios*" in Puerto Rico. [1]

The census shapefile maintains all the information and formatting of the .shp file generated by ArcGIS when imported into Google Earth and converted into a .KML file. Part of the information provided for each polygon includes total population, total land area and total water area. These two areas are provided in m^2. The total population is also subdivided into categories such as age, sex, employment, etc. these factors could also be plotted easily. The desired parameter, population density, is not included in the shape file. It is then calculated and incorporated in the new .KML file. Although area is provided in m^2, it is more convenient to calculate population density in people/km^2. It should be noted that the 1,000,000 factor in equation (12) is just the conversion from m^2 to km^2. The calculation, a simple one, is as follows:

$$Total\ Area = Land\ Area + Water\ Area\ (m^2) \tag{11}$$

$$Population\ Density = \frac{Total\ Population * 1,000,000}{Total\ Area} \left(People/_{km^2} \right) \tag{12}$$
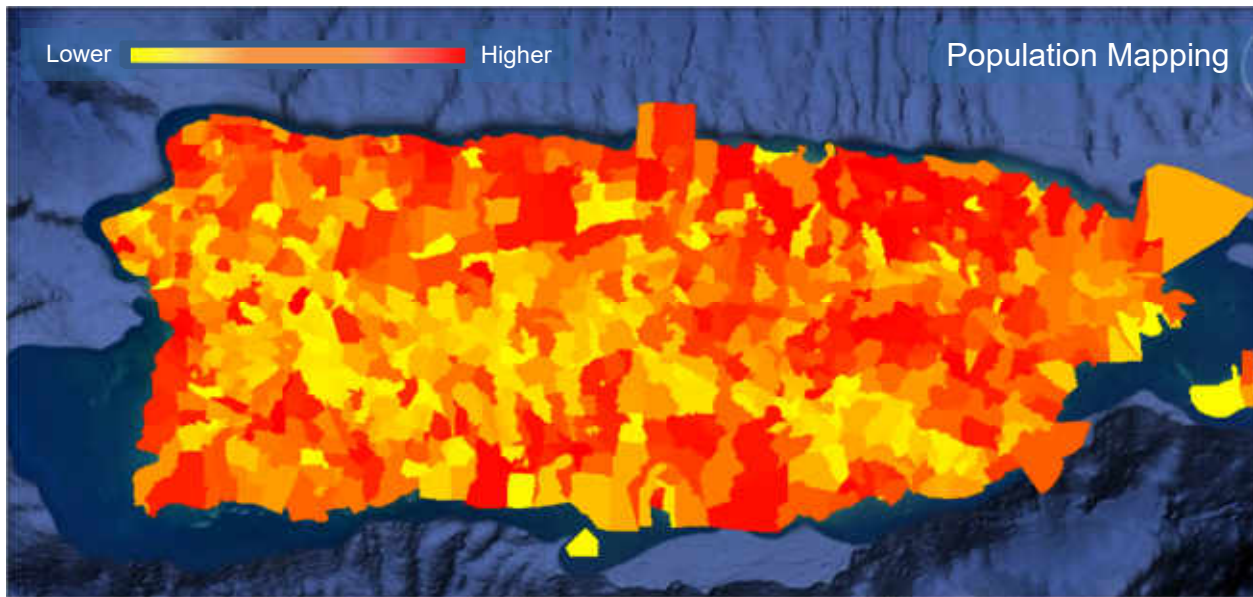
Figure 35 Population Color Mapped County Sub-Divisions. Color map: yellow (lowest) to red (highest).
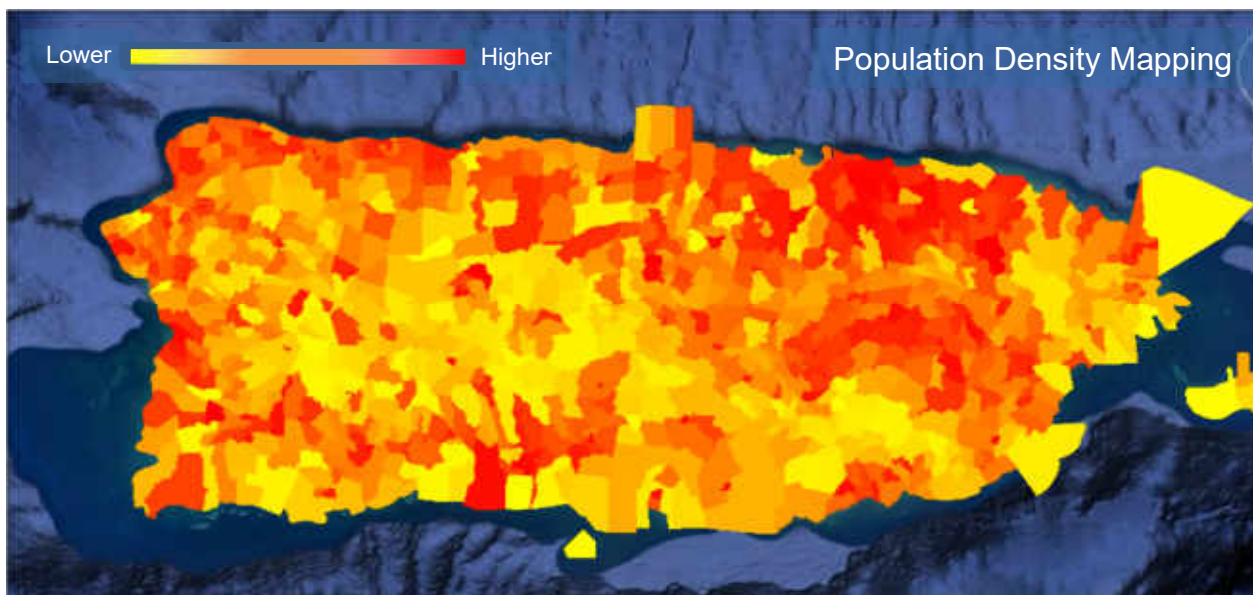
Figure 36 Population Density Color Mapped County Sub-Divisions. Color map: yellow (lowest) to red (highest).

Having all the data in KML files is very convenient, but these only serve to plot, all processing must be done with python scripts that read and write to KML files. The goal of this part of the workflow is to estimate the amount of people in the affected blackout areas. The first idea that comes to mind is to overlay the blackout areas and match how much of each intersects with the sub-division polygons and then multiply the area of the intersection with the population density value and obtain the estimate number of people in the affected area. As with the contour finding, this is something that a human can do intuitively while a computer cannot. This is where the python package Shapely [36] becomes very useful. This package allows for the creation, and manipulation of planar geometry, as long as all the objects under evaluation are in the same coordinate plane. All the polygons under evaluation are in the same coordinate plane, latitude longitude, but it is inconvenient to calculate area in this coordinate system and the current density population data is in people/km^2 therefore a conversion to meters would useful. The best way would be to represent each of the features on the Universal Transverse Mercator coordinate system (UTM), as the fundamental units of this system are already meters and has lower distortion of projected features than other map projection systems. This was not done because the area under evaluation (the whole island of Puerto Rico) was divided into two different UTM zones, instead, a traditional Mercator projection was used. The equations used in the conversion are shown below. The main difference from this conversion process and the previous pixel to latitude conversion is the use of a known radius for earth. The radius of the earth is latitude dependent. The latitude selected for this work was 18.2350°N, the corresponding radius of earth at this location is 6376059m, the calculation for this can be done using [37]. The λ_0 can be any arbitrary longitude if it is between the most eastward point on the map and the prime meridian; -65.0° was

selected. It is important to note that equations (13) through (16) are written for coordinates in radians; the conversion factors for degrees to radians were omitted for simplicity.

Turn latitude and longitude into X-Y meter coordinates

$$X = R * (\lambda - \lambda_0) \tag{13}$$

$$Y = R * ln\left[\tan\left(\frac{\pi}{4} + \frac{\varphi}{2}\right)\right] \tag{14}$$

To turn X-Y meter coordinates back into latitude longitude:

$$\lambda = \lambda_0 + \frac{X}{R} \tag{15}$$

$$\varphi = 2 * \tan^{-1}\left[exp\left(\frac{Y}{R}\right)\right] - \frac{\pi}{2} \tag{16}$$

Equations (13) through (16) are the true Mercator projection equations and can be found in [38]. The reader need not worry themselves with their derivation, only their usage; they have been around since 1569! On their usage, equation (13) can use any unit of length since the radius of earth R will determine the units of the distance X, as mentioned, λ_0 can be any longitude from zero up to the first interaction with the map. A reference latitude is not needed as in the previous set of transformations. The range of values for latitude are [90,-90] in degrees and for longitude they are [-180,180].

The method by which the intersection areas are found and calculated are nothing if not simple. While the evaluation of many polygons quickly becomes time consuming, it is straightforward and is as follows: the intersection of a single blackout polygon and each of the county sub-division polygons is individually evaluated, if the intersection, equation (17), is non zero (True) the area of intersection and resulting polygon are stored in a new list. This is done for each blackout polygon and for all the sub-divisions each time. The reason for this is to consider the possibility of one blackout polygon falling into more than one sub-division; blackout areas do not care about arbitrary political boundaries. Consider the worst case for this work, with 904 county sub-divisions and around 22,000 single blackout area polygons, there are close to 20 million intersection evaluations done. Again, the shapely package becomes extremely important. The package employs functions *object.intersects(other)"* and *"object.intersection(other)."* The first function determines whether the intersection is non-zero and if non-zero, the second function calculates de area and coordinates for the intersection.

$$Blackout\ Polygon\ Area = Blackout\ Polygon \cap County\ Sub.Polygon \qquad (17)$$

$$Pop.for\ Blackout\ Polygon = \ Blackout\ Polygon\ Area * Pop.Density \qquad (18)$$

The population estimation per blackout area is done using the recently generated intersection area and multiplying by the average population density from the particular county sub-division from which the intersection was created, equation (18). These new intersection areas are then sorted by amount of people estimated to be within that area; an example of the sorting can be seen in Figure 38, the whole result can be seen in Figure 37. The reader may notice that the result in Figure 37 has significantly less features than the mask in Figure 25, this is because prior to sorting, all polygons that are estimated to contain 5 people or less were discarded from the list

44

prior to plotting. The reasoning behind this is, "more bang for your buck;" eliminating clusters as small as this allows the rest of the processing and filtering to focus on higher priority locations.
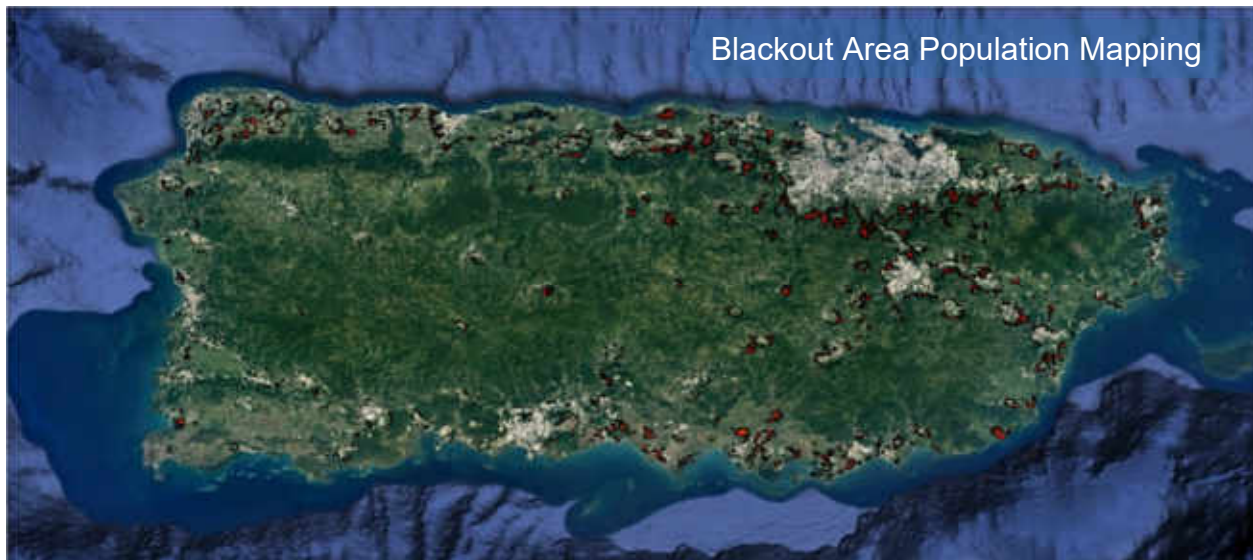
Figure 37 Final Result, all groups of blackout areas with population data.
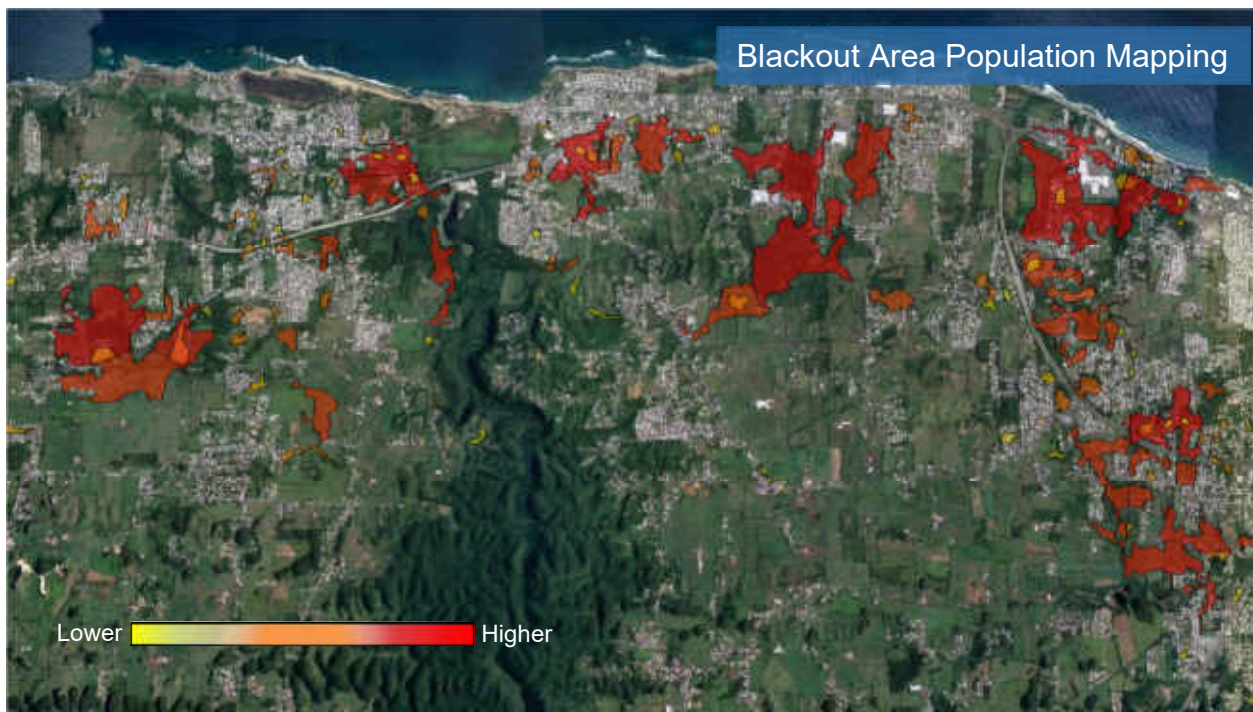
Figure 38 Close up of all groups of blackout areas with population data. Color map: yellow (lower number of people) to red (higher number of people).
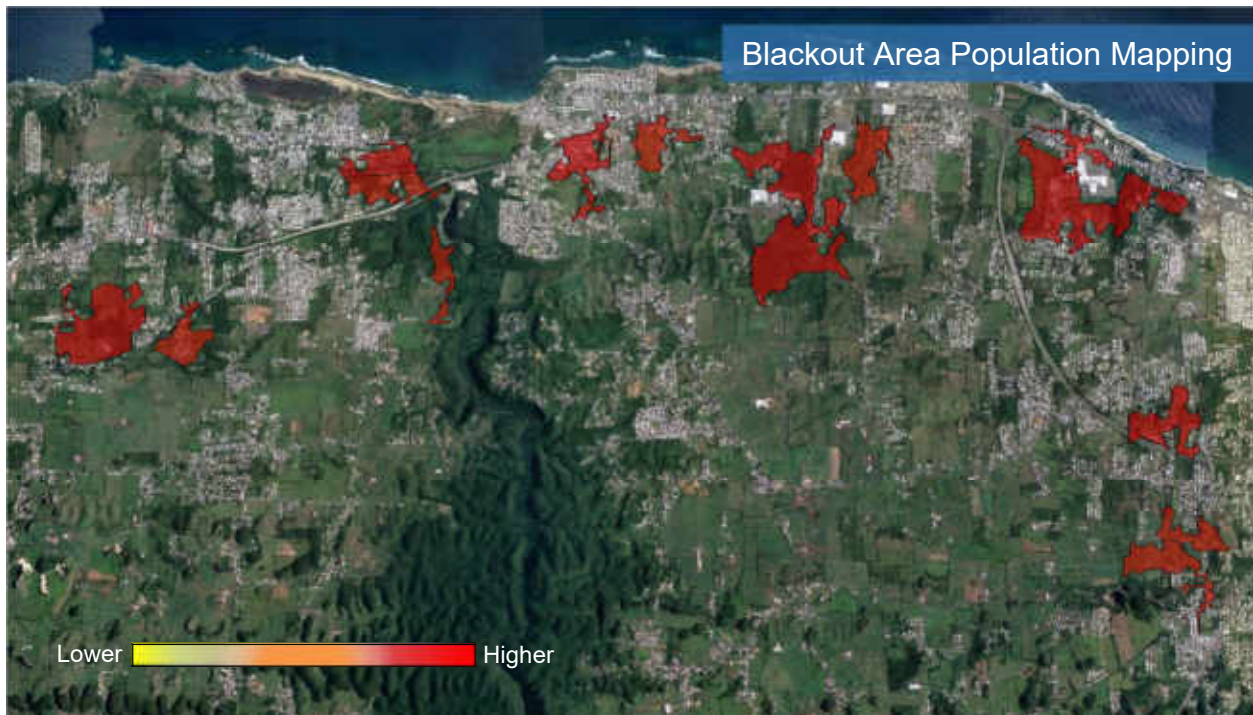
Figure 39 Closeup of blackout areas ranked by population, only a sample including the top 10% most populated areas are shown.
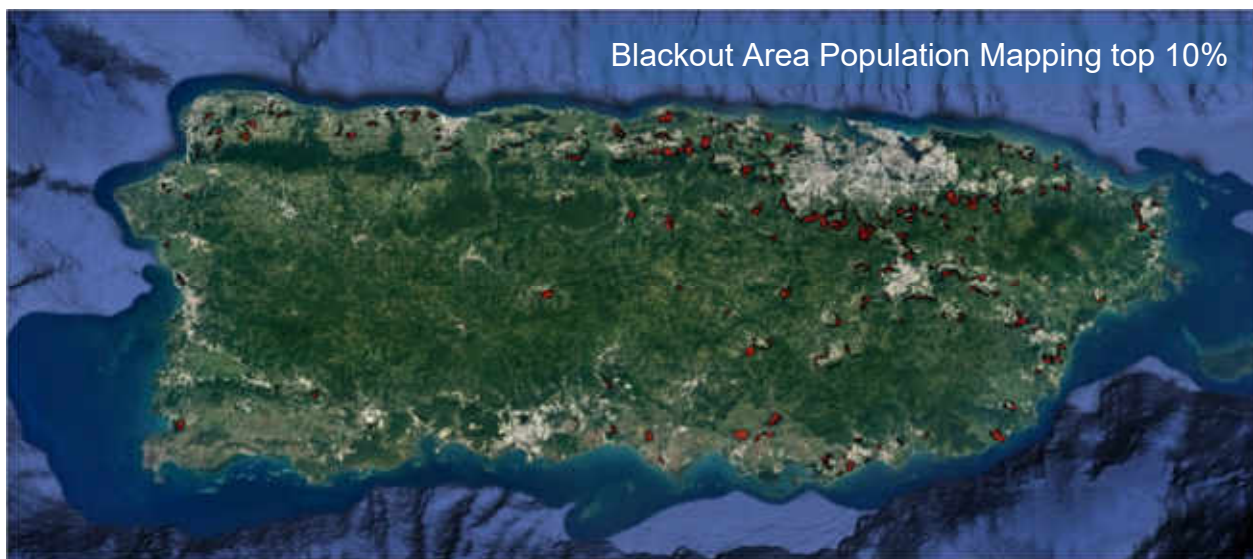
Figure 40 Final Result, blackout areas with population data. Only top 10% of most populated areas are shown.

As previously mentioned, an average population density parameter is used to estimate the amount of people in a given blackout area. This means that very small blackout areas, single pixels or only a few pixels in size, will return an unreasonably low number of people per area. These single pixel areas will most times return a value of less than one person per area, for this work these rounded to the nearest integer which results in many of these areas returning a value of zero. A visualization of how many times this happens can be seen in the distribution for group sizes in Figure 41. For the case being presented for the third stage blackout in this work, a whopping 70.56% of the total 23,911 groups generated. A group with a value of 0 persons per area is unrealistic and is considered noise for the purpose of this work. The second largest percentage for any group is the 1 to 4 people per blackout area group. These made up 17.46% of all the generated groups, and as with the zero people case, they are due to low average density and a very small area. These too can be regarded as noise.

Number of People Group Size Distribution for All Groups
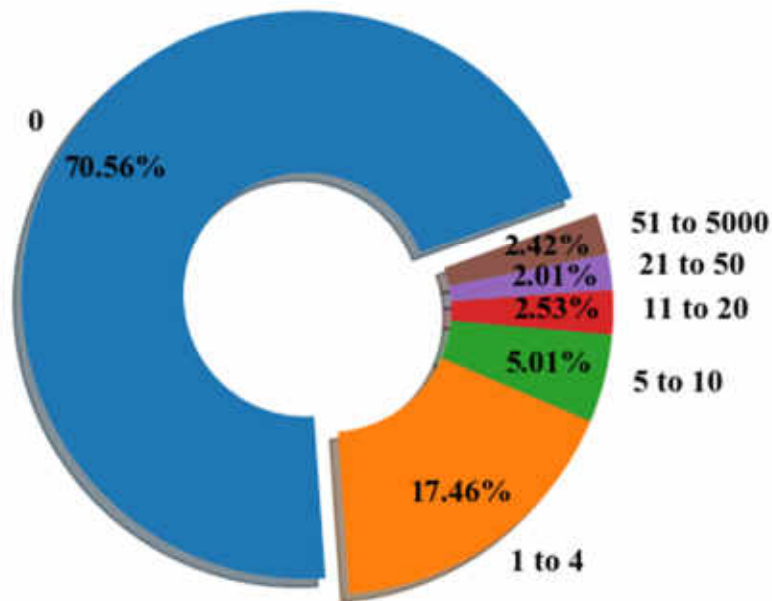
Figure 41 Pie Chart of Distribution of amount of people per blackout area for all groups.

A previously mentioned threshold value of 5 people or more per blackout area was imposed, this reduced the total number of groups from 23,911 to 2,863. The resulting percent distribution can be seen in Figure 42. This reduction results in better resolution, specifically in the 51 to 5000 range, this can now be subdivided into a 51 to 100, 101 to 500 and over 500 groupings. This improvement in resolution is why only the top ten percent largest groups are plotted in Figure 40, this range groups the over 500 and part of the 101 to 500 groups and therefore all the groups being considered have at least 101 people in them, which guarantees a broader impact.

Number of People Group Size Distribution for All Groups with More than 5 People
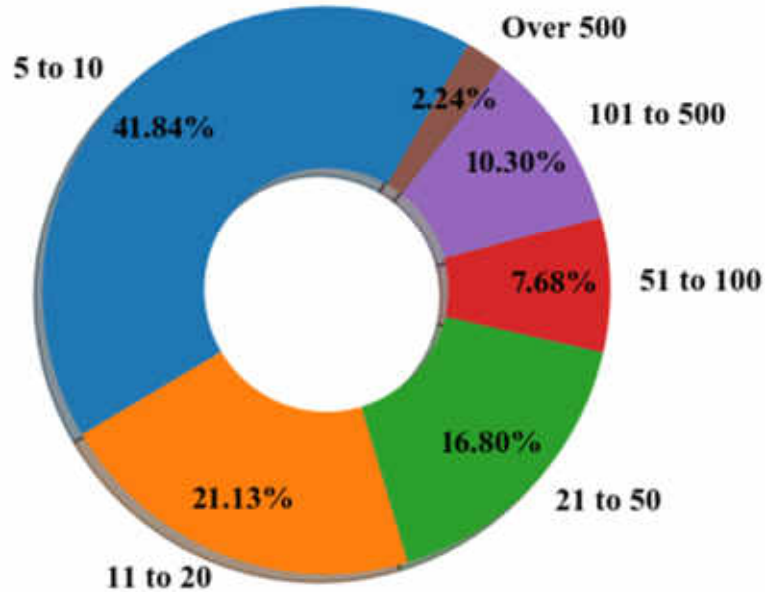
Figure 42 Pie Chart of Distribution of amount of people per blackout area with lower threshold of 5 people or more per polygon imposed.

3.3   Infrastructure Identification

The types of loads to be evaluated are derived from the types of infrastructure available in the area under study. Higher priority is assigned to infrastructure deemed critical, these tend to serve multiple clients at the same time and their service area may extend beyond the region under study, either downstream or upstream on the grid. These include but are not limited to radio towers, cellphone towers, wells, pumping systems, fuel supply, shelters, food supply chain. Infrastructure loads are not the only ones that are considered for the analysis. Non-critical public and private loads are included, such as: hospitals, pharmacies, police stations, fire stations, restaurants, government offices, places of worship etc. A more comprehensive list of these non-critical loads can be found in Table 3. These loads are included in the analysis, but are, of course,

49

given a lower priority. They are included in the analysis because they may be physically close to the critical infrastructure and it may be beneficial to include them in the load clusters in order to increase the amount of people impacted by the microgrid.

Table 3 Types of Infrastructure Included in Search

Airport	Dentist	Police
Atm	Doctor	Post Office
Bakery	Fire Station	School
Bank	Gas Station	Supermarket
Transit Station	Place of Worship	Café
City Hall	Hospital	Restaurant
Convenience Store	Local Govt. Office	Shelters
Courthouse	Pharmacy	Clinic
Water Pumping Station	Telecom Towers	Electric Power Substation

Ideally the information would be gathered from open sources such as Google Earth or Google Maps. All the unshaded categories listed in Table 3 can be found using Google Earth, the added benefit of finding infrastructure this way is that it can be directly exported into a KML file. Another source for critical infrastructure is the Homeland Infrastructure Foundation-Level Data (HIFLD) open data base; this is the best source for the shaded items in Table 3. [8] This is the best source for US based infrastructure. It covers everything from schools, shelters, hospitals to power generation, telecommunication etc.
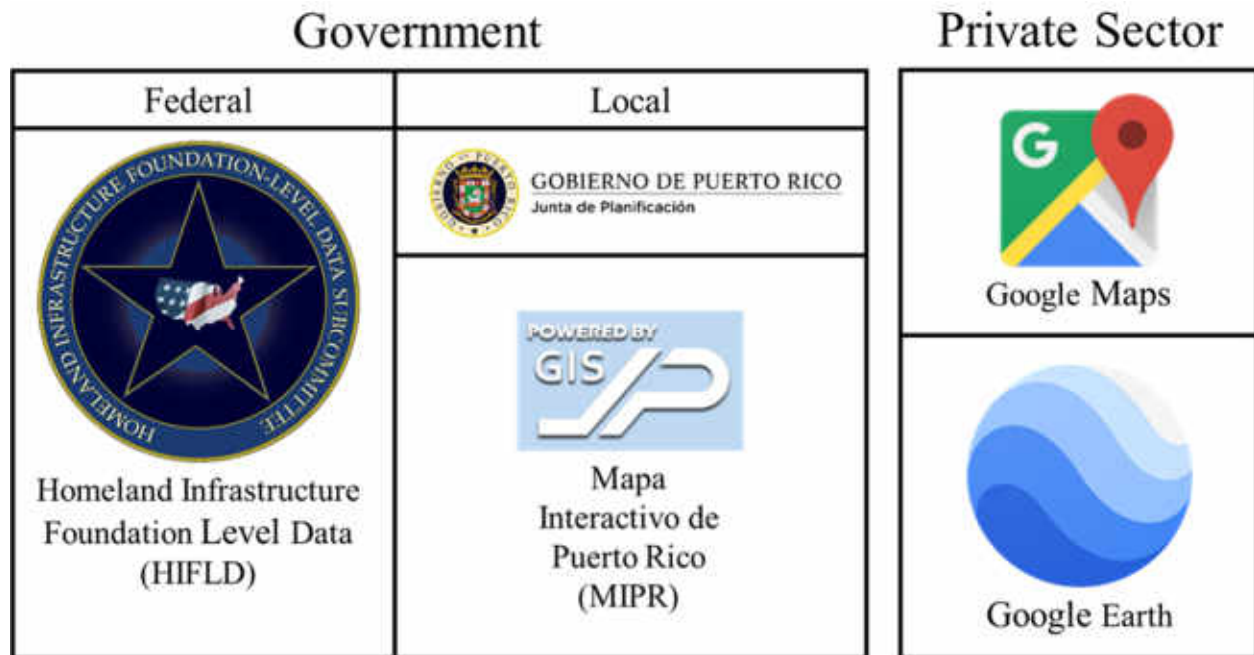
Figure 43 Infrastructure data sources

FS	Pumping Station
P	Well
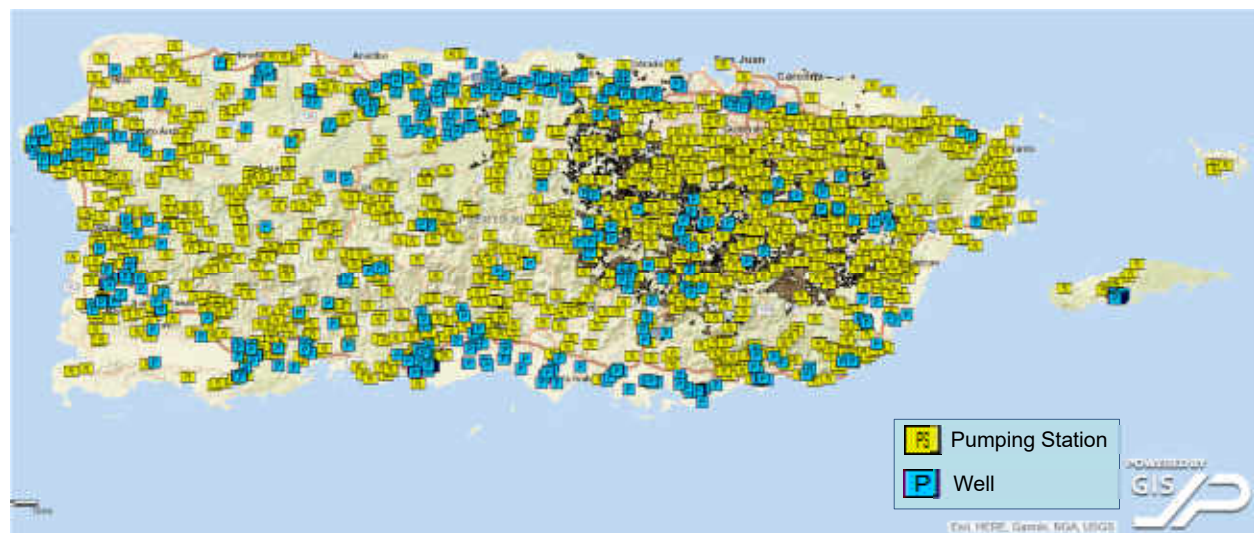
Figure 44 GIS water resource data overlay of Puerto Rico. Pumping stations are shown in yellow, wells are shown in blue, the dark brown area on the center of the island identifies the non PRASA service area. [39]

Figure 45 GIS radio and telecom data overlay of Puerto Rico. AM radio towers are shown in green; FM radio towers are shown in blue, the remaining icons show telecomunications towers. [39]

At this point in the workflow, the researcher has determined what the area under study is going to be and has found all the loads and infrastructure of interest. The next step in the process requires the inclusion of some type of feeder circuit or line geometry. An example of what a pre-processed line circuit segment and a selection of loads around said segment would look like is shown in Figure 46. The green line represents a feeder circuit segment and the yellow push-pin markers represent all the loads within the area of interest.

The researcher should not make any attempt to eliminate loads based on proximity or load type at this stage. Non-critical loads may be near critical loads or even near the interconnection point, any hasty removal of loads would bias the outcome. An opposing situation that could occur is that of a critical load, so far removed from the interconnection point, that the researcher might be tempted to remove it prior to analysis, but it might be so critical that all other factors would outweigh the proximity issue.

52
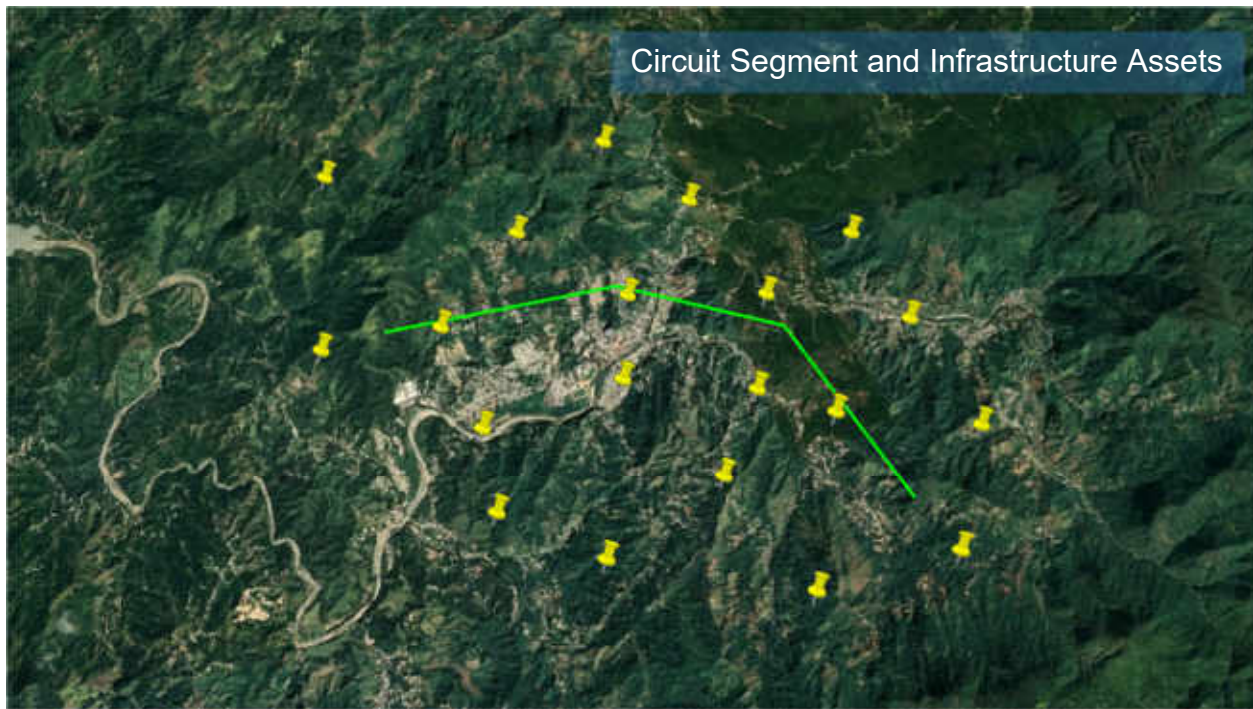
Figure 46 Hypothetical circuit line with hypothetical infrastructure assets.

The next step in the workflow is to define the distances for the limits of the bounding areas around the feeder circuit segment. Going back to the Shapely Python package, the easiest way to do this is by defining a buffer area using the *"object.buffer(distance)"* function. This will create an area representing all the possible points a set distance from the line. This function also has other inputs that define things such as the join style between buffer areas and the cap style. The work done here used the default round, join and cap style. The round cap style creates a semi-circle perpendicular to the end of the feeder segment which creates a truly equidistant perimeter. The flat and square ends could allow for the inclusion of loads that are not truly the maximum distance from the end of the line, as the perimeter created would not be equidistant.
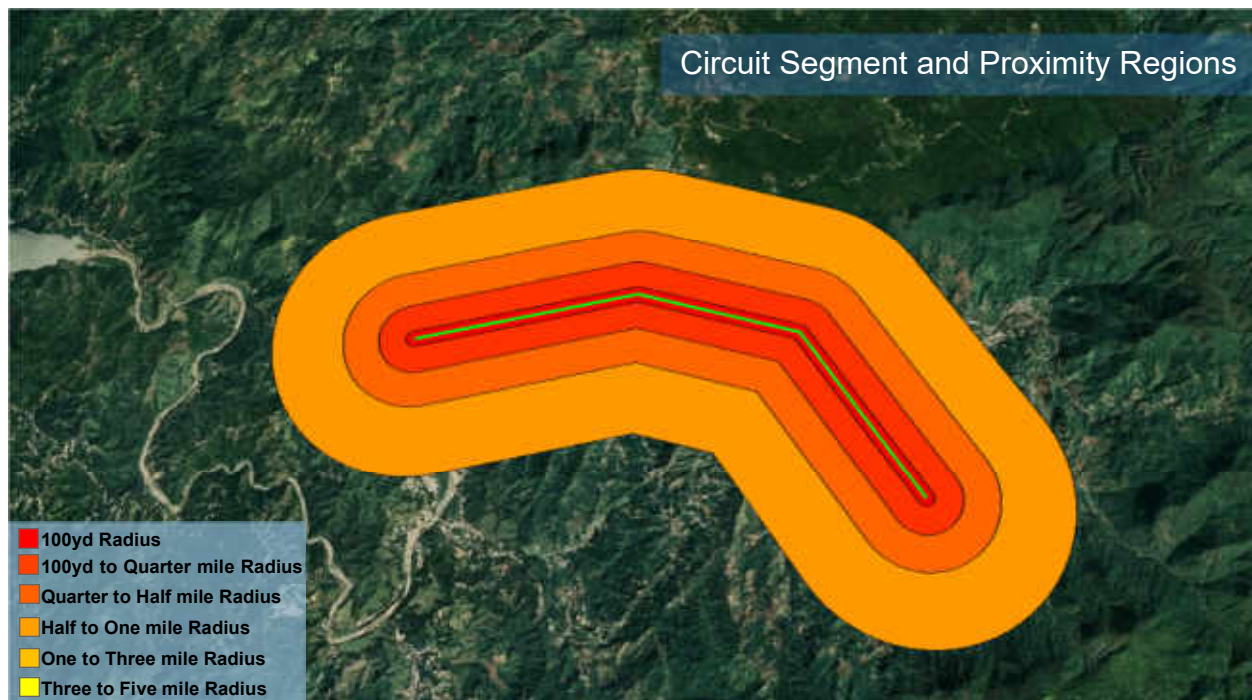
Figure 47 Circuit line with buffer areas around it.
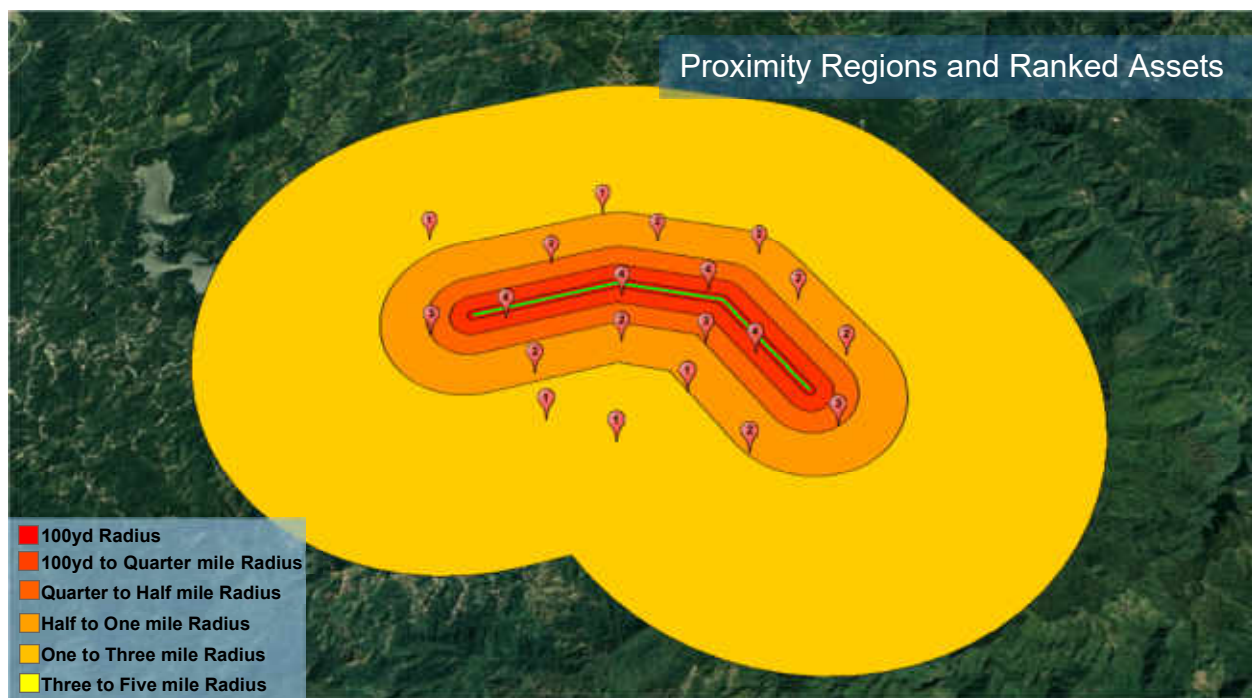
Figure 48 Circuit line with buffer area; markers have now been ranked according to where they lie in relation to the circuit line. Ranked from closest (5) to farthest (0).

3.4   Microgrid Design

The previous steps in this methodology all lead up to the load selection process. This next step aims to help the researcher select which loads from the previously selected loads should be connected to a microgrid. The decision matrix included in this work has six categories, each with a ranking system that ranges from 5 (most desirable) to 0 (least desirable). Each load is assigned a rating for all categories, the sum of the ratings per category for a load determine if that load will be included in the final microgrid or not. A load will be discarded if it is rated at 18 or lower out of the maximum rating of 30 points, this is equivalent to scoring 60% or less. These categories are proximity to connection point, load type, cluster size (or number of loads per microgrid), system size, cost to power and location accessibility. They are explained in further detail in the following sections. A table containing the criteria can be found in Table 4; a hypothetical use case can be found in Table 5 and Table 7.

3.4.1   Proximity to Distributed Generation Node:

The first processing of assets is done based on the proximity to a boundary area created around a distribution system feeder. These areas can be seen for an example segment in Figure 48. The distances are as follows: 100yds, ¼ mile, ½ mile, 1 mile, 3 miles. In practice these values should be adjusted according to the terrain being evaluated, difficult terrain should have shorter distances while open terrain could have a dilation of the selected values. This potential for adjustability is part of the methodology's design and is meant to be scalable and transferable to other places in the world.

3.4.2 Load Type:

The proposed critical infrastructure is listed in Table 4. This again could be changed according to the criteria of the researcher. The proposed hierarchy for this work was done by assigning higher values to services and infrastructure that could impact both locally and the surrounding regions and then lower values to things that would only have local impact to a lower number of people. While residential Loads were given a rating of 0, and were not included as part of this work, this does not mean that they could not be included. As mentioned before in Infrastructure Identification, critical loads may benefit from the proximity of non-critical loads and this may include residential loads.

3.4.3 Potential Size of Cluster with Included Load:

This factor is just a descriptor and is straightforward. Clusters with a larger number of loads are favored over ones with individual loads but does not differentiate between small and large loads. Great importance in placed on the possibility of a broader impact with the implementation of the microgrid. Integration efforts and logistics would be easier if focus is placed on a small number of clusters with many loads rather than many clusters with a small number of loads, even if the total number of loads impacted by each case is the same. The ranking for cluster sizes, as with all the criteria in the methodology, may be adjusted.

3.4.4 Size of System:

It is important to note that this is evaluated PER LOAD and is, again, something that can be adjusted depending on the area that is being evaluated. Smaller loads are favored as these would be less costly to power. Smaller distributed generation assets are also easier to deploy and would be given priority, this is not invalidated by a large total load due to clustering. A cluster with a large total load may have an agglomeration of smaller distributed generation assets to power it (e.g. rooftop solar). Even within clusters with large loads, or remote single loads, the rating scale for this parameter allows the loads to not get lost in the rating process.

3.4.5 Cost to Power:

In line with the theme of the previous categories, a lower cost is given priority over a higher cost. This work, in its inception, considered the most vulnerable populations, the ones that had endured the severe blackout, to be the priority. More remote locations and rural communities might not have the same buying power as a more urban center. More than likely the urban centers would have been powered early in the grid recovery efforts. The range and specific values could be adjusted by taking the areas' economic health and resources into consideration.

3.4.6 Accessibility:

This parameter becomes relevant if the terrain is rough or varies within the area under study. Loads located in accessible places are favored over loads located in very remote regions. It is important to note that relative accessibility is to be considered when assigning a rating to each load. Due to the nature of the locations of the areas under study, the sector may be in a hard to access place when compared to an urban center and thus all loads might be incorrectly classified as inaccessible. The ranking system developed for this work, and the example presented in TEST CASE: Jayuya, assumes the majority of the loads are located in areas with paved roads in good

condition. This might be unsuitable for all cases and it is up to the researcher to select the appropriate criteria used to create the ranking for their area under study. The presented criteria would be used as a guide, should a new ranking system be required.

3.4.7 Decision Matrix:

The reasoning behind the ranking system has been explained in the previous sections. It can be organized into a decision matrix for easier processing is found in Table 4 below. The ranking values are in the first column, the categories are in the first row from the second column onward. The categories are in no particular order, but the rows are ordered from most desirable (second row) to least desirable (last row).

Table 4 Proposed Load assessment rating system for a microgrid

Rating	Proximity to Distributed Generation Node	Load Type	Potential Size of Cluster with Included Load	Size of System	Cost to Power	Accessibility
5	Direct connection	Infrastructure (radio, water, telecom, food supply, shelters, fuel)	Five or More Loads Served	Less than 10kW	Less than $20k	More than one access point
4	Less than 1/4 mile (1320 ft)	Healthcare Facilities	Four Loads Served	Less than 50kW	Less than $75k	Single access point (e.g. dead-end road, cul-de-sac)
3	Less than 1/2 mile (2640 ft)	Emergency Personnel	Three Loads Served	Less than 100kW	Less than $250k	Unpaved access points, but in good condition
2	Less than 1 mile (5280 ft)	Govt. Offices or Public Buildings	Two Loads Served	Less than 500kW	Less than $500k	Access points are in poor condition
1	Less than 3 miles	Private Businesses	Single Load Served	Less than 1MW	Less than $1M	Access points are damaged but can be repaired
0	Several Miles	Residential Loads	Single Load Served, no possibility of multiple connection points	Several MW	Requires significant investment	Remote location, cannot be reached unless special equipment is deployed

There are three hypothetical clusters, ranging from 2 to 6 loads per cluster. The reader may notice in the fourth column of Table 5 that clusters are of a mixed load type, with the most diverse cluster being the third one. A similar phenomenon can be observed in the sixth column; loads within the same cluster are of different sizes as well. Interestingly, the third cluster has an example of a load that does not meet the minimum 19 points required for inclusion in the microgrid. This load is highlighted in Table 5. When this happens, the researcher has two options: remove the load and continue as before or split the cluster to try to accommodate all the loads. The first case can be seen in Table 6, the uncompliant load, the Government Office is removed. The load cluster is no longer 6 items, but because the maximum rating is based off 5 or more loads, this parameter is unchanged, and all remaining loads comply.

The standard procedure should be to remove the load and continue with the evaluation, if the researcher deems the uncompliant load to be sufficiently important to warrant keeping, the cluster can be split. The split case can be seen in Table 7. When doing this splitting, two parameters will change, and the split must be done in a strategic manner as to not have these to become the reason all loads are uncompliant and the whole cluster disappears. These two parameters are the proximity to the node and the cluster size. The cluster size will immediately decrease, and this factor will be negatively impacted, therefore the difference and the rating that must be increased must be the proximity rating. This is where the strategic planning comes in. The telecom tower, the supermarket and the government office all have the lowest rating for proximity, presumably these are all far away from the interconnection point but are close to each other. Therefore, these three loads should be grouped together, as done in the Third Cluster B on Table 7, a new common interconnection point would be generated for this cluster and their proximity rating would increase enough to surpass the drop in cluster size and be compliant. The

60

other half of the loads, Third Cluster A, had a high enough rating that the drop in cluster size did

not negatively affect their compliance.

Table 5 Three cluster example using the assessment criteria of Table 4

	Load	Proximity to Distributed Generation Node	Load Type Ranking	Potential Size of Cluster with Included Load	Size of System	Cost to Power	Accessibility	Totals per load
First Cluster	Pumping Station	5	5	2	5	5	3	25
	Police Station	3	3	2	4	4	5	21
Second Cluster	Radio Tower	4	5	3	5	4	5	26
	Fire Station	5	3	3	4	3	5	23
	Shelter	1	5	3	4	3	5	21
Third Cluster	Telecom Tower	3	5	5	5	5	2	25
	Community Hospital	5	4	5	3	2	5	24
	Community Center	5	2	5	4	2	4	22
	Govt. Office	0	2	5	3	3	5	18
	Bank	4	1	5	4	3	4	21
	Supermarket	3	5	5	2	2	4	21

Table 6 Third Cluster, uncompliant load removed

	Load	Proximity to Distributed Generation Node	Load Type Ranking	Potential Size of Cluster with Included Load	Size of System	Cost to Power	Accessibility	Totals per load
Third Cluster	Telecom Tower	3	5	5	5	5	2	25
	Community Hospital	5	4	5	3	2	5	24
	Community Center	5	2	5	4	2	4	22
	Bank	4	1	5	4	3	4	21
	Supermarket	3	5	5	2	2	4	21

Table 7 Third cluster is split into sub-clusters and now all loads comply with threshold value

	Load	Proximity to Distributed Generation Node	Load Type Ranking	Potential Size of Cluster with Included Load	Size of System	Cost to Power	Accessibility	Totals per load
Third Cluster A	Community Hospital	5	4	3	3	2	5	22
	Bank	4	1	3	4	3	4	19
	Community Center	5	2	3	4	2	4	20
Third Cluster B	Telecom Tower	5	5	3	5	5	2	25
	Govt. Office	3	2	3	3	3	5	19
	Supermarket	5	5	3	2	2	4	21

3.4.8 Microgrid Design Process Flow

This section outlines the process flow and the limitations and decision criteria that are involved in each of the stages. This step is necessary after the creation and evaluation of the clusters formed in the decision matrix of section 3.4.7. A flow chart of the process decision flow can be seen in Figure 49, a detailed explanation of each of the steps is found in the following section.

3.4.8.1 MG 1 – Microgrid stage 1

This stage, the determination of the amount of load to be served in the microgrid, is tied to the output of the decision matrix. The researcher should know by this stage what the load to be served will be due to the previous clustering; unwanted loads (those that failed the criteria for being included in a cluster) have been eliminated. It is included as a first step such that the process flow can be adapted to works outside this thesis.

3.4.8.2 MG 2 –Microgrid stage 2

This stage, the figuring out of the surplus factor is an optional one. The factor ranges from $(1,5]$, this means that after multiplication the design load for the microgrid can be up to 500% of the original load. This factor can be used to account for the inherent inefficiencies of a generation system by increasing the system requirements. In a more strategic sense, designing a microgrid for a load much larger than the currently existing one, leaves the possibility for future growth of said microgrid; this site would then become a prime candidate for the infrastructure expansion of an area.

3.4.8.3   R 1 – Renewable stage 1

If the researcher has reached this decision point, it means that there is an interest in the inclusion of renewable energy solutions in the microgrid. At this point it is not necessary to know exactly how much of the system size is required to be renewable. If in doubt the researcher should pick 50% as a starting point, the next step will determine if this percentage is possible. It is the author's preference to pick somewhere between 50% and 75% renewable. While an effort should be made to shy away from non-renewable energy resources, there are still some limitations of 100% renewable energy microgrids that may be easily overcome with the implementation of some non-renewable energy sources such as common diesel generators.

3.4.8.4   R 2 – Renewable stage 2

A realistic approach to the previously established renewable target is taken in this step. The researcher should be acutely aware of the advantages, disadvantages of the commonly available renewable energy resources as well as the interaction with the desired location of the microgrid. The more common sources are, solar photovoltaic, wind turbines, hydroelectric specifically small hydro. Some are more exotic such as solar concentrating, geothermal. The five technologies mentioned here have two things in common, they require a thorough study of the location's weather and topology and are extracted from the natural forces of the earth that would otherwise go unused. These forces, topologies and weather patterns do not express themselves homogeneously throughout the earth, and as such we may not be able to implement the technologies in the locations or at the scale that we would like. There are other renewable energy sources that require more human intervention, and some could argue would not be considered renewable if not for their careful conservation. One of these is the burning of biomass and

biodiesel. These more closely resemble the technologies found on the non-renewable side of the equation.

Some limitations and considerations in the case of solar photovoltaic: the amount of daily sunlight, the weather (is it cloudy or clear sky most of the year), the topology (is it too steep, is it economically feasible to install panels at this location?), the amount of land available for this operation, what is the cost of opportunity of using tracts of land for solar vs some other operation.

Some limitations and considerations for the case of wind power, just as with the sun in solar case, what is the wind profile of the location, how will the placement of these turbines impact the local fauna, the view of the land etc. In conclusion for this section, the goal is to be creative in the selection of the renewable technologies for a location and verify how much is available.

3.4.8.5 R 3 – Renewable stage 3

This is the sanity check section of the renewable energy implementation section of the design of a microgrid. Hopefully there is enough available to meet the percentage, a happy surprise would be that there is more than required and the percentage could be increased, but more than likely this is not the case. The researcher might find that there is not enough for the target established in 3.4.8.3. There are three choices should this happen: make the maximum available renewable energy, the target and continue with the evaluation of the microgrid, establish an even lower target or abandon the idea of renewable completely. For example, say that the target 40% of renewable energy was not met, but only a 36% is possible. The researcher performs an economic analysis and determines that the incremental cost of making a 30% renewable microgrid to a 36% renewable microgrid is too great to warrant the cost; there the researcher would elect to design around this new 30% target or decide that the 40% original target was the pass/fail criteria for renewables in this microgrid and opt to do a completely non-renewable microgrid.

3.4.8.6 RS 1 – Renewable Storage stage 1

This section might seem counterintuitive, why would there only be storage if there is renewable generation? The simple answer is, the non-renewable sources all require that there be some type of reserve that guarantees their operation, i.e. the storage portion is already built into the non-renewable energy technologies. There is a special case of storage that does not care where the power generation is coming from: pumped hydro storage, but this is only currently used at very large scales, outside the scope of this work.

3.4.8.7 RS 2 – Renewable Storage stage 2

All of those who advocate for the exclusion of renewable energy sources have the same complaint: renewable energy is intermittent and affects the grid operation! While this is true there are ways to reduce, but not yet eliminate, that impact, one of those ways is with the use of storage. The added benefit of storage is that is also helpful during the times when the grid is down; it allows the loads that have some type of storage to continue operating at some level for some time, hopefully enough such that the grid power is reestablished.

Which leads into the most important question when it comes to storage: how much is enough? One might be tempted to put in so much storage as to appear to be like a dragon hoarding its gold, but quickly the realities of size, cost and available technologies make that notion disappear. The large-scale storage projects around the world are a testament to the current limitations, most offer less than an hour in duration and are not used as a resiliency improving trick but more of a way to mitigate the aforementioned intermittence problems associated with renewable energy. For design purposes the researcher should not try to create solutions that are more than a few days length.

Most people hear of storage and think battery, but even within that there are many types of batteries, with research being done into making them, cheaper, safer, more energy dense and more useful than before. There are also other, non-chemical ways of storing energy one popular choice is the use of flywheels to mechanically store rotational energy.

3.4.8.8   NR 1 – Non-Renewable stage 1

This stage is only accessed in microgrids that are not purely renewable. The percentage of non-renewable generation varies from (0,100-*percentage of renewable generation*]. The sum of this non-renewable and renewable generation should not exceed 100% as the surplus factor in 3.4.8.2 already inflates the size of a microgrid.

3.4.8.9   NR 2 – Non-Renewable stage 2

As with the renewable energy generation options, one must keep an open and creative mind when it comes to the selection of non-renewable energy sources. The restrictions here are different. A restriction here are the fuel costs and cost fluctuations, fuel supply chain, environmental regulations on the technologies being utilized, etc. There are some very good arguments to be made for these sources. A 1 MW generator can be hooked up to a trailer and hauled into place *pro re nata,* as was the case for the island municipalities of Vieques and Culebra when they were isolated from the mainland's power supply. A 1 MW generator is several orders of magnitude smaller than a comparable 1 MW solar photovoltaic operation.

3.4.8.10   NR 3 – Non-Renewable stage 3

As mentioned, the non-renewable energy sources have inherent storage and is much easier to store large quantities of energy, as the common sources tend to be more energy dense than their counterparts; still the researcher should not try to make the storage last more than a few days.
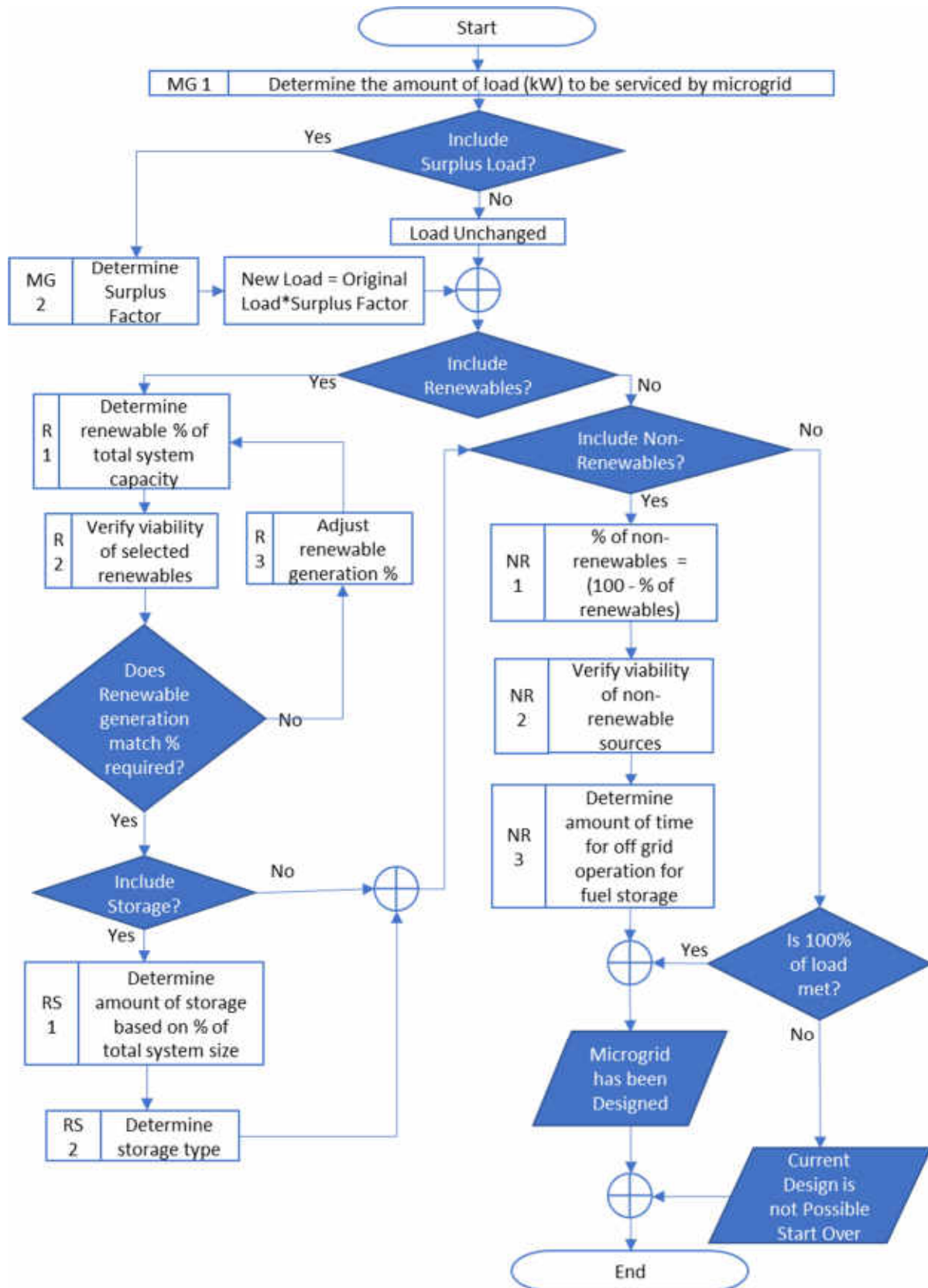
Figure 49 Microgrid Design Process Flow flowchart

Chapter 4: TEST CASE: Jayuya

The previous chapters of this work have been a combination of real data and hypothetical cases to show the reader how the methodology works. Though it has been mentioned extensively throughout this text, the reader should take note that the purpose of this work is not to make a microgrid in Jayuya, but present the methodology and showcase how it would work by providing a hybrid example composed of real-world and hypothetical data. The information and examples presented in Chapter 3:, excluding the decision matrix and cluster examples presented in Table 5, Table 6, Table 7 are done with real world data and could be used to perform actual studies. The goal of this section is to present how that information is used in a real-world example. The area presented here is the town of Jayuya in Puerto Rico. All infrastructure asset data presented for Jayuya is real except for the circuit geometry presented. The distribution circuit geometry used here is not of a real circuit in Jayuya but modified and based off another place in the world with similar characteristics regarding population and terrain; this place shall remain anonymous. The use of hypothetical circuit geometry does not invalidate the purpose of this example, which is to show how the full methodology is performed.

4.1 Why Jayuya?

Jayuya is one of the 78 municipalities of the island of Puerto Rico. It lies in the central part of the island. Its location can be observed in Figure 50 as the yellow groping of polygons. The yellow polygons show the county sub-divisions, known as *"barrios"*. The town has 11 barrios and total population of 16,642 (2010 Census) [1]. The names of the different *barrios* can be seen in Table 8. The most populated of these is Veguitas, with a population of: 3,685 [1].

Jayuya is an ideal candidate for use as a test case for a few reasons, its location, population size, assets type and distribution and the peculiar industry that lies there. The central part of Puerto Rico is mountainous, and access is usually in the form of two-lane winding roads that have been cut into the mountains, surrounded by varied tropical vegetation. These roads make travel take longer than what would be expected. Jayuya is in the middle of this area and is a very nice representation of all the other towns located in the mountainous part of Puerto Rico. While the center of the town, the barrio called Jayuya Pueblo, may be called urban in the sense that there is a concentration of businesses, government offices and some housing, most of the population lives outside of this area towards the rural outskirts. As a point of comparison, the population of Jayuya Pueblo was 1,222 [1] whereas the total population was 16,642 [1] as previously mentioned, roughly 7% of the population lives in the "urban" area. A few well-placed microgrids would greatly impact the population of Jayuya, whereas the same number of microgrids' effect would only impact the people living closest to the microgrid in a place such as the capital, San Juan, that has a population of 395,326.

The peculiar industry is the Baxter International manufacturing plant located in Jayuya which employs around 800 people. This plant is one of three located in Puerto Rico. The line of products they produce for different markets such as fluid therapy, anesthesia, critical care, oncology, bioscience, renal care, nutrition, and specialized pharmacy [40]. The hurricane caused minor structural damage to the facility but decimated the electrical infrastructure that supplied power to the plant and surrounding areas it also caused road damage and obstructions on the already small two-lane roads. As such, there was no power and getting diesel fuel and supplies to continue manufacturing operations was difficult if not impossible for some time. Baxter accounts for 43% of the IV saline solution market, and most of that is produced in Puerto Rico this caused

an IV bag shortage in Puerto Rico and the U.S. [41] For this and all the other previously mentioned reasons, Jayuya is the ideal candidate to showcase the methodology.

Table 8 County Sub-Divisions of Jayuya, known as *"Barrios"*

Jayuya's *"Barrios"*					
Pica	Jauca	Collores	Zamas	Saliente	Veguitas
Jayuya Pueblo	Coabey	Rio Grande	Jayuya Abajo	Mameyes Arriba	
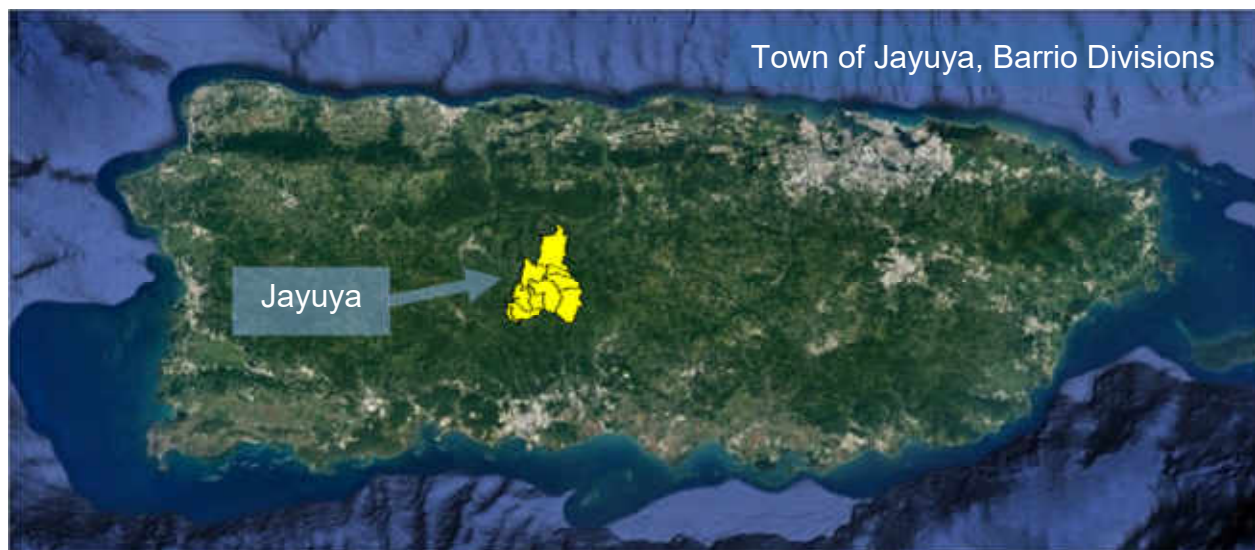
Figure 50 Town of Jayuya with barrio divisions.

The blackout identification step, shown in 3.2 Number of Affected Customer Estimation, and the data generated also form the basis for the selection of Jayuya. The original image can be seen in Figure 37 and the reduced grouping that shows the top 10% largest groups can be seen in Figure 40. A blackout polygon in the region of Jayuya shows up in the initial analysis and a polygon of the same size persists in the second image, meaning that that portion remained without power for at least 6 months and was one of the largest within the island! Figure 51 highlights the blackout area, notice how isolated it is when compared to the other large blackout groups. A close-up of the blackout area is presented in Figure 52.
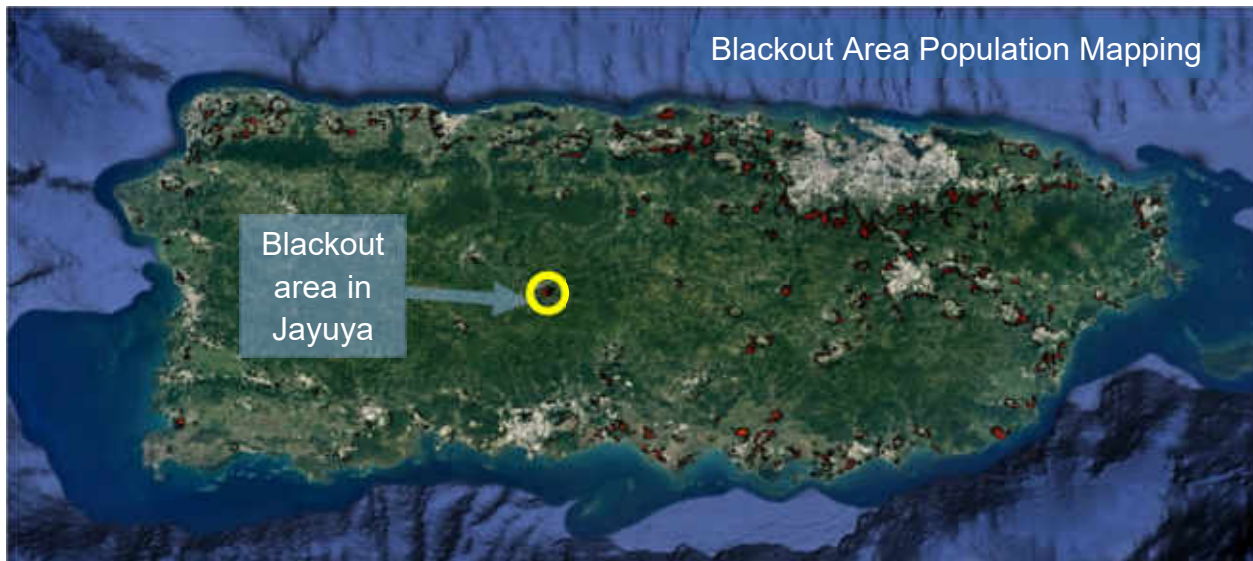
Figure 51 Blackout area in town of Jayuya identified in yellow circle on blackout areas with population data.
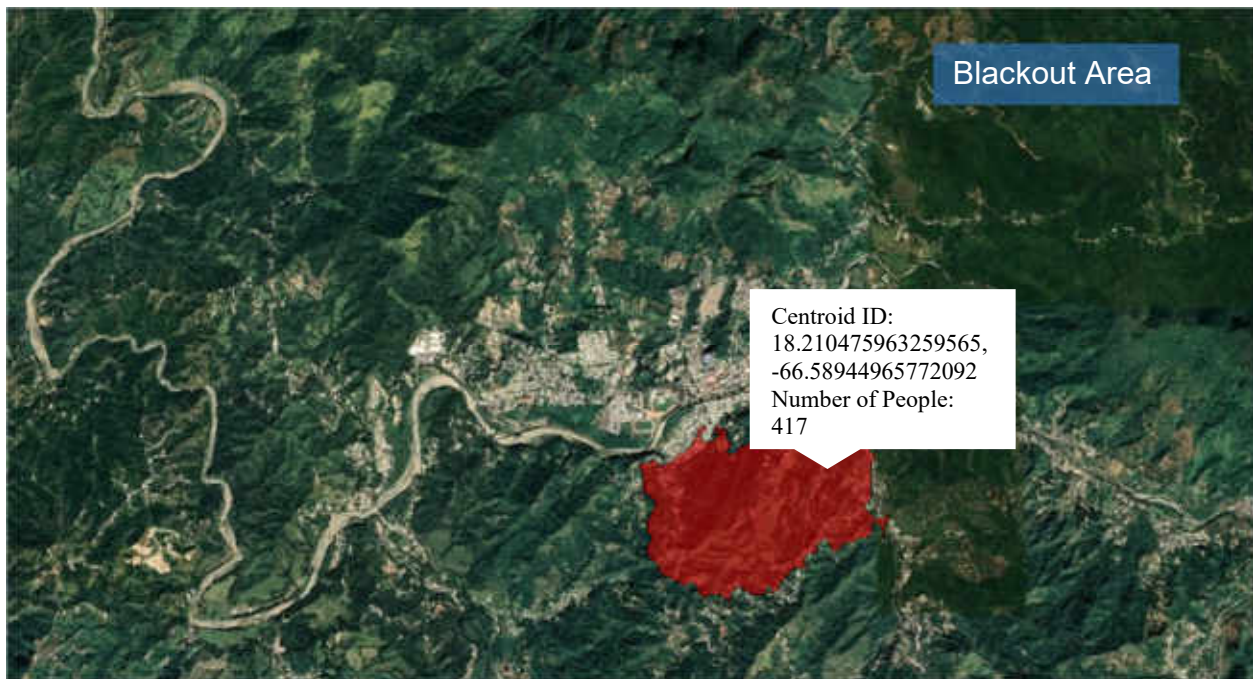
Figure 52 Blackout area in Jayuya (red polygon); Centroid ID and Population estimate can be seen in balloon (417).

4.2   Circuit Overlay and Asset Identification

Ideally the researcher would have a circuit model for the area under study, at the very least the circuit geometry would be enough for this step. At the moment of writing, the geometry of the real feeder circuit for Jayuya could not be obtained, instead the geometry of a feeder from a region with comparable geography and population was used. The circuit geometry and its placement over Jayuya can be seen in Figure 53, the white line denotes the three phase backbone, the different colored lines denote the single phase branches and their secondary circuits. The denser parts of the feeder are located over the urban areas with some parts of the circuit branching out into the more rural areas.
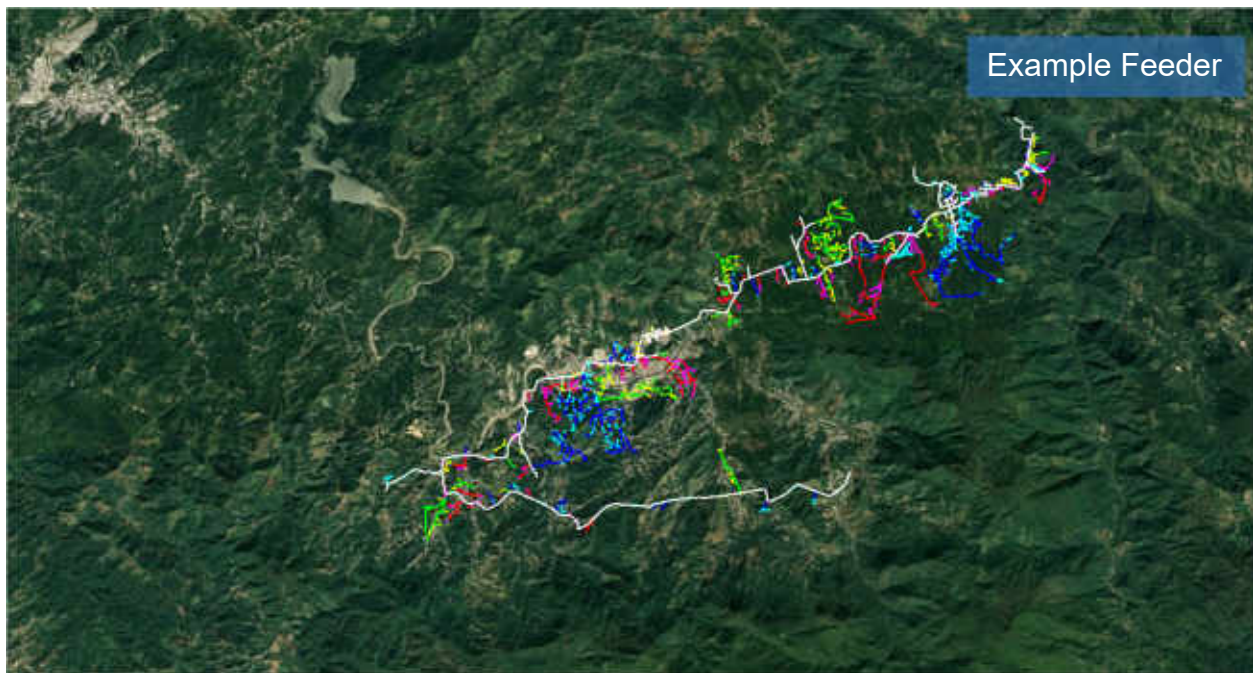
Figure 53 Hypothetical distribution feeder overlay.

The next step is to find and geolocate all the infrastructure of interest. As mentioned in the methodology, a good source for this is google earth or google maps. All the real-world infrastructure of interest for Jayuya can be found in Figure 54, denoted by the yellow pushpins. As with the densest part of the circuit being over the urban area, the largest concentration of infrastructure is at the urban area and thins out as one moves out into the surrounding rural area. The use of a hypothetical feeder for this work means some loads are not connected to the main feeder. In a real-world case this could represent loads on an adjacent feeder, which would still be of interest for the researcher, and loads which are off-grid. The case of an off-grid water pump or telecom tower would not be out of the question for a remote location. For the purpose of this work, the feeder is considered the chosen connection point and all loads not close to the feeder are off-grid.
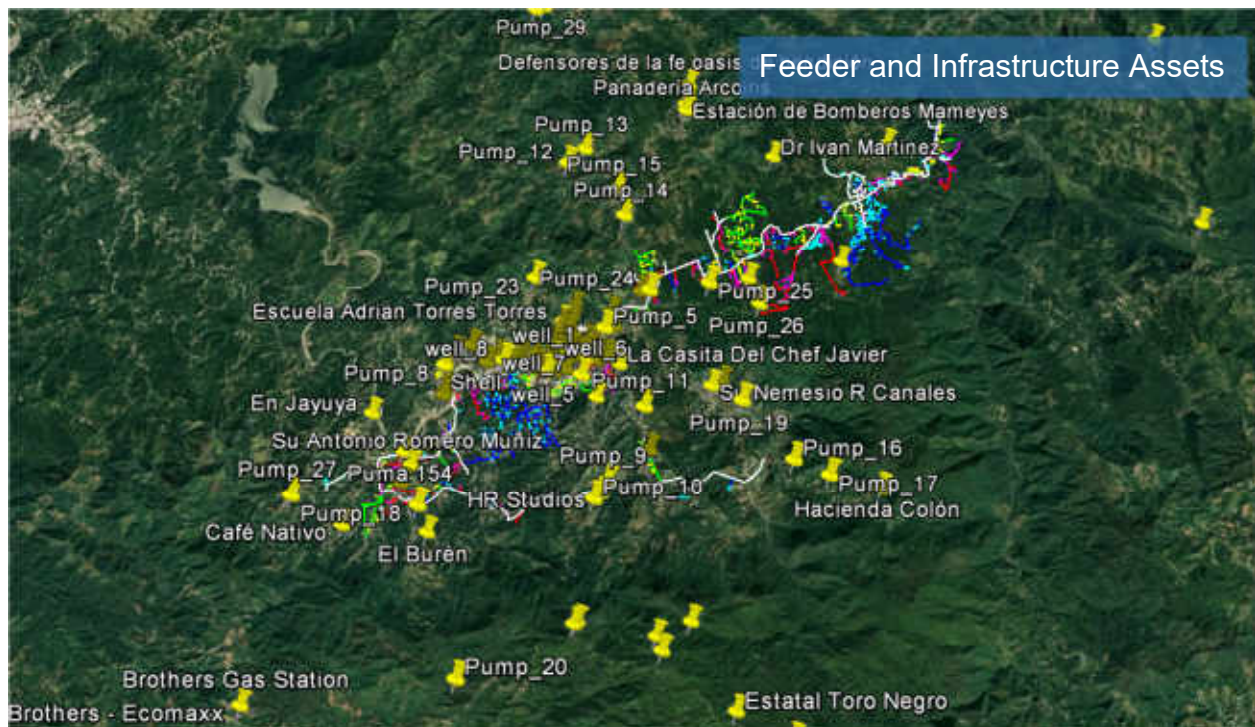
Figure 54 All real infrastructure assets around example feeder.

4.3   Load Classification and Clustering

The feeder and infrastructure assets are now located in the same space as shown in Figure 54. This representation is a good way to get an idea of how dense or sparse are the critical loads near the connection point, but this does not aid in further load classification.   Further load classification is done according to proximity to a desired connection point.   The visual representation for the Jayuya case is shown in Figure 55. The first three boundary areas are a lot closer as these have a larger bearing on the classification and importance of a load. The difference between a load with a direct connection and a load that is close by is the capital cost required to include them in the grid.   Both loads would be high priority because they are close to the connection point, but one would incur much lower integration costs and therefore be favored. The last three are rather large and provide less information, they would tell the researcher that a load is far away or very far away, in either case the load would not be a good candidate for a grid connected microgrid. If the connection point is picked carefully, most of the loads should fall within the first three classifications, as is the case with Jayuya where the densest part of the circuit also contains the most loads and these are in turn classified as high priority due to proximity. Loads should not be discarded on this classification alone, high priority infrastructure loads such as water pumps, and telecom towers and radio wave repeaters are generally in remote places and could be inadvertently discarded. Loads are classified but not yet clustered at this point.
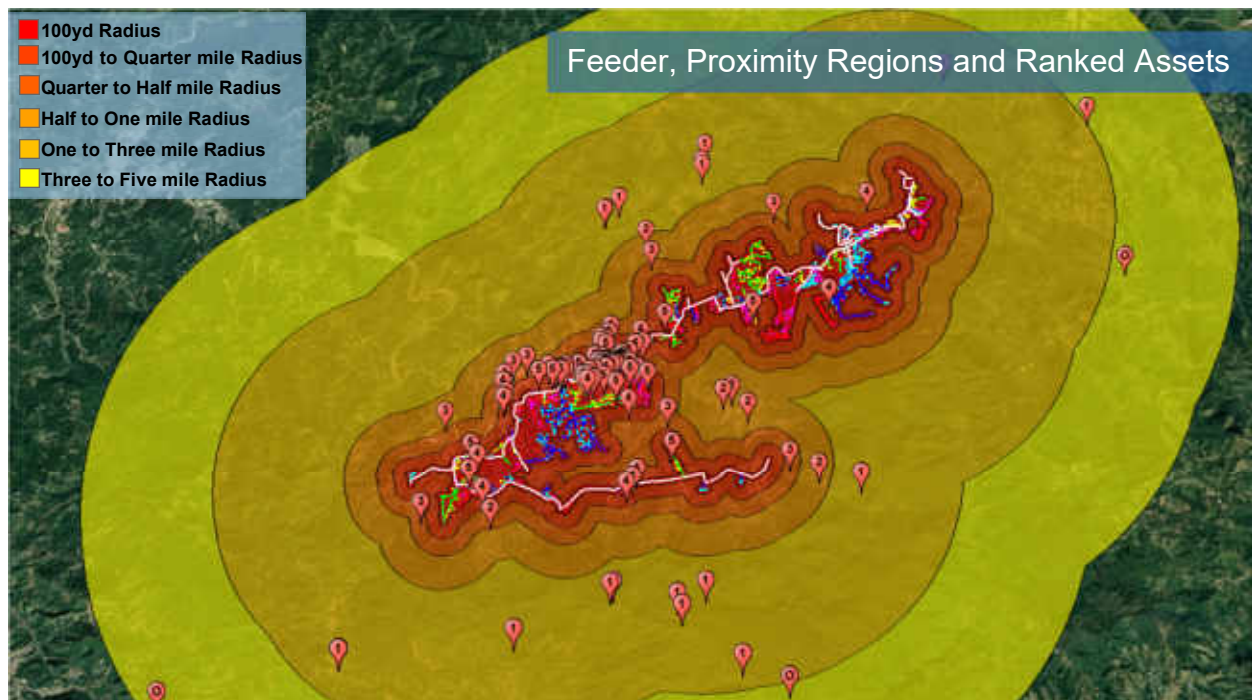
Figure 55 Proximity regions defined, and assets sorted by proximity.

There is no automated clustering done in this work, a feature such as this would be an expansion and powerful addition to the methodology, the implementation of a tree partitioning algorithm would perform this task quite elegantly. This is where the use of GIS and google earth really shine. The graphical representation allows the researcher to use their judgment when selecting the clusters by simply drawing a polygon around the loads they want to group together, shown in Figure 56. The load locations and the polygon locations are then imported into python and are grouped using the relationship between the intersection of the locations and the polygons. This allows for the automated creation of a table that includes the cluster names, the load names within that cluster and their proximity rating. This encompasses the first three columns of Table 9
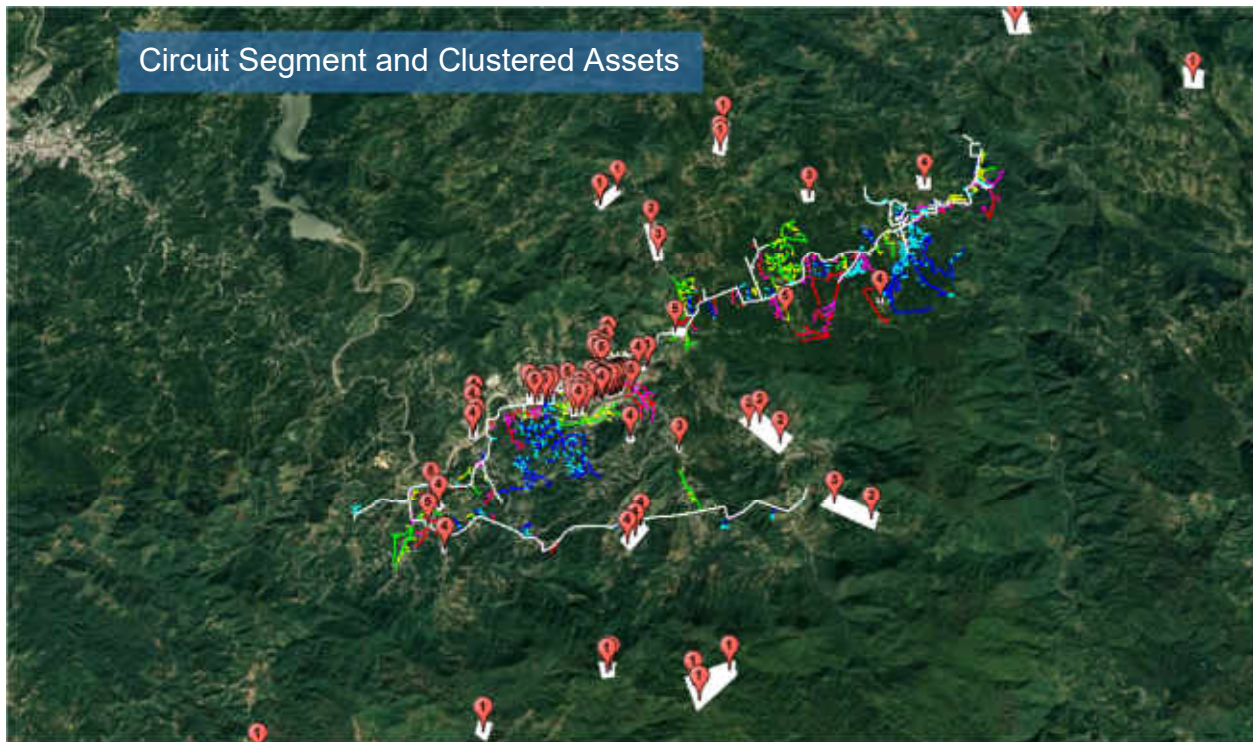
Figure 56 Load clusters around the hypothetical feeder for the Jayuya case. Clusters are represented by the white rectangles under the loads.

A close-up image of how loads can be clustered at the ends of the single-phase feeder segments is shown in Figure 57. There are three clusters in the center of the figure that exemplify why the researcher must be smart in their decision when clustering. These three clusters group a total of 7 loads, initially one could be tempted to just create a single large cluster with all of them, but upon closer inspection it is evident this would not be a wise choice. Grouping these seven loads under one cluster would mean using three different connection points across the feeder and in at least two cases it would be connecting different phases of the circuit, identified by the different colors of the circuit lines in Figure 57. A better choice is the one finally implemented, three distinct clusters: a four-load cluster in the center, a single load cluster and the two-load cluster above the four-load cluster. The single load is isolated due to the river, the two-load cluster is isolated due to being connected to a different phase in the circuit. This example highlights the importance of considering the electrical and geographical characteristics of the area under study.

76

Figure 57 Close up of the densest part of the feeder circuit and loads for the Jayuya case. Clusters are represented by the white polygons.

The following table, Table 9, contains the result of the full analysis of the clusters with respect to the ranking system described in Table 4. The clusters are not ranked and are only placed in order of creation. There are three general rules in the creation of the clusters, these can be extrapolated from the careful evaluation of Table 9. The first rule: not all loads have to be served as part of a cluster, the second rule: all clusters are non-coincident, the third rule: single load clusters are not advised, but may be included in the analysis if the load is deemed important. There are a total of 39 clusters, these do not contain all the original loads found and presented in Figure 54; following the first general rule, it is up to the researcher to decide if all loads must be served. The clusters are non-coincident as stated in the second rule, meaning that if a load is served by a cluster, it cannot be served in another cluster. Another way to explain is rule is that clusters cannot overlap in their servicing areas or in the loads they serve. The reasoning behind the third rule can also be explained with the results from the analysis. Out of a total of 39 clusters, 18 were single

77

load clusters, out of these 18, 4 were not load type 5 (highest priority) and were all discarded per the analysis. It must be mentioned that being the highest priority load does not guarantee that the cluster will be selected as two of the single load highest priority clusters were eliminated. The last column of Table 9 has the total per load; all totals highlighted in red did not make the cut and were subsequently removed from further analysis.

After the non-compliant loads have been removed, the "potential size of cluster with load" value is adjusted for the clusters which have lost loads. This in turn, may cause other loads or clusters to drop out if they now become non-compliant. This did not happen for the Jayuya case.

Table 9 Example of Loads, Clusters and Ratings for Jayuya

Cluster Name	Load Name	Proximity to Distributed Generation Node	Load Type	Potential Size of Cluster with Included Load	Size of System	Cost to Power	Accessibility	Totals Per Load
Cluster_1	HR Studios	4	1	3	4	4	5	21
	Pump_9	4	5	3	4	4	5	25
	Pump_10	4	5	3	4	4	3	23
Cluster_2	Acueducto Jayuya	1	5	3	1	0	5	15
	Pump_12	1	5	3	4	4	5	22
	Pump_13	1	5	3	4	4	3	20
Cluster_3	Angela Calvani	5	5	5	4	3	5	27
	Farmacia Hayuya	5	4	5	3	3	5	25
	Ferreteria Gilbes and Bycicle Shop	5	1	5	4	3	5	23
	Panadería (Bakery) Santa Clara	5	1	5	3	3	5	22
	Iglesia Del Nazareno - Jayuya Pueblo (Town)	5	1	5	4	4	5	24
	well_8	5	5	5	4	5	3	27
	Iglesia La Nueva Jerusalén C.L.A.	4	1	5	4	4	5	23
Cluster_4	well_2	5	5	4	4	4	4	26
	well_3	5	5	4	4	4	5	27
	well_4	4	5	4	4	4	3	24
	well_5	4	5	4	4	5	4	26
Cluster_5	Escuela Angelica Toro Rodriguez	5	2	4	3	3	5	22
	Estación de Bomberos Jayuya	5	3	4	4	3	5	24
	Baxter Credit Union	5	1	4	3	3	5	21
	Escuela Adrian Torres	4	5	4	2	3	5	23

Cluster Name	Load Name	Proximity to Distributed Generation Node	Load Type	Potential Size of Cluster with Included Load	Size of System	Cost to Power	Accessibility	Totals Per Load
Cluster_6	Estación de Bomberos Mameyes	1	3	3	4	4	5	20
	Panadería Arcoiris	1	1	3	3	3	5	16
	Defensores de la fe oasis de bendición	1	1	3	4	4	5	18
Cluster_7	Total Avenida Vicens	5	5	4	3	3	5	25
	Farmacia Lizette	4	4	4	4	4	5	25
	Oficina Dr. Fernando Carreras Coello	4	1	4	4	4	5	22
	JayuCoop - Coorperativa de Ahorro y Crédito de Jayuya	4	1	4	4	3	5	21
Cluster_8	Cuartel Dtto. Jayuya	5	3	4	4	3	5	24
	Jayuya County Mayor	5	2	4	3	3	5	22
	CDT Mario Canales Torresola	5	4	4	2	1	5	21
	La Placita De Jayuya	5	1	4	4	4	5	23
Cluster_9	Pump_5	4	5	3	4	4	5	25
	Pump_6	4	5	3	4	4	4	24
	Pump_7	4	5	3	4	4	4	24
Cluster_10	Pump_18	4	5	0	4	4	5	22
Cluster_11	Su Nemesio R Canales	2	5	3	2	3	5	20
	Hacienda Santa Marina	2	1	3	3	3	5	17
	Pump_19	2	5	3	4	4	5	23
Cluster_12	Telecom Tower Carr 533 Bo. Toro Negro Rio Cialito	4	5	0	5	5	3	22

Table 7 Continued

Cluster Name	Load Name	Proximity to Distributed Generation Node	Load Type	Potential Size of Cluster with Included Load	Size of System	Cost to Power	Accessibility	Totals Per Load
Cluster_13	Jayuja Metropolitana	5	1	5	4	3	5	23
	Gulf	5	5	5	3	3	5	26
	Los Domplines	5	1	5	4	3	5	23
	COGOP Jayuya (Iglesia de Dios de la Profecía)	5	1	5	4	4	5	24
	Cafetería Rodríguez	4	1	5	4	4	5	23
	Policlínica Castañer Jayuya	4	4	5	3	3	5	24
	Farmacia Padua	4	4	5	3	3	5	24
	Medicaid	4	2	5	4	4	5	24
	JAYUYA VETERINARY SERVICES	4	4	5	4	4	5	26
	Breban Beauty Supply	4	1	5	4	4	5	23
	EZ Payments Inc.	4	1	5	4	4	5	23
	Oficina Dr. Luis A. Rivera "Lucho"	4	1	5	4	3	5	22
	Popular Bank - Sucursal Jayuya	4	1	5	3	3	5	21
	Paliques Café	4	1	5	3	3	5	21
	Parroquia Nuestra Señora de la Monserrate	4	1	5	4	4	5	23
	Iglesia Metodista Hill Memorial	4	1	5	4	4	5	23
Cluster_14	El Yocahú	5	1	2	4	3	5	20
	Iglesia Cristiana Carismatica Jesus Vive	4	1	2	4	4	5	20
Cluster_15	Telecom Tower carr 141 Km 5.7 Monte Gregorio	5	5	0	5	5	3	23
Cluster_16	Pump_14	3	5	2	4	4	5	23
	Pump_15	2	5	2	4	4	3	20

Cluster Name	Load Name	Proximity to Distributed Generation Node	Load Type	Potential Size of Cluster with Included Load	Size of System	Cost to Power	Accessibility	Totals Per Load
Cluster_17	La Casona	4	1	5	4	4	5	23
	Napoli Pizza	4	1	5	4	4	5	23
	Shell	4	5	5	3	3	5	25
	Panadería La Jayuyana	4	1	5	3	3	5	21
	Pump_8	4	5	5	4	4	5	27
Cluster_18	Puma 154	5	5	2	4	3	5	24
	Su Antonio Romero Muñiz	4	5	2	3	3	5	22
Cluster_19	Telecom Tower Carr 143 Km 17.2 Cerro Puntas	1	5	2	5	5	4	22
	Telecom Tower Carr 143 Km 17.4 Interior bo. Zamas Cerro Punta	1	5	2	5	5	4	22
Cluster_20	Telecom Tower Carr 143 Bo Punta	1	5	3	5	5	0	19
	Telecom Tower Carr 143 Cerro Punta	1	5	3	5	5	0	19
	Telecom Tower Carr 143 Km 18.5 Int Bo. Saliente	1	5	3	5	5	3	22
Cluster_21	United States Postal Service	5	2	2	4	4	5	22
	Pump_2	5	5	2	4	4	5	25
Cluster_22	Josefina Leon Zayas	5	2	0	3	3	5	18
Cluster_23	Dr Ivan Martinez	3	1	0	4	4	4	16
Cluster_24	Telecom Tower Carr 614 Km 6.2 Bo. Cialitos	4	5	0	5	5	3	22
Cluster_25	Telecom Tower Carr 149 Caminos las Ca@as	1	5	0	5	5	3	19
Cluster_26	Telecom Tower Carr 615 Km 7.1 Int. Bo Toro Negro	1	5	0	5	5	5	21
Cluster_27	Gasolinera Brothers - Ecomaxx	1	5	0	3	3	5	17
Cluster_28	Telecom Tower Carr 143 Bo. Portuguez	0	5	0	5	5	5	20
Cluster_29	Pump_20	1	5	0	4	4	3	17

Table 7 Continued

Cluster Name	Load Name	Proximity to Distributed Generation Node	Load Type	Potential Size of Cluster with Included Load	Size of System	Cost to Power	Accessibility	Totals Per Load
Cluster_30	Econo	5	5	0	2	2	5	19
Cluster_31	Telecom Tower Carr 144 Bo. Veguitas	4	5	0	5	5	4	23
Cluster_32	Pump_11	3	5	0	4	4	5	21
Cluster_33	well_1	5	5	2	4	4	5	25
	well_6	5	5	2	4	5	5	26
Cluster_34	Pump_1	5	5	0	4	4	3	21
Cluster_35	Telecom Tower Carr 533 Bo. Toro Negro Rio Cialito	4	5	0	5	5	3	22
Cluster_37	Pump_16	3	5	2	4	4	5	23
	Pump_17	2	5	2	4	4	5	22
Cluster_38	Ferreteria El Gigante #2	5	1	0	3	3	5	17
Cluster_39	ESCUELA ELEMENTAL RAFAEL MARTINEZ NADAL	5	2	0	3	3	5	18

Table 7 Continued

A more detailed explanation of where the cost to power values were obtained for the Jayuya Case, can be found in Table 12. The first two columns of this table are the same as the original cluster output table. This table instead includes four new columns, the first of these is the estimated total cluster cost, next is the system size per load, the last two are the estimated system size and the number of critical loads per cluster. This las column considers how many 5 ranked loads exist in the cluster. This can be used to differentiate the relative importance of same sized clusters or at an even more basic level, if a cluster can be considered critical at all.

The cost estimates per system size were taken from the work done in [42] and are based on the dollar amount per kW of installed generation or storage. These values turned out to be constant and are represented in Figure 58 for the three types considered in this work: PV, diesel and battery. It is apparent that the renewable is the most expensive, followed by diesel and battery storage. The summary can be found in Table 10. This work considered an equivalent system cost based on a system composed of 50% PV, 50% Diesel and the capability to store 25% of what was generated. The equivalent installed system cost per kW is $1975/kW; the derivation is found in Table 11. At this point no attempt is made to confirm whether the topography and resources at each cluster will allow for the 50% PV rule, but as PV is the most expensive of the options, any substitution for the other resources would just lower the cost of the cluster implementation. PV is considered as the prices have dropped in recent times and more people are become familiarized with the technology, if other types of renewables are available in the area (geothermal, micro-hydro, wind power, etc.) they should be included in the analysis as part of the generation portfolio. The data presented in this section serve as an example for how the analysis could be conducted and do not, as with the hypothetical feeder, represent real-world load values.

84
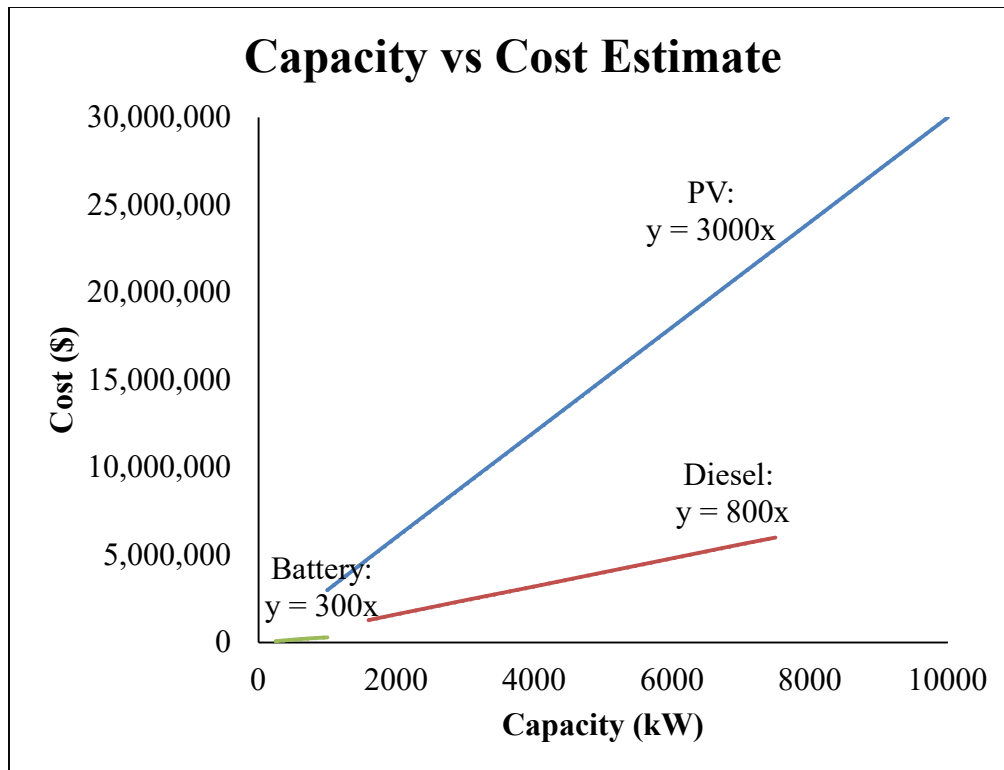
Figure 58 Cost estimate per system size of installed PV, Diesel and Battery systems. Taken from. [42]

Table 10 Summary of cost and system size estimates multipliers derived from Figure 58

System Type	Cost/System size ($/kW)
PV	3000
Diesel	800
Battery	300

Table 11 Derivation of equivalent cost and system size multiplier for systems in Jayuya Case

Fraction of Load	Source	Cost/System size ($/kW)
0.5	PV	1500
0.5	Diesel	400
0.25	Battery	75
	Equivalent	**1975**

Table 12 Clusters with estimated cost and number of critical loads per cluster

Cluster Name	Load Name	Estimated Cluster Cost	Estimated System Size (kW)	Estimated Cost	Number of Critical Loads
Cluster_1	HR Studios	$ 118,500.00	30	$ 59,250.00	2
	Pump_9		15	$ 29,625.00	
	Pump_10		15	$ 29,625.00	
Cluster_2	Pump_12	$ 59,250.00	15	$ 29,625.00	2
	Pump_13		15	$ 29,625.00	
Cluster_3	Angela Calvani	$ 590,525.00	40	$ 79,000.00	2
	Farmacia Hayuya		80	$ 158,000.00	
	Ferreteria Gilbes and Bycicle Shop		49	$ 96,775.00	
	Panadería (Bakery) Santa Clara		60	$ 118,500.00	
	Iglesia Del Nazareno - Jayuya Pueblo (Town)		30	$ 59,250.00	
	well_8		10	$ 19,750.00	
	Iglesia La Nueva Jerusalén C.L.A.		30	$ 59,250.00	
Cluster_4	well_2	$ 98,750.00	12	$ 23,700.00	4
	well_3		13	$ 25,675.00	
	well_4		15	$ 29,625.00	
	well_5		10	$ 19,750.00	
Cluster_5	Escuela Angelica Toro Rodriguez	$ 523,375.00	80	$ 158,000.00	1
	Estación de Bomberos Jayuya		50	$ 98,750.00	
	Baxter Credit Union		45	$ 88,875.00	
	Escuela Adrian Torres		90	$ 177,750.00	
Cluster_7	Total Avenida Vicens	$ 375,250.00	70	$ 138,250.00	1
	Farmacia Lizette		35	$ 69,125.00	
	Oficina Dr. Fernando Carreras Coello		35	$ 69,125.00	
	JayuCoop - Coorperativa de Ahorro y Crédito de Jayuya		50	$ 98,750.00	
Cluster_8	Cuartel Dtto. Jayuya	$ 1,027,000.00	50	$ 98,750.00	0
	Jayuya County Mayor		90	$ 177,750.00	
	CDT Mario Canales Torresola		350	$ 691,250.00	
	La Placita De Jayuya		30	$ 59,250.00	

Cluster Name	Load Name	Estimated Cluster Cost	Estimated System Size (kW)	Estimated Cost	Number of Critical Loads
Table 10 Continued					
Cluster_9	Pump_5	$ 88,875.00	15	$ 29,625.00	3
	Pump_6		15	$ 29,625.00	
	Pump_7		15	$ 29,625.00	
Cluster_10	Pump_18	$ 29,625.00	15	$ 29,625.00	1
Cluster_11	Su Nemesio R Canales	$ 266,625.00	120	$ 237,000.00	2
	Pump_19		15	$ 29,625.00	
Cluster_12	Telecom Tower Carr 533 Bo. Toro Negro Rio Cialito	$ 19,750.00	10	$ 19,750.00	1
Cluster_13	Jayuja Metropolitana	$ 1,362,750.00	50	$ 98,750.00	1
	Gulf		70	$ 138,250.00	
	Los Domplines		40	$ 79,000.00	
	COGOP Jayuya (Iglesia de Dios de la Profecía)		30	$ 59,250.00	
	Cafetería Rodríguez		35	$ 69,125.00	
	Policlínica Castañer Jayuya		60	$ 118,500.00	
	Farmacia Padua		60	$ 118,500.00	
	Medicaid		30	$ 59,250.00	
	JAYUYA VETERINARY SERVICES		35	$ 69,125.00	
	Breban Beauty Supply		20	$ 39,500.00	
	EZ Payments Inc.		30	$ 59,250.00	
	Oficina Dr. Luis A. Rivera "Lucho"		40	$ 79,000.00	
	Popular Bank - Sucursal Jayuya		65	$ 128,375.00	
	Paliques Café		60	$ 118,500.00	
	Parroquia Nuestra Señora de la Monserrate		35	$ 69,125.00	
	Iglesia Metodista Hill Memorial		30	$ 59,250.00	
Cluster_14	El Yocahú	$ 148,125.00	40	$ 79,000.00	0
	Iglesia Cristiana Carismatica Jesus Vive		35	$ 69,125.00	
Cluster_15	Telecom Tower carr 141 Km 5.7 Monte Gregorio	$ 19,750.00	10	$ 19,750.00	1
Cluster_16	Pump_14	$ 59,250.00	15	$ 29,625.00	2
	Pump_15		15	$ 29,625.00	

			Estimated		Number
			System		of
Cluster Name	Load Name	Estimated Cluster Cost	Size (kW)	Estimated Cost	Critical Loads

Table 10 Continued

Cluster Name	Load Name	Estimated Cluster Cost	Estimated System Size (kW)	Estimated Cost	Number of Critical Loads
Cluster_17	La Casona	$ 414,750.00	35	$ 69,125.00	2
	Napoli Pizza		30	$ 59,250.00	
	Shell		65	$ 128,375.00	
	Panadería La Jayuyana		65	$ 128,375.00	
	Pump_8		15	$ 29,625.00	
Cluster_18	Puma 154	$ 296,250.00	50	$ 98,750.00	2
	Su Antonio Romero Muñiz		100	$ 197,500.00	
Cluster_19	Telecom Tower Carr 143 Km 17.2 Cerro Puntas	$ 39,500.00	10	$ 19,750.00	2
	Telecom Tower Carr 143 Km 17.4 Interior bo. Zamas Cerro Punta		10	$ 19,750.00	
Cluster_20	Telecom Tower Carr 143 Bo Punta	$ 59,250.00	10	$ 19,750.00	3
	Telecom Tower Carr 143 Cerro Punta		10	$ 19,750.00	
	Telecom Tower Carr 143 Km 18.5 Int Bo. Saliente		10	$ 19,750.00	
Cluster_21	United States Postal Service	$ 98,750.00	35	$ 69,125.00	1
	Pump_2		15	$ 29,625.00	
Cluster_24	Telecom Tower Carr 614 Km 6.2 Bo. Cialitos	$ 19,750.00	10	$ 19,750.00	1
Cluster_25	Telecom Tower Carr 149 Caminos las Ca@as	$ 19,750.00	10	$ 19,750.00	1
Cluster_26	Telecom Tower Carr 615 Km 7.1 Int. Bo Toro Negro	$ 19,750.00	10	$ 19,750.00	1
Cluster_28	Telecom Tower Carr 143 Bo. Portuguez	$ 19,750.00	10	$ 19,750.00	1
Cluster_30	Econo	$ 296,250.00	150	$ 296,250.00	1
Cluster_31	Telecom Tower Carr 144 Bo. Veguitas	$ 19,750.00	10	$ 19,750.00	1
Cluster_32	Pump_11	$ 29,625.00	15	$ 29,625.00	1
Cluster_33	well_1	$ 43,450.00	12	$ 23,700.00	2
	well_6		10	$ 19,750.00	
Cluster_34	Pump_1	$ 29,625.00	15	$ 29,625.00	1
Cluster_35	Telecom Tower Carr 533 Bo. Toro Negro Rio Cialito	$ 19,750.00	10	$ 19,750.00	1
Cluster_37	Pump_16	$ 59,250.00	15	$ 29,625.00	2
	Pump_17		15	$ 29,625.00	

The result of all the cluster processing can be summarized in Table 13, which can facilitate the decision making of someone who is in charge of actually financing and implementing the clusters. This table ranks the clusters according to cost (left side) or number of critical loads (right). The observant reader may note that there is no real correlation between cost and how many critical loads are impacted. This is wonderful news if an area is dealing with limited recovery funds and wants to impact the largest number of critical loads for a defined budget. Let us consider the costliest cluster, cluster 13, with an estimated implementation cost of $1.36 million. While it is true that this cluster serves 16 separate loads, there is only one critical load contained within it. If the first five clusters on the list on the right are considered, they sum of their estimated costs is $1.25 million, but their total contribution is that of 14 critical loads and 22 total loads served when the non-critical loads in those clusters are considered.

Table 13 Clusters sorted by cost (left side) Clusters sorted by number of critical loads (right side)

Cluster Name	Estimated Cluster Cost	Number of Critical Loads	Cluster Name	Estimated Cluster Cost	Number of Critical Loads
Cluster_13	$ 1,362,750.00	1	Cluster_4	$ 98,750.00	4
Cluster_8	$ 1,027,000.00	0	Cluster_9	$ 88,875.00	3
Cluster_3	$ 590,525.00	2	Cluster_20	$ 59,250.00	3
Cluster_5	$ 523,375.00	1	Cluster_3	$ 590,525.00	2
Cluster_17	$ 414,750.00	2	Cluster_17	$ 414,750.00	2
Cluster_7	$ 375,250.00	1	Cluster_18	$ 296,250.00	2
Cluster_18	$ 296,250.00	2	Cluster_11	$ 266,625.00	2
Cluster_30	$ 296,250.00	1	Cluster_1	$ 118,500.00	2
Cluster_11	$ 266,625.00	2	Cluster_2	$ 59,250.00	2
Cluster_14	$ 148,125.00	0	Cluster_16	$ 59,250.00	2
Cluster_1	$ 118,500.00	2	Cluster_37	$ 59,250.00	2
Cluster_4	$ 98,750.00	4	Cluster_33	$ 43,450.00	2
Cluster_21	$ 98,750.00	1	Cluster_19	$ 39,500.00	2
Cluster_9	$ 88,875.00	3	Cluster_13	$ 1,362,750.00	1
Cluster_2	$ 59,250.00	2	Cluster_5	$ 523,375.00	1
Cluster_16	$ 59,250.00	2	Cluster_7	$ 375,250.00	1
Cluster_20	$ 59,250.00	3	Cluster_30	$ 296,250.00	1
Cluster_37	$ 59,250.00	2	Cluster_21	$ 98,750.00	1
Cluster_33	$ 43,450.00	2	Cluster_10	$ 29,625.00	1
Cluster_19	$ 39,500.00	2	Cluster_32	$ 29,625.00	1
Cluster_10	$ 29,625.00	1	Cluster_34	$ 29,625.00	1
Cluster_32	$ 29,625.00	1	Cluster_12	$ 19,750.00	1
Cluster_34	$ 29,625.00	1	Cluster_15	$ 19,750.00	1
Cluster_12	$ 19,750.00	1	Cluster_24	$ 19,750.00	1
Cluster_15	$ 19,750.00	1	Cluster_25	$ 19,750.00	1
Cluster_24	$ 19,750.00	1	Cluster_26	$ 19,750.00	1
Cluster_25	$ 19,750.00	1	Cluster_28	$ 19,750.00	1
Cluster_26	$ 19,750.00	1	Cluster_31	$ 19,750.00	1
Cluster_28	$ 19,750.00	1	Cluster_35	$ 19,750.00	1
Cluster_31	$ 19,750.00	1	Cluster_8	$ 1,027,000.00	0
Cluster_35	$ 19,750.00	1	Cluster_14	$ 148,125.00	0

4.4   Example microgrid: Cluster 4

As a conclusion to the test case, cluster 4 was selected. This cluster had the highest number of critical loads, while not being the most expensive cluster making it a good choice as an example to showcase the complete methodology. An isolated Google Earth overlay of cluster 4 is found in Figure 59. Cluster 4 contains four freshwater wells with pumps, an ideal cluster as pumps are on the top of the priority list of critical infrastructures. It is important to note, that as there is no real information about the underlying electrical infrastructure, all clusters are created using proximity and the hypothetical feeder that has been placed over Jayuya. Those pumps have the possibility of helping the nearest communities as well as extend further due to the water pipe network.

Figure 59 Google Earth overlay of cluster 4; four wells with pumps. Red flags indicate the location of the pumps
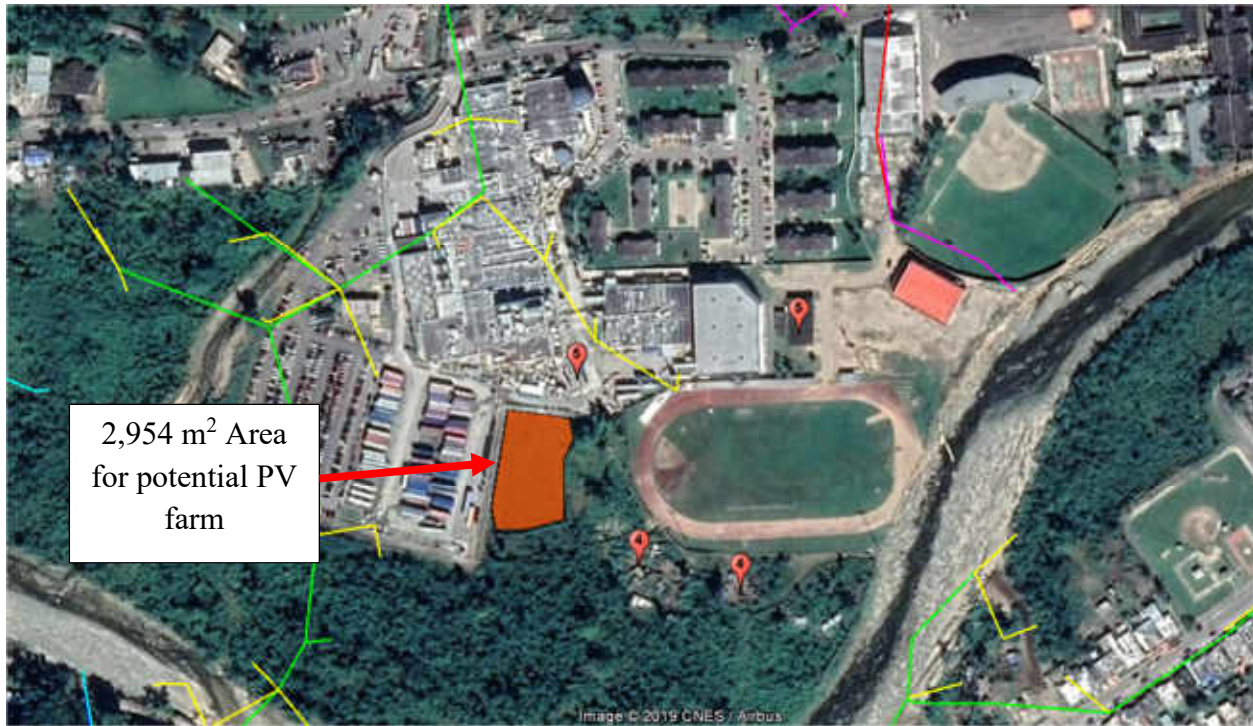
Figure 60 Potential for PV farm near cluster 4. PV area shown by orange polygon

Table 12 includes the estimated system size per load for cluster 4, which comes out to a total of 50 kW. A surplus factor of 1.25 was selected as a consideration for system inefficiencies when calculating the required powers and energies for the loads in the microgrid, which turned the new load into 62.5 kW Water pumps are not all turned on at the same time and are not always on either, much like the on-off cycles of an air conditioner compressor. An average on time of 12 hours for the regular use case was selected to calculate the required energy, yet the design for the worst case must consider the peak load to be all the pumps turned on at the same time. The split between renewable and non-renewable stayed the same, 50/50. The daily energy requirement for each of the halves assuming a flat loadshape with the value of peak load and an on time of 12 hours is 375 kWh. The summary for all of this is found in Table 14.

Table 14 Initialization of microgrid characteristics. This table is a combination of the M 1, M 2, R 1 and NR 1 stages.

Microgrid Sizing Characteristics	
Total load from cluster (kW)	50
Surplus factor	1.25
New total load (kW)	62.5
Percent Renewable	50%
Percent Non-renewable	50%
Peak power supplied by Renewable (kW)	31.25
Peak power supplied by Non-renewable (kW)	31.25
Average amount of time Pumps will run per day (hrs)	12
Amount of energy required of Renewable (kWh/day)	375
Amount of energy required of Non-renewables (kWh/day)	375

For the 50% renewable source, photovoltaic panels were selected. Specifically, the CHSM6612M Series 370W monocrystalline PV module. Its efficiency and area can be found in [43] and Table 15. The effective daylight hours or the annual average global horizontal irradiance (GHI) of the location in Jayuya must also be known to estimate the physical size of the required system. The GHI for Jayuya can be found in NREL's NSRDB in [44] and its value also in Table 15. The total panel area is found using equation (19) in square meters; verification of viability was done by creating a polygon of at least that area and overlaying it near where cluster 4 was located. The result of this can be seen in Figure 60. The required panel area was around 400 square meters, finding a place for this amount of PV was not a problem. The area of the orange polygon is close to 3000 square meters, well above the required minimum. The number of panels is rounded up to the nearest integer, therefore the result of 200.6 panels turns into 201 panels.

$$Total\ Panel\ Area = \frac{\frac{Daily\ Energy\ Requirement}{Daily\ GHI}}{Panel\ Efficiency}\ (m^2) \qquad (19)$$

$$Number\ of\ Panels = \frac{Total\ Panel\ Area}{Area\ per\ Panel} \qquad (20)$$

93

Table 15 Renewable generation solution evaluation R 2 stage.

Solar System Sizing	
GHI for Jayuya (kWh/sq.m/day)	5.062
Selected solar module efficiency	0.191
Total panel area (sq.m)	387.861
Area of selected panel (sq.m)	1.93446
Number of panels	200.501

Now the process continues to storage (RS 1). The rules of operation change under an emergency condition. The pumps will no longer be required to run for 12 hrs, their run time is reduced to 8 hrs per day a 33% reduction in up time. This has de effect of conserving fuel and battery charge and therefore allows for a smaller storage system which has a lower cost. A grid-less operation time of 8 hrs a day for 3 days is selected, again in the hopes of allowing for a smaller storage system. The math for Table 16 is fairly simple: a 25% size of the load is taken as the peak load, the required energy is the total up time in hours (8x3=24 hours) multiplied by the peak output power. This results in a storage system that must supply at least 375 kWh [45].

Table 16 Renewable storage requirements RS 1 stage.

Storage Requirements for emergency operation	
Percent of total system size	25%
Storage peak power (kW)	15.625
Isolated operation duration (days)	3
Average amount of time Pumps will run per day (hrs)	8
Total operation time (hrs)	24
Total energy required from storage (kWh)	375

Table 17 Renewable storage solution evaluation RS 2 stage.

Lead Flooded battery sizing per storage requirements	
Depth of discharge penalty(only allowed 50% depth of discharge)	2
Actual needed installed capacity (kWh)	750
Usable energy of selected module (kWh)	95.616
Number of modules needed	15.6878

94

The technology selected to act as the storage are common flooded lead acid batteries, this model however promises an extended life of 10 years which is around double what is expected from this type of flooded batteries. The model is the Solar-One HUP SO-6-125-33 48V Flooded Battery, more information about it can be found here: [46]. Flooded batteries must not be discharged below 50% of their usable kWh rating, nor should they be discharged faster than their Ah rating, therefore the amount of batteries you need is actually double that of the nameplate rating of the battery [47], this is why the actual installed capacity shown in Table 17 is double what was calculated in stage RS 1. The number of modules is found using equation (21) and results in 15.7 modules which is again rounded up and now equal to 16 modules.

$$Number\ of\ Battery\ Modules = \frac{Needed\ Installed\ Capacity}{Usable\ Module\ Capacity} \qquad (21)$$

Table 18 Non-renewable viability check. NR 1 and NR 2 stage.

Diesel generator system sizing	
Peak power supplied by Non-renewable (kW)	31.25
Fuel tank capacity of selected generator (gallons)	260
Peak power rating of selected generator (kW)	40

Table 19 Fuel requirements estimation for non-renewables. NR 3 stage

Fuel requirements estimation	
Days of fuel required	3
Average amount of time Pumps will run per day (hrs)	8
Average fuel consumption at 75% load (gal/hr)	3.2
Estimated required fuel (gallons)	76.8
Does fuel tank meet minimum requirements	Yes

The final stretch of the microgrid design process flow, NR 1 through NR 3, Table 18 and Table 19. The percent of renewables established at the beginning was 50% and it held through, therefore the rest of the load must be served via the non-renewable source. A diesel generator was selected as the non-renewable source. These are rated by peak load unlike the previously discussed things which have been selected based on energy. Generators also come in discrete ratings; therefore, the closest largest generator should be selected to service the load a much larger generator should not be used as it would not operate near its rating and be less fuel efficient as well as being costlier. Smaller generators could be connected to serve a single load, but that tends to add more complication than it is worth and more possible failure points. For a peak load of 31.2 kW, there are two options: a 38kW and a 40kW generator. The 40kW Generac generator [48] was selected due to its form factor; this generator included a rather large tank (260 gallons) for the storage portion of this section.

The amount of fuel required is calculated based on the efficiency curves found in [49]. For a 40kw generator operating at 75% rated load, assuming the microgrid's load is the flat peak discussed earlier, the fuel consumption will be 3.2 gallons/hour and for the 24 hour required run time, this equates to 76.8 gallons of fuel. The selected generator can handle the peak load and has some room for expansion as well as a large enough tank to accommodate 10 days of 8hr per day run time and complies with the design.

Table 20 Simplified bill of materials (BOM) for cluster 4

Simplified BOM			
Item	Quantity	Cost each	sub total
CHSM6612M Series 370W Monocrystalline PV module	201	$ 262.00	$ 52,662.00
Sunny TriPower Core1 62-US 62kW	1	$ 6,875.00	$ 6,875.00
Solar-One HUP SO-6-125-33 48V Flooded Battery	16	$ 29,250.00	$ 468,000.00
Generac SD40 40kW 3ph diesel generator w/ 260-gallon tank	1	$ 13,250.00	$ 13,250.00
Total			**$ 540,787.00**

Table 20 includes the costs of the simplified bill of materials for cluster 4. It is almost 6 times that of the original estimate in Table 13, this is due to the high cost of the battery storage and the duration of the expected outage. When the storage is removed a total of $72,787.00 is achieved, which is much closer to the original estimate. Something that has not been discussed before is the TriPower inverter, it is a 62kW 3ph inverter with grid tied functionality as well as 6 mppt channels for up to 12 strings of modules. The solar panels could be arranged in four pairs of strings of 20 modules each for the first four mppt channels, the fifth channel would have a single string of 20 and the last channel a string of 21.

As a final analysis of energy availability during the outage and taking advantage of the large capacity fuel tank and battery storage system, look to Table 21. Under standard operating conditions the generator goes unused while the battery and PV system provide grid support for four pumps which are on 12 hours a day. Under emergency conditions the grid is lost, and the generator comes in with a new schedule of 8 hours a day for the pumps. The reader should remember the pumps will not be on all at the same time and the 8 hours a day is distributed according to a predetermined cycle such that there may be the water resource for most of the day. In fact, the new operation regimen means a reduction to 2/3 of the original available water.

Should the microgrid have a smart schedule to dispatch a mix of renewable, non-renewable and storage it may be possible to extend way beyond the designed 3-day limit. Taking for example a full tank of diesel fuel and a fully charged battery system prior to the outage and using the scheduling shown in Table 21. The scheduling assumes that the PV system is able to take in all of its rated power which is not real, but taking the ideal example shown below it is shown that the microgrid would be able to continue on with the reduced 2/3 regimen for up to 24 days without resorting to intermittent water service! A definite improvement over instantly losing the water service and not gaining it for weeks. The scheduling shown below also tries to use the generator sparingly as to allow for the opportunity of refueling after the emergency and before the intermittent water service, therefore improving both the resilience of the community and their water availability.

Table 21 Rudimentary scheduling of generation and storage assets to extend working period during emergency situation.

All units in kWh								
Day of outage	**Generator Energy consumed by the pumps**	**Generator remaining energy**	**PV Energy consumed by the pumps**	**Energy given by the Battery**	**Energy received from PV to the Battery**	**Net allowable discharge for battery**	**Consumed by Pumps**
1	0	1750	250	250	150	775	500
2	0	1750	250	250	150	675	500
3	0	1750	250	250	150	575	500
4	0	1750	250	250	150	475	500
5	0	1750	250	250	150	375	500
6	0	1750	250	250	150	275	500
7	0	1750	250	250	150	175	500
8	250	1500	250	0	150	325	500
9	0	1500	250	250	150	225	500
10	250	1250	250	0	150	375	500
11	0	1250	250	250	150	275	500
12	0	1250	250	250	150	175	500
13	250	1000	250	0	150	325	500
14	0	1000	250	250	150	225	500
15	250	750	250	0	150	375	500
16	0	750	250	250	150	275	500
17	0	750	250	250	150	175	500
18	250	500	250	0	150	325	500
19	0	500	250	250	150	225	500
20	250	250	250	0	150	375	500
21	0	250	250	250	150	275	500
22	0	250	250	250	150	175	500
23	250	0	250	0	150	325	500
24	0	0	250	250	150	225	500

Chapter 5:   CONCLUSION

This work shows how to use the nighttime satellite imagery provided by NASA and create map overlays using open source software that can then be combined with free access GIS databases and geocoded information to aid in microgrid planning. The aim of which is to be able to provide an easier entry to researchers interested in resilience planning without all the burden of cost or information unavailability in the hopes that in the future distribution system planning and the use of GIS data sets are combined to provide more holistic solutions.

The methodology presented here aims to frontload all the decision criteria into the setup of the methodology to help remove some of the bias during the evaluation process. The process will always be influenced by the decisions and experience of the researcher, but by frontloading the criteria it is hoped that they are not changed on the fly should the result of the methodology not favor a particular interest. There is only one case where the results of the methodology should be re-evaluated, this is the case where the positive impact to the community can be broadened or improved upon from the initial solution. The main advantage of using satellite imagery to identify the blackout areas is that the interests of any one group are eliminated from the identification stage; facts are facts and priority is assigned to those locations without power for the longest duration.

This is another important difference between the methodology presented here and traditional distribution system planning and microgrid resource allocation methods, the segmentation of a circuit is not done with the power system as a priority. The grids are centered around load criticality with respect to the local community impact as well as the potential to impact the surrounding communities, which gives the potential for human benefit more importance. This is not to say the power system challenges regarding the implementation of such a microgrid are to

be ignored. The technical implementation challenges can be incorporated as part of the decision process which should involve the local utility. This work presents a different way in which to look at energy availability for critical loads because it forces the researcher to define what they consider to be the critical loads before looking at who is being affected by power outages. It would be truly impossible to undertake the creation microgrids based on those communities that had no power for months after Hurricane María without knowing the electrical infrastructure of at least the affected areas. Therefore the utility must be involved for something like this to happen; something that would improve the lives of those who suffered most.

Chapter 6:   FUTURE WORK

There are several ways in which this work can be expanded. The clustering methodology could be expanded by including an automatic clustering algorithm. This could be a graph theory based approach, as previously mentioned, by including a tree partitioning algorithm and then a clustering ranking system. If a complete circuit model of an area under study is obtained, a power flow based partitioning could also be applied. The assignment of generation portfolios could be evaluated by including things such as the renewable energy alternatives for each area, land use constraints.

When assigning cluster priority, other considerations such as demographics and economic improvement of an area could be added. Although these would require the input of sociology, as pure engineering approaches often ignore these factors. The inclusion of microgrid planning as part of the economic development of an area looking at the future of a community. It is important that resilience not only be approached from a purely power systems approach; the impact to people should be at the heart of any resilience efforts.

The two-year anniversary of the hurricane was a month ago, but still work is being done with the development of solutions for powering critical loads during emergencies. Take the work done by C. Keerthisinghe et. al [50], it was presented in January this year and they also used Jayuya as a test case. They provide solutions to power individual loads but provide no guidance as to how to select the locations for these emergency power solutions. The methodology presented in this thesis could be used to complement such solutions, which answer how to power a high priority load, by providing the answer to the important question of where the high priority loads are and how to group them.

References

[1] United States Census Bureau, "Geographies: TIGER/Line with Selected Demographic and Economic Data," 2010. [Online]. Available: https://www.census.gov/geographies/mapping-files/time-series/geo/tiger-data.2010.html. [Accessed 31 January 2019].

[2] Aeepr.com, "Sistema Electrico," 2017. [Online]. Available: https://www.aeepr.com/Aeees/sistema_electrico.asp. [Accessed 30 October 2017].

[3] R. Avila, "Apagón de Puerto Rico es el más largo en la historia de la nación americana," Metro, 2017. [Online]. Available: https://www.metro.pr/pr/noticias/2017/10/26/apagon-puerto-rico-mas-largo-la-historia-la-nacion-americana.html. [Accessed 30 October 2017].

[4] NATIONAL RESEARCH COUNCIL OF THE NATIONAL ACADEMIES, Terrorism and the Electric Power Delivery System, Washington: THE NATIONAL ACADEMIES PRESS, 2012.

[5] C. Otero, "Impacto multibillonario de María," El Vocero de Puerto Rico, 2017. [Online]. Available: http://www.elvocero.com/economia/impacto-multibillonario-de-mar-a/article_5f364bf0-a176-11e7-892a-ff1a85c871da.html. [Accessed 31 October 2017].

[6] Energia.pr.gov, "Distribución Porcentual de la Generación de Energía por Tipo – Comisión de Energía de Puerto Rico," 2017. [Online]. Available: http://energia.pr.gov/datos/distribucion-porcentual-de-la-generacion-de-energia-por-tipo/. [Accessed 30 October 2017].

[7] Energia.pr.gov, "Consumo Energético Municipal (2004-2014) – Comisión de Energía de Puerto Rico," 2017. [Online]. Available: http://energia.pr.gov/datos/consumo-municipal/. [Accessed 10 October 2017].

[8] U. D. o. H. Security, "Homeland Infrastructure Foundation-Level Data (HIFLD) Open Data," 2017. [Online]. Available: https://hifld-geoplatform.opendata.arcgis.com/. [Accessed 26 June 2019].

[9] CB en Español, "Huracán María provoca que AAA pierda sistema de visualización de sus plantas," 2017. [Online]. Available: http://cb.pr/huracan-maria-provoca-que-aaa-pierde-sistema-de-visualizacion-de-sus-plantas/. [Accessed 31 January 2019].

[10] C. Heredia-Rodriguez, "Water quality in Puerto Rico remains unclear months after Hurricane Maria," 2019. [Online]. Available: https://www.pbs.org/newshour/health/water-

quality-in-puerto-rico-remains-unclear-months-after-hurricane-maria. [Accessed 31 January 2019].

[11] Metro PR, "Metro Pavia y hospitales afiliados listos para brindar ayuda," Metro PR, 2017. [Online]. Available: https://www.metro.pr/pr/estilo-vida/2017/09/22/metro-pavia-hospitales-afiliados-listos-brindar-ayuda.html. [Accessed 31 October 2017].

[12] Telemundo PR, "Crítica situación en los hospitales de Puerto Rico tras paso del huracán María," Telemundo, 2017. [Online]. Available: http://www.telemundo.com/noticias/2017/09/25/critica-situacion-en-los-hospitales-de-puerto-rico-tras-paso-del-huracan-maria. [Accessed 31 October 2017].

[13] El Nuevo Dia, "Sigue en aumento el restablecimiento de energía eléctrica y agua potable," 2017. [Online]. Available: https://www.elnuevodia.com/noticias/locales/nota/sigueenaumentoelrestablecimientodeenergiaelectricayaguapotable-2367357/. [Accessed 31 October 2017].

[14] El Nuevo Dia, "Telecomunicaciones: 30.5% del servicio se ha restablecido," 2017. [Online]. Available: https://www.elnuevodia.com/negocios/empresas/nota/telecomunicaciones3050delservicioseharestablecido-2361611/. [Accessed 31 October 2017].

[15] G. Lopez-Cardalda, M. Lugo-Alvarez, S. Mendez-Santacruz, E. Rivera and E. Bezares, "Learnings of the Complete Power Grid Destruction in Puerto Rico by Hurricane Maria," in *2018 IEEE International Symposium on Technologies for Homeland Security (HST)*, Woburn, MA, 2018.

[16] N. Brown, R. Respaut and J. Resnick-Ault, "Special Report: The bankrupt utility behind Puerto Rico's power crisis," Reuters, 4 October 2017. [Online]. Available: https://www.reuters.com/article/us-usa-puertorico-utility-specialreport/special-report-the-bankrupt-utility-behind-puerto-ricos-power-crisis-idUSKBN1C92B5. [Accessed 14 October 2019].

[17] NOTICEL, "A seis meses de María así está Puerto Rico," 2018. [Online]. Available: https://www.noticel.com/ahora/a-seis-meses-de-mara-as-est-puerto-rico/716861339. [Accessed 31 January 2019].

[18] Svs.gsfc.nasa.gov, "Transcripts of 12616_BlackMarblePR_FINAL_youtube_720," 2019. [Online]. Available: https://svs.gsfc.nasa.gov/vis/a010000/a012600/a012616/12616_BlackMarblePR_FINAL-transcript.html. [Accessed 31 January 2019].

[19] M. O. Román, Z. Wang, Q. Sun, V. Kalb, S. D. Miller and E. al., "NASA's Black Marble nighttime lights product suite," *Remote Sensing of Environment,* vol. 210, pp. 113-143, 2018.

[20] M. O. Roman, E. C. Stokes, R. Shrestha, Z. Wang, L. Schultz, E. A. S. Carlo and e. al., "Satellite-based assessment of electricity restoration efforts in Puerto Rico after Hurricane Maria," *PLoS ONE,* 28 June 2019.

[21] Z. Li and M. Shahidehpour, "Role of microgrids in enhancing power system resilience," in *2017 IEEE Power & Energy Society General Meeting*, Chicago, IL, 2017.

[22] R. Mathew, S. Ashok and S. Kumaravel, "Resilience assessment using microgrids in radial distribution network," in *2016 IEEE 7th Power India International Conference (PIICON)*, Rajasthan, India, 2016.

[23] M. Saleh, A. Althaibani, Y. Esa, Y. Mhandi and A. Mohamed, "Impact of clustering microgrids on their stability and resilience during blackouts," in *2015 International Conference on Smart Grid and Clean Energy Technologies (ICSGCE)*, 2015.

[24] NREL, "SMART-DS: Synthetic Models for Advanced, Realistic Testing: Distribution Systems and Scenarios | Grid Modernization | NREL," 2019. [Online]. Available: https://www.nrel.gov/grid/smart-ds.html. [Accessed 31 January 2019].

[25] NASA, "NASA World View," [Online]. Available: https://worldview.earthdata.nasa.gov/?p=geographic&l=VIIRS_SNPP_DayNightBand_E NCC&t=2019-03-11. [Accessed 26 July 2019].

[26] Esri ArcGIS, "VIIRS DNB Nighttime Lights Monthly Composites," [Online]. Available: https://www.arcgis.com/home/webmap/viewer.html?useExisting=1&layers=d7c95b2da6fd 43cd9dec19b212f145db. [Accessed 26 July 2019].

[27] NASA Goddard Space Flight Center, "NASA Facts," 15 February 2013. [Online]. Available: https://web.archive.org/web/20130215071955/http://npp.gsfc.nasa.gov/images/NPP%20Fa ctSheet_Final.pdf#. [Accessed 26 July 2019].

[28] D. Netburn, "The making of NASA's super hi-res blue marble Earth image," L.A. Times, 26 1 2012. [Online]. Available: https://latimesblogs.latimes.com/technology/2012/01/nasa-super-hi-res-earth.html. [Accessed 26 7 2019].

[29] K. E. f. t. S. V. Studio, "NASA's Black Marble night lights used to examine disaster recovery in Puerto Rico," 9 December 2018. [Online]. Available: https://svs.gsfc.nasa.gov/4658. [Accessed 26 7 2019].

[30] S. v. d. Walt, J. L. Schönberger, J. Nunez-Iglesias, F. Boulogne, J. D. Warner, N. Yager, E. Gouillart, T. Yu and s.-i. contributors, "scikit-image: Image processing in Python," *PeerJ,* p. 2:e453, 14 June 2014.

[31] S. v. d. Walt, S. C. Colbert and G. Varoquaux, "The NumPy Array: A Structure for Efficient Numerical Computation," *Computing in Science & Engineering,* vol. 13, no. 2, pp. 22-30, March 2011.

[32] scikit-image, "RGB to HSV," [Online]. Available: https://scikit-image.org/docs/stable/auto_examples/color_exposure/plot_rgb_to_hsv.html#sphx-glr-auto-examples-color-exposure-plot-rgb-to-hsv-py. [Accessed 15 June 2019].

[33] P. Osborne, "The Mercator Projections," Zenodo, Edinburgh, 2013.

[34] Google , "What is KML?," [Online]. Available: https://developers.google.com/kml/. [Accessed 31 January 2019].

[35] esri, "Shapefiles," esri, [Online]. Available: https://doc.arcgis.com/en/arcgis-online/reference/shapefiles.htm. [Accessed 30 July 2019].

[36] S. Gillies, O. Tonnhofer, J. Arnott and E. al., "Shapely 1.6.4.post2," 18 July 2018. [Online]. Available: https://pypi.org/project/Shapely. [Accessed 15 June 2019].

[37] J. Kummer, "Earth Radius by Latitude Calculator," [Online]. Available: https://rechneronline.de/earth-radius/. [Accessed 20 June 2019].

[38] W. MathWorld, "Mercator Projection," Wolfram, [Online]. Available: http://mathworld.wolfram.com/MercatorProjection.html. [Accessed 10 June 2019].

[39] Junta de Planificacion de Puerto Rico, "Mapa Interactivo de Puerto Rico MIPR," [Online]. Available: http://gis.jp.pr.gov/mipr/. [Accessed 30 May 2019].

[40] Baxter, "About Baxter Puerto Rico," [Online]. Available: www.baxter.com.pr/about_baxter/about_baxter_pr.html. [Accessed 8 8 2019].

[41] W. Konrad, "Why so many medicines are in short supply months after Hurricane Maria," CBS News, 12 2 2018. [Online]. Available: https://www.cbsnews.com/news/why-so-many-medicine-arel-in-short-supply-after-hurricane-maria/. [Accessed 8 8 2019].

[42] R. F. Jeffers, M. J. Baca, A. M. Wachtel, S. DeRosa, A. Staid, W. Fogleman, A. Outkin and F. Currie, "Analysis of Microgrid Locations Benefitting Community Resilience for Puerto Rico," Sandia National Laboratories, Albuquerque, 2018.

[43] Astroenergy, "AstroHalo CHSM6612M Monocrystalline PV Module 350W~370W," Astroenergy, 2018.

[44] NREL, "NSRDB Data Viewer Multi Year PSM Global Horizontal Irradiance," NREL, Denver, Colorado, 2019.

[45] G. Lopez-Cardalda, E. I. Ortiz-Rivera, M. Lugo-Alvarez, R. Darbali-Zamora and R. Broderick, "Puerto Rico as an Example for Energy Storage Evaluation and Selection Assessment," in *TPEC2020*, College Station. TX, 2019.

[46] Northwest Energy Storage, "Solar One batteries with Hup technology," Northwest Energ Storage, 2016.

[47] Wholesale Solar, "Off-Grid Battery Bank Sizing," Wholesale Solar, 3 December 2019. [Online]. Available: https://www.wholesalesolar.com/solar-information/battery-bank-sizing. [Accessed 3 December 2019].

[48] Diesel Service & Supply, "Genrac 40kW," Diesel Service & Supply, 3 December 2019. [Online]. Available: https://www.dieselserviceandsupply.com/Used-Generators/Generac-40-2090233.aspx. [Accessed 3 December 2019].

[49] Supply, Diesel Service &, "Approximate Diesel Fuel Consumption Chart," Diesel Service & Supply, 3 December 2019. [Online]. Available: https://www.dieselserviceandsupply.com/Diesel_Fuel_Consumption.aspx. [Accessed 3 December 2019].

[50] C. Keerthisinghe, M. Ahumada-Paras, L. D. Pozzo, D. S. Kirschen, H. Pontes, W. K. Tatum and M. A. Matos, "PV-Battery Systems for Critical Loads During Emergencies," *IEEE Power & Energy Magazine,* pp. 82-92, January 2019.